



THE UNIVERSITY OF  
**WAIKATO**  
*Te Whare Wānanga o Waikato*

Research Commons

<http://researchcommons.waikato.ac.nz/>

## Research Commons at the University of Waikato

### Copyright Statement:

The digital copy of this thesis is protected by the Copyright Act 1994 (New Zealand).

The thesis may be consulted by you, provided you comply with the provisions of the Act and the following conditions of use:

- Any use you make of these documents or images must be for research or private study purposes only, and you may not make them available to any other person.
- Authors control the copyright of their thesis. You will recognise the author's right to be identified as the author of the thesis, and due acknowledgement will be made to the author where appropriate.
- You will obtain the author's permission before publishing any material from the thesis.

**Process Sedimentology of the Waikato River Mouth, Port Waikato, New  
Zealand:**

**The depositional record of a mixed-energy river mouth**

A thesis  
submitted in partial fulfilment  
of the requirements for the degree  
of  
**Master of Science (Research) in Earth Sciences**  
at  
**The University of Waikato**  
by  
**Anya Podrumac**



THE UNIVERSITY OF  
**WAIKATO**  
*Te Whare Wānanga o Waikato*

2020

# Abstract

---

Interacting fluvial and marine processes at the Waikato River mouth control sedimentation patterns at the sand spit. These interacting processes cause tidal asymmetry between the ebb and flood tide, and produce multidirectional currents, orientated east, west, north, north-west, and south. Depositional processes at the Waikato River mouth are recorded using oceanographic instrumentation, and are linked to their corresponding sedimentary deposits. Sedimentary bedforms on the sand spit include wave- and combined-flow ripples and dunes, and planar bedding, produced from interacting fluvial and wave currents. Despite tides directly controlling sediment deposition, tides manifest as rising and falling water levels, affecting current magnitude and velocity, but are not directly indicated in terms of “tidal” sedimentary structures. Preservation potential of bedforms are low, with the sedimentary recorded dominated by structureless sand, from rarely occurring low flow velocity periods in the early- to mid-ebb tide. The Waikato River mouth is classified as wave-dominated, fluvially influenced and tide affected (Wft).

**Keywords:** Process sedimentology; mixed-energy; river mouth; Waikato River; Port Waikato.

# Acknowledgements

---

This thesis could not have been made possible without the very many people involved in this work.

My biggest thanks go to my supervisor Dr. Andrew La Croix for all his efforts navigating this project. I am very honoured to be Andrew's first student, and grateful for his support throughout these past 2 years. His knowledge and passion for sedimentology and ichnology is inspiring and he has challenged me in the best ways.

My thanks also go to my secondary supervisor Dr. Julia Mullarney. From her efforts in the field and lab, to helping me work through a complex dataset. Julia has broadened my knowledge in coastal processes, for which I am very thankful.

Data collection could not have been possible without the help of my supervisors, and the universities wonderful (former) technicians: Dean and Noel. The long days, and short nights and heavy lifting were strenuous; thank you everyone for your hard work, and for boosting my confidence in the field.

Thank you to the Waikato Regional Council, particularly Dr. Stephen Hunt. Your financial support, made the field work, and ultimately this entire project possible.

Thank you to the local Iwi, Richard Thompson and Barry Baquié; for your blessing for us to work on the sand spit, and your happiness to teach us about the history of the Waikato River.

A big thank you to Chris and Kirsty for all their help in the lab, cutting and x-raying cores, and to Rochelle and Peter for their insightful discussions in the office. To my classmates George, Ashley, Tori, Ben, Bérengère, and the 'Kamped' team; your company and support have gone a long way. Thank you for making me laugh, even when things were tricky through a very strange 2020.

Finally, I would like to thank my family who always support me through my life's endeavours. An extra thank you to my older brother Alyosha for his guidance and edits through this thesis, and my boyfriend Josh who is always by my side.

# Table of Contents

---

<b>Abstract</b> .....	<b>i</b>
<b>Acknowledgements</b> .....	<b>ii</b>
<b>Table of Contents</b> .....	<b>iii</b>
<b>List of Figures</b> .....	<b>v</b>
<b>List of Tables</b> .....	<b>vii</b>
<b>Chapter 1 Introduction and Literature Review</b> .....	<b>1</b>
1.1 Introduction .....	1
1.2 Background Literature .....	2
1.2.1 Facies Models .....	2
1.2.2 Coastal Depositional System Classification Based on the Sedimentary Record .....	2
1.2.3 Burrowing Infauna .....	8
1.3 Regional Context of the Waikato River Catchment .....	10
1.3.1 The Waikato River .....	10
1.3.2 Geological History of the Waikato River .....	11
1.3.3 Anthropogenic Impacts on the Waikato River .....	12
1.3.4 Weather and Climatic Setting .....	13
1.3.5 Sub-surface Geology of the Waikato River Catchment .....	14
1.3.6 Sediment in the Waikato River .....	15
1.4 Geology of the Port Waikato Region .....	16
1.5 The Coastal Setting of Port Waikato .....	18
1.5.1 Estuarine Classification in New Zealand .....	18
1.5.2 Morphology of the Waikato River Mouth .....	19
1.5.3 Tides in Estuaries .....	20
1.5.4 Estuarine Sedimentation .....	21
1.6 Summary .....	22
1.7 References .....	24
<b>Chapter 2 Process Sedimentology of the Waikato River Mouth, Port Waikato, New     Zealand</b> .....	<b>29</b>
2.1 Introduction .....	29
2.1.1 Sedimentology and Ichnology of Barriers and Mouth Bars .....	30
2.2 Study Area .....	31

2.2.1	Waikato River, New Zealand .....	31
2.3	Methods.....	34
2.3.1	Sediment Samples.....	36
2.3.2	Topography & Bathymetry Survey .....	36
2.3.3	Oceanographic Instruments .....	37
2.3.4	Vibracore .....	38
2.4	Results .....	39
2.4.1	Hydrodynamic Processes.....	39
2.4.2	Topography and Bathymetry of the Waikato River Mouth.....	42
2.4.3	Sedimentology of the Waikato River Mouth.....	44
2.5	Discussion .....	49
2.5.1	Process Sedimentology at the River Mouth.....	49
2.5.2	Relative Importance of River Flow, Waves and Tides.....	53
2.5.3	Implications for the Global Rock Record.....	54
2.6	Conclusions .....	56
2.7	References .....	58
<b>Chapter 3</b>	<b>Conclusions .....</b>	<b>63</b>
3.1	References .....	67
<b>Appendices .....</b>	<b>.....</b>	<b>69</b>
Appendix A.	Grainsize data.....	69
Appendix B.	Topography and Bathymetry.....	80
Appendix C.	Process Data from Oceanographic Instruments .....	81
Appendix D.	Core Logs.....	103
Appendix E.	Core X-rays .....	113

# List of Figures

---

Figure 1.1: Ternary diagram of coastal classification modified from Boyd et al. (1992) after Dalrymple et al. (1992).....	3
Figure 1.2: Schematic of the shoreface and beach profile. Showing the shoreface depositional environments (zones), wave zones, fair-weather wave base (FWWB), and low tide and high tide marks. Modified from Dashtgard et al. (2012). .....	4
Figure 1.3: Coastal depositional environment classification on both prograding and transgressive coasts. Showing increasing tidal power towards the left, and increasing wave power to the right. Modified from Boyd (2010) after Boyd et al. (1992). .....	5
Figure 1.4: (A) energy distribution, (B) morphology, and (C) longitudinal sedimentary facies, in a tide-dominated estuary (left) and wave-dominated estuary (right) modified after Dalrymple et al. (1992). .....	8
Figure 1.5: Distribution of marine ichnofacies, and their common trace fossils and trace fossil assemblages. From Gingras et al. (2011), after Seilacher (1967).....	9
Figure 1.6: Waikato River and Waipa River in central North Island, New Zealand. Paleo Waikato River course adapted from Manville & Wilson (2004). (Image Source: USGS). .....	11
Figure 1.7: Hydrographs of the Waikato River's six largest flood peaks at Ngaruawahia (1958-2008). Modified from Brown (2010) after Mighty River Power (2001).....	15
Figure 1.8: Geology and structural features of the Port Waikato region. Modified after Barker et al. (2016) and Edbrooke (2005).....	17
Figure 1.9: Morphological features of the Waikato River mouth. (Image Source: Google Earth, 2019).....	20
Figure 2.1: Site locations in the field area at the Waikato River mouth, Port Waikato, New Zealand. (Image Source: USGS and Google Earth). .....	33
Figure 2.2: Air photo of Waikato River mouth in 2012. Colour outlines show the changes in position of the shoreline and sand spit between 1942 and 2017. Modified from WRC (2018).....	34
Figure 2.3: Photos of research equipment: (A) Mastersizer® particle-size analyser used for grain size analysis of surface and channel sediment samples, (B) Site C: Nortek Vector, with velocity sensor mounted on the left pipe and Optical back scatter (OBS; turbidity) sensor on the right, (C) Site E: Nortek Aquadopp in front, and RBR Concerto behind. OBS sensors attached to the pipe, (D) echosounder used for the bathymetry survey of the river channel, (E) Vibracore collecting core sample. ....	35

Figure 2.4: Flow velocity and direction across two tides, recorded from ADCPs and ADVs. Colour represents time relative to high tide, and length of arrow denotes flow velocity. Each arrow shows averages over 15 minutes.....	41
Figure 2.5: Elevation of study area; topography of sand spit, and bathymetry of the Waikato River channel.....	43
Figure 2.6: Grainsize distribution of the study area. ....	44
Figure 2.7: Facies characteristics of selected intervals: (A) Facies 1, trough cross-bedded sand, in core 3, (B) facies 2, wave-ripple laminated sand in core 3, (C) facies 3, planar laminated sand, in core 3, (D) facies 4a structureless sand, in core 8, and (E) facies 4b shelly structureless sand, in core 9. ....	46
Figure 2.8: Bedforms visible on the surface of the sand spit: (A) Combined-flow dunes located between Sites E and F. Photo facing east; (B) Symmetrical, Wave dunes at Site D. Photo facing south-east; (C) Combined-flow ripples at Site E. Photo facing north east; and (D) Wave ripples at Site C. Photo facing east. ....	47
Figure 2.9: Vibracore cross-sections for (A) Cores 1-3, (B) Cores 4-6, and (C) Cores 7-9. NZVD2016 0 m elevation is used as the datum, although it is noted that the datum occurs above the cores since cores are intertidal. Inset map shows core locations in study area. ....	48
Figure 2.10: Hjulstrom diagram, showing sediment erosion, transport, and deposition as a function of flow velocity and sediment grain size. There is no assumed water depth. The range of grain sizes present on the sand spit are highlighted in green. Modified after Hjulstrom (1935).....	49
Figure 2.11: Horizontal flow velocities at Sites C, D, E, F, and H, recorded over a 24 hr period; from 12 am 20th to 12 am 21st January 2020. With erosion at flow velocities faster than 0.4 m/s, transport between 0.06-0.4 m/s, and deposition at flow velocities slower than 0.06 m/s. ....	50
Figure 2.12: Sedimentary bedforms development in combined flow conditions, as a function of unidirectional flow velocity and orbital flow velocity. Assuming an average grain size of 0.25 mm diameter (upper fine sand). Overlain with data recorded from each site, where green is Site C, yellow is Site D, light blue is Site E, red is Site F, and dark blue is Site H. Modified after Perillo et al. (2014).....	52
Figure 2.13: Process based classification modified after Ainsworth et al. (2011), with the Waikato River mouth plotted using the sedimentological dataset in red, and combined sedimentological and hydrodynamic datasets in blue.....	55
Figure 3.1: Waikato River mouth classified from Ainsworth et al. (2011). Classified as Wft using combined hydrodynamic and sedimentological dataset (blue), and Wf using only sedimentological data set (red).....	65



# List of Tables

---

Table 2.1: Vibracores and oceanographic instruments deployed at each site. All hydrodynamic instruments also had additional optical backscatter sensors (OBS); Nortek instruments were paired with Campbell Scientific OBS3+ sensors and the RBR instruments were paired with Seapoint turbidity sensors. ....	35
Table 2.2: Oceanographic instrumentation deployed in the field, with information regarding the deployment location and inbuilt sensors. ....	37
Table 2.3: East, west, north and south orientated flow velocity at each site recorded by the ADVs and ADCPs. ....	40

# Chapter 1

## Introduction and Literature Review

---

### 1.1 Introduction

The fluvial-to-marine transition (FMT) has become one of the most studied depositional zones from a sedimentological, ichnological, and stratigraphic standpoint. It is a complex region where the interactions between fluvial-alluvial and marine processes result in significant variability in physical and chemical conditions that affect sedimentation patterns and infaunal distributions. Sedimentological facies models are built from the prevailing physical sedimentological and ichnological aspects within these environments, using modern observations as their background. Currently, facies models fail to adequately capture all the processes and depositional products occurring within the FMT, where mixing of river flow, tides and waves is dynamic, with changing conditions over short time scales (hourly, daily, and annually).

Despite being the longest river in New Zealand, information on the Waikato River mouth is limited, particularly with regards to its morphology, infauna and sedimentology. This thesis focuses on the sediments deposited at the intertidal portion of the sand spit at the mouth of the Waikato River with the purpose of answering the following questions:

- 1) *Can depositional processes be recorded using oceanographic instrumentation and linked to the corresponding sedimentary deposits?*
- 2) *Is the sedimentary record biased towards certain processes operating at specific timeframes?*

These questions will be answered by characterising the sedimentology and ichnology of the mouth of the Waikato River, and using oceanographic data to build process-response linkages. This thesis is written in “paper format” and is divided into three chapters. Chapter one provides background information on sedimentology and

ichnology of shallow marine and river mouth environments. Chapter one also presents a review on the current state of knowledge regarding the Waikato River. Chapter two presents the study area, methods employed, and the research data collected in this study. Lastly, chapter three summarises the findings of this thesis, and how they address the research questions.

## **1.2 Background Literature**

### **1.2.1 Facies Models**

Facies models have long been under development and refinement. As noted by Dalrymple (2010a), the term facies was first created by Gressly (1838), to describe the lithology and paleontology of a stratigraphic unit. Although, today the term facies is used to describe a rock body that is different from those surrounding it, in regards to its lithology, and physical and biological structures (Dalrymple, 2010a). One of the first uses of facies models were to aid in predicting and identifying the distribution and arrangement of depositional units (e.g. Potter, 1959). The '*Facies Models*' books were first developed by Walker (1979), in which facies models were created and used for a range of depositional environments. The facies-analysis approach is in widespread use by sedimentary geologists to interpret the sedimentary record. For this reason, facies models have been further developed by Walker (1984), Walker and James (1992), Posamentier and Walker (2006), and James and Dalrymple (2010), to update the material and methods used, as hundreds of geologists across the decades have progressed the research on depositional processes and environments.

### **1.2.2 Coastal Depositional System Classification Based on the Sedimentary Record**

Coastal depositional environments are classified based on the dominant physical processes that affect the morphology of the shoreline shown in Figure 1.1. The relative influence of waves and tides are measured on the horizontal axis, and relative fluvial influence on the vertical axis.

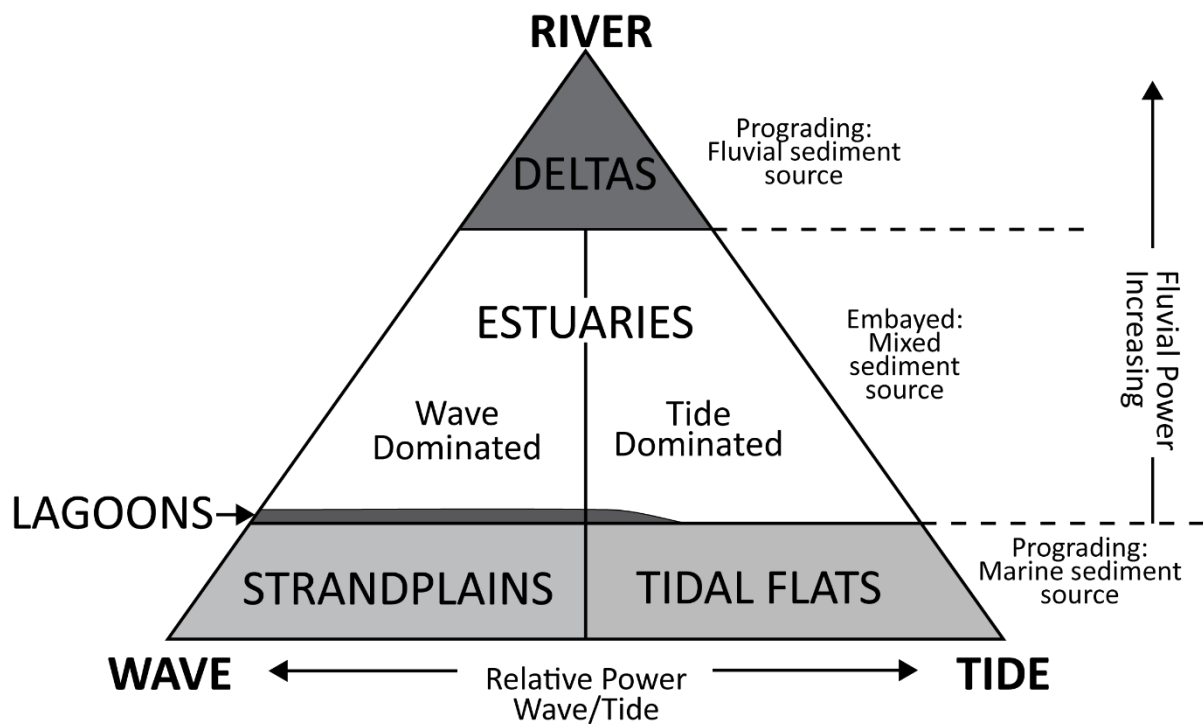


Figure 1.1: Ternary diagram of coastal classification modified from Boyd *et al.* (1992) after Dalrymple *et al.* (1992).

In this research, three coastal environments are of interest; strandplain shorefaces, deltas, and estuaries. Strandplains are not influenced by rivers and are dominated by wave energy, whereas estuaries and deltas form at rivers mouths as a result of interactions between long term sediment supply (to the basin) and available accommodation space. If the rate of sediment supply is greater than the creation of accommodation space, a delta forms and there is net regression of the shoreline. By contrast, if the creation of accommodation space is greater than the rate of sediment supply, then an estuary forms and there is net transgression of the shoreline (Boyd *et al.*, 1992; Prothero & Schwab, 2004). As indicated by the top triangle of Figure 1.1, deltas are dominated by river power, whereas, estuaries form the centre trapezoidal area, on wave- or tide-dominated shorelines (Boyd *et al.*, 1992; Dalrymple *et al.*, 1992). A wave-dominated coast is described as “*those where wave action causes significant sediment transport and predominates over the effect of tides*” (Heward, 1981, p. 223), and a similar definition can be applied for tide-dominated coasts.

The first depositional environment of interest, strandplains, are shore-parallel sand bodies containing beaches and dunes (Boyd *et al.*, 1992). The strandplain shoreface is permanently subaqueous, comprising the zone between mean low tide and the lower

limit of fair-weather wave base (approximately 10 m deep), and the foreshore is an intertidal zone above the low tide mark (Figure 1.2).

There are three sections of the shoreface, each of which contain different physical and biogenic sedimentary characteristics: upper, middle, and lower. The upper shoreface is a high energy environment with breaking waves and offshore-directed currents (Figure 1.2). The upper shoreface comprises well sorted cross-bedded sand, shore elongated sand bars, and trace fossils attributed to the *Skolithos* Ichnofacies (MacEachern *et al.*, 2010; Plint, 2010). The foreshore is dominated by wave action and comprises planar laminated sands, and trace fossil assemblages of the *Skolithos* Ichnofacies (MacEachern *et al.*, 2010; Plint, 2010).

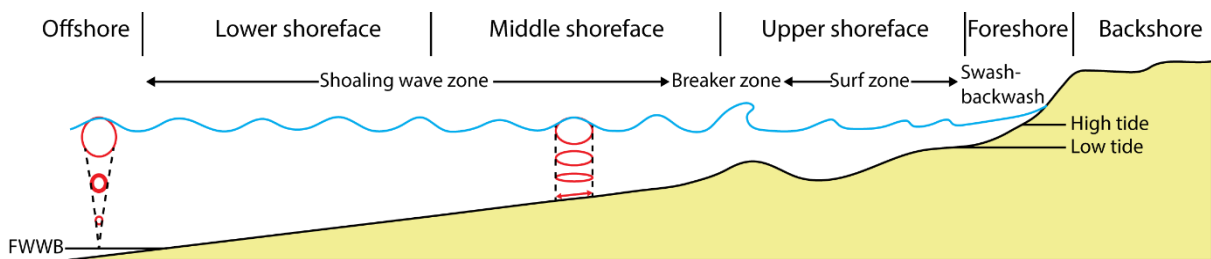


Figure 1.2: Schematic of the shoreface and beach profile. Showing the shoreface depositional environments (zones), wave zones, fair-weather wave base (FWWB), and low tide and high tide marks. Modified from Dashtgard *et al.* (2012).

Deposition on the shoreface is also affected by storm events. These storm deposits, known as tempestites, consist of swaley cross-stratified (SCS) and hummocky cross-stratified (HCS) structures (Dumas & Arnott, 2006; Plint, 2010). Storms do not represent the ambient conditions within the environment, although can be used to infer the intensity or frequency of storm activity, or both, based on the relative amount of tempestites present. Hence, shorefaces can be described as either strongly storm-dominated, comprising almost entirely storm beds; moderately storm-dominated, comprising laminated-to-burrowed sequences (lam-scam); or, weakly storm-influenced with bioturbated fair-weather deposits and little to no preserved tempestites (Plint, 2010).

With increasing proximity to river mouths, shorefaces pass along strike into deltas and estuaries (Figure 1.3). The influence of freshwater and river-derived sediment increases the complexity of processes and deposits of deltas and estuaries.

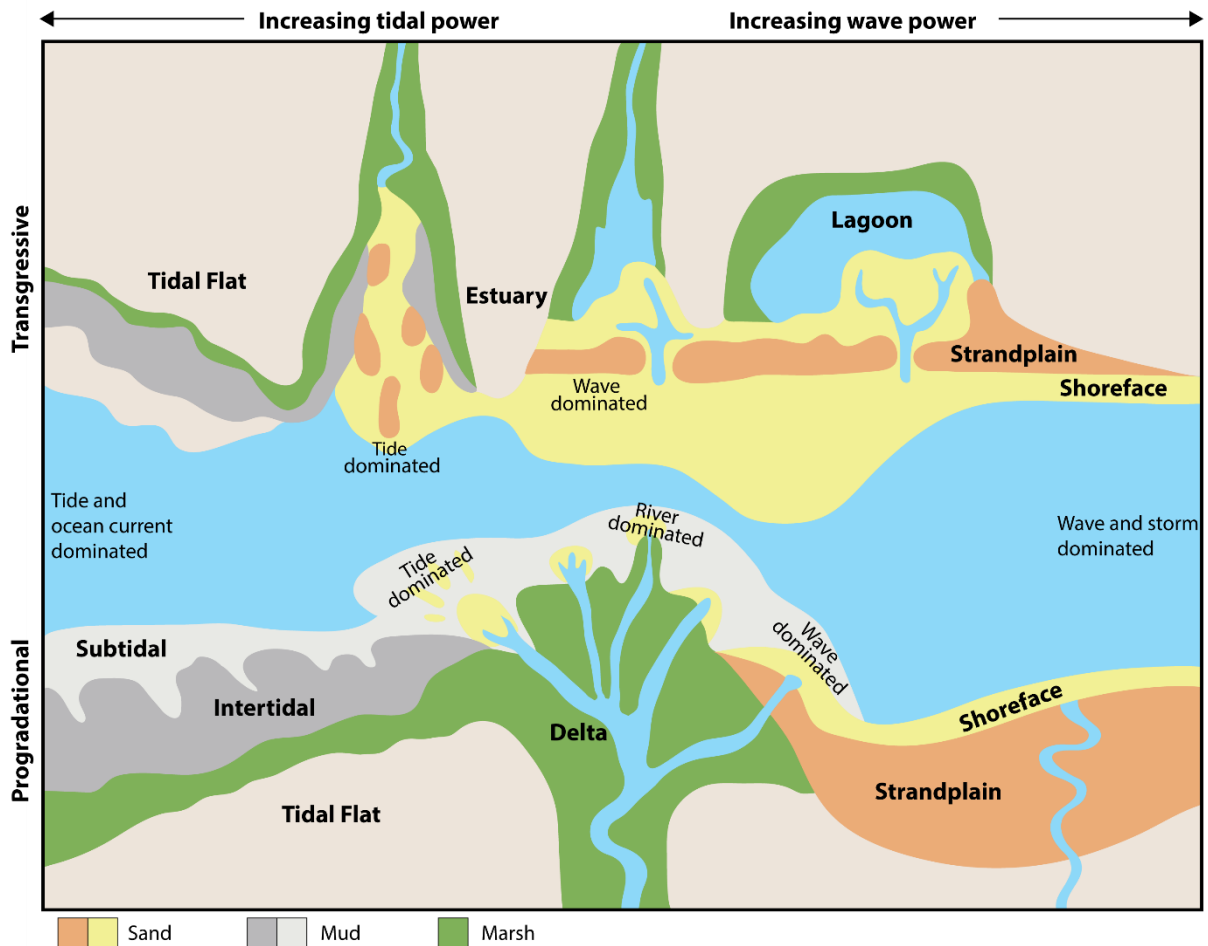


Figure 1.3: Coastal depositional environment classification on both prograding and transgressive coasts. Showing increasing tidal power towards the left, and increasing wave power to the right. Modified from Boyd (2010) after Boyd *et al.* (1992).

Deltas are characteristic of prograding shorelines (Figure 1.3), where their deposits build out over (geological) time, forming progradational successions where more proximal deposits overlie distal deposits (Dalrymple & Choi, 2007). The morphology and characteristics of deltas depend on the interactions between waves, storms, tides and fluvial input (Boyd *et al.*, 1992). Galloway (1975) developed a morphological classification of deltas based on the distribution and shape of sand bodies at the delta front. Galloway's classification defines deltas as either river-, wave- or tide-dominated, although, most deltas are of mixed-influence.

The delta front is controlled by marine processes (waves and tides), and the relative density of fluvial input (combined freshwater and sediment) with respect to the water in the receiving basin. Fluvial input is either more dense (hypopycnal), less dense (hypopycnal), or of equal density (homopycnal) to the receiving basin water. Hypopycnal flow is usually the result of a high suspended sediment load ( $36-43 \text{ kg m}^{-3}$ )

and can occur during high river flow conditions such as in floods, or from small- to medium-size rivers (with annual discharge of  $380\text{--}460\text{ m}^3\text{ s}^{-1}$ ), particularly if draining steep slopes (Mulder & Syvitski, 1995; Mulder *et al.*, 2003). Hypopycnal conditions are most common at the mouths of rivers flowing into marine basins, where the river flows at the water's surface, depositing fine sediment from suspension to form very gentle delta front slopes (Mulder *et al.*, 2003). Lastly, homopycnal flow is most common in lacustrine deltas, or coarse-grained marine deltas. The river flow rapidly decelerates and deposits sediment to form discrete topset, foreset and bottomset beds (i.e., "Gilbert deltas"; Mulder *et al.*, 2003).

From a geographical perspective, deltas can be divided into three main zones: delta plain, delta front, prodelta (Bhattacharya, 2010). The delta plain is relatively flat and is the zone including the permanently subaerial (exposed) through to the low tide mark (intertidal). The delta front is the deltaic equivalent to the strandplain shoreface, being the zone between low tide and the lower limit of fair-weather wave base. The delta front is a seaward dipping shoreface or bar-front that is sand-, or gravel-dominated, and may contain mud if it is tide-influenced. The prodelta is situated the furthest offshore, with lower energy, and is mud-dominated. Thus, vertical facies successions in deltas are characterised by coarsening (or sanding) upwards from the mud-dominated prodelta to sand-dominated delta front and delta plain.

In contrast, estuaries reflect either net transgression (by relative sea level rise) or low sediment supply to the coast, and so have retrogradational stacking patterns as they are infilled with the creation of accommodation space (Dalrymple *et al.*, 1992; Dalrymple & Choi, 2007). An estuary is defined sedimentologically in terms of sedimentary facies distributions, and is defined by Dalrymple *et al.* (1992) as:

*The seaward portion of a drowned valley system which receives sediment from both fluvial and marine sources and which contains facies influenced by tide, wave and fluvial processes. The estuary is considered to extend from the landward limit of tidal facies at its head to the seaward limit of coastal facies at its mouth* (p. 1132).

Similar to deltas, estuaries are morphologically classified based on the dominant processes controlling sedimentation, with either wave- or tide-dominated end members (Dalrymple *et al.*, 1992). Fluvial influence is also a major characterisation factor,

although Dalrymple *et al.* (1992) state that including a river-dominated category is unnecessary as the influence of a river does not alter the morphology of an estuary, only the rate at which the estuary infills. However, Cooper (1993) argues that a river-dominated classification should exist, where, fluvial discharge dominates over wave and tidal influence. Cooper (1993) describes that the morphology of a river-dominated estuary is characterised by shallow water levels, and that the fluvial influence extends to the mouth of the estuary, influencing the sedimentary record.

The hydrodynamics of FMT areas are exceedingly complex due to the interactions between fluvial and marine processes (Dalrymple & Choi, 2007). The energy levels in an estuary, are a sum of the tide, waves and river, and these vary spatially and temporally. Dalrymple *et al.* (1992) describe three main zones of an estuary based on relative energy (Figure 1.4A): (1) a river-dominated inner zone; (2) a relatively low-energy central zone, where river currents and marine energy (generally tidal currents) are approximately balanced; and (3) a marine-dominated (by waves or tides) outer zone. These zones correspond to net bedload transport direction and influence deposition of sediments and corresponding sedimentary facies (Figure 1.4B & C; Dalrymple *et al.*, 1992).

Barriers (Figures 1.3 & 1.4) also form during transgression and may intersect estuary mouths along shore, separating it from the marine environment. Boyd *et al.* (1992) define a barrier as an “*elongate, shore-parallel sand body which may consist of a number of sandy units including beach, dunes, tidal deltas, washovers, and spits*” (p.142).



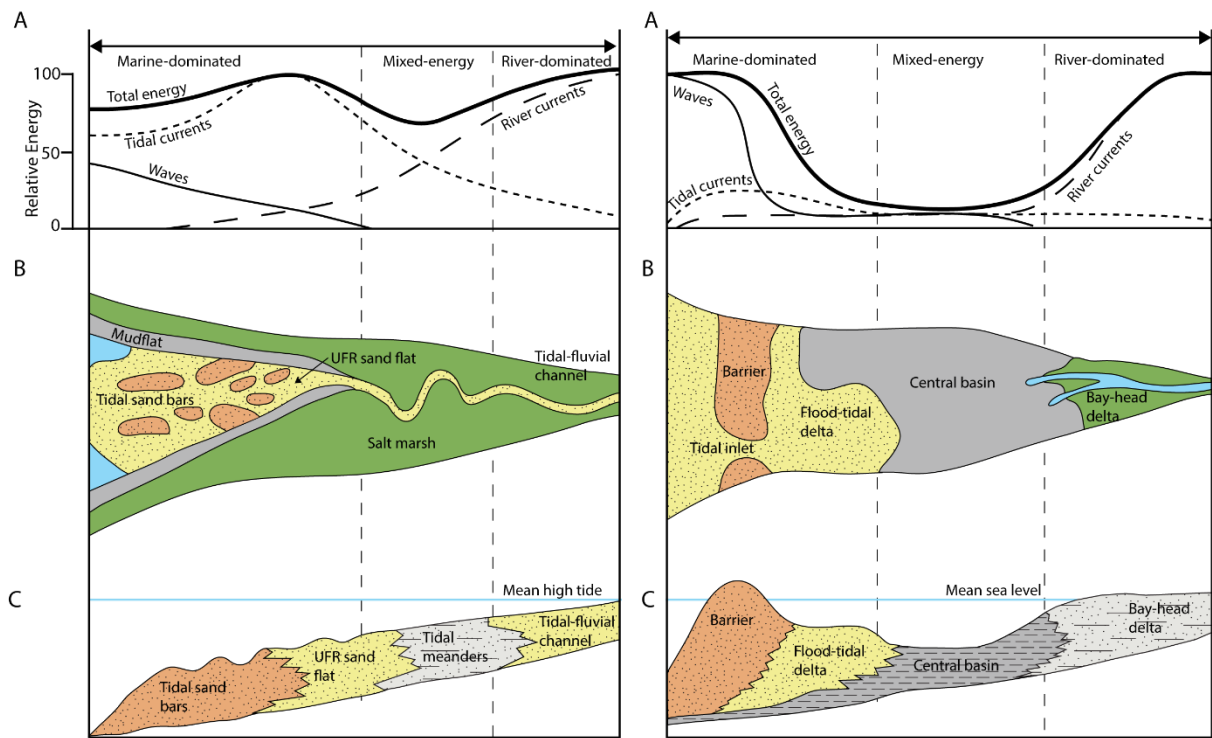


Figure 1.4: (A) energy distribution, (B) morphology, and (C) longitudinal sedimentary facies, in a tide-dominated estuary (left) and wave-dominated estuary (right) modified after Dalrymple *et al.* (1992).

### 1.2.3 Burrowing Infauna

Ichthyology is the study of biogenic structures produced by organisms burrowing the sediment they inhabit. Bioturbation disrupts the sediment, leaving behind structures such as tracks, trails, and burrows (MacEachern *et al.*, 2010). Neoichthyology is the study of modern trace-making organisms, and the present-day relationship between traces and the sediment (MacEachern *et al.*, 2010). Burrowing organisms are very sensitive to their environment, and their traces reflect their behaviours, and provide information about the physical and chemical environmental conditions that physical sedimentology cannot (e.g. salinity, temperature and oxygen; MacEachern *et al.*, 2010).

Ichnofacies are recurring trace fossil assemblages that are characteristic of animal-sediment responses to the depositional environment (Figure 1.5; MacEachern *et al.*, 2010). Traces typical to FMT zones are formed by marine organisms who have evolved to withstand lowered and variable salinity (i.e., brackish-water conditions; Dalrymple & Choi, 2007; La Croix *et al.*, 2015). Environmental conditions in the FMT are biologically stressful due to freshwater input, reducing salinity, subaerial exposure, daily and seasonal energy and temperature changes, and often high water-turbidity and

variable sedimentation rates. Hence, most organisms burrow into the substrate where conditions are generally more stable (Dalrymple & Choi, 2007). Burrows in brackish-water settings are generally small and the population density is variable, with patchy distributions of areas of high densities of a single species, and an overall reduction in trace diversity (Dalrymple & Choi, 2007; Gingras *et al.*, 2011). The trace-making organisms are small and create simple structures of which common structures include *Skolithos*, *Thalassinoides*, *Arenicolites*, *Cylindrichnus*, *Gyrolithes*, and *Planolites* (Figure 1.5; Gingras *et al.*, 2011).

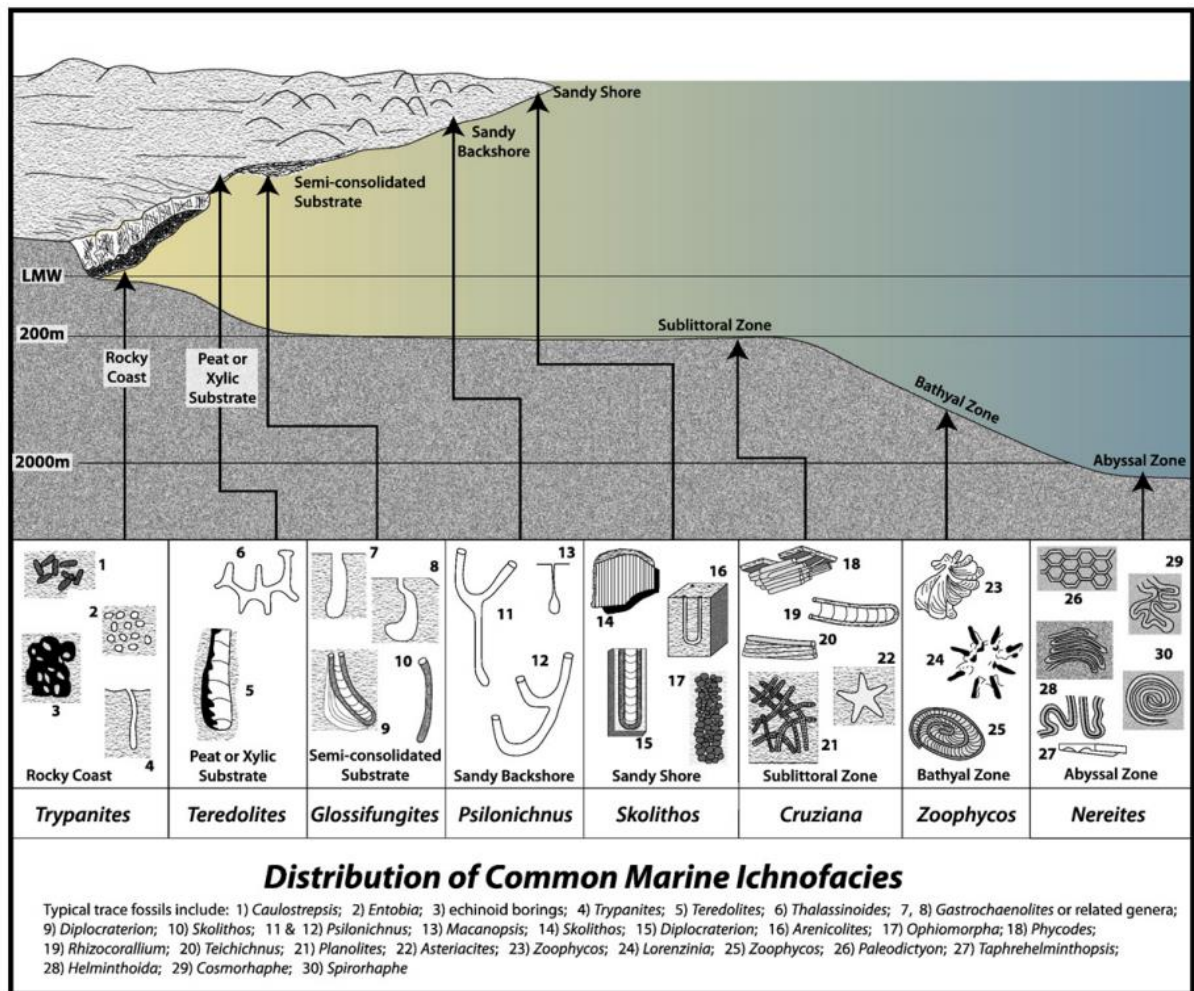


Figure 1.5: Distribution of marine ichnofacies, and their common trace fossils and trace fossil assemblages. From Gingras *et al.* (2011), after Seilacher (1967).

## **1.3 Regional Context of the Waikato River Catchment**

### **1.3.1 The Waikato River**

At 425 km long, the Waikato River, is the longest river in New Zealand and drains a catchment area of 14, 260 km<sup>2</sup> (Manville, 2002; Williams, 2017). The headwaters of the Waikato are located at Mt Ruapehu in the central region of the North Island. Streams originate at the mountain and first join with the Tongariro River before flowing in to Lake Taupo, the largest freshwater lake in the Southern Hemisphere (Brown, 2010; Williams, 2017). From the northern outlet of Lake Taupo, the Waikato River proper flows north through the Waikato Region, debouching at Port Waikato into the Tasman Sea (Figure 1.6). The Waipa River is the largest tributary, which drains a catchment area of 3, 060 km<sup>2</sup> and joins the Waikato River at Taupiri Gap in Ngaruawahia (Manville, 2002; Williams, 2017).

Mean annual river discharge of the Waikato River is approximately 600 m<sup>3</sup> s<sup>-1</sup> (Jones & Hamilton, 2014). The Waipa River contributes approximately 20% of the total river flow (90 m<sup>3</sup> s<sup>-1</sup>), and because it has not been dammed, high flows occur in the Lower Waikato River (Fenton, 1989; Williams, 2017).

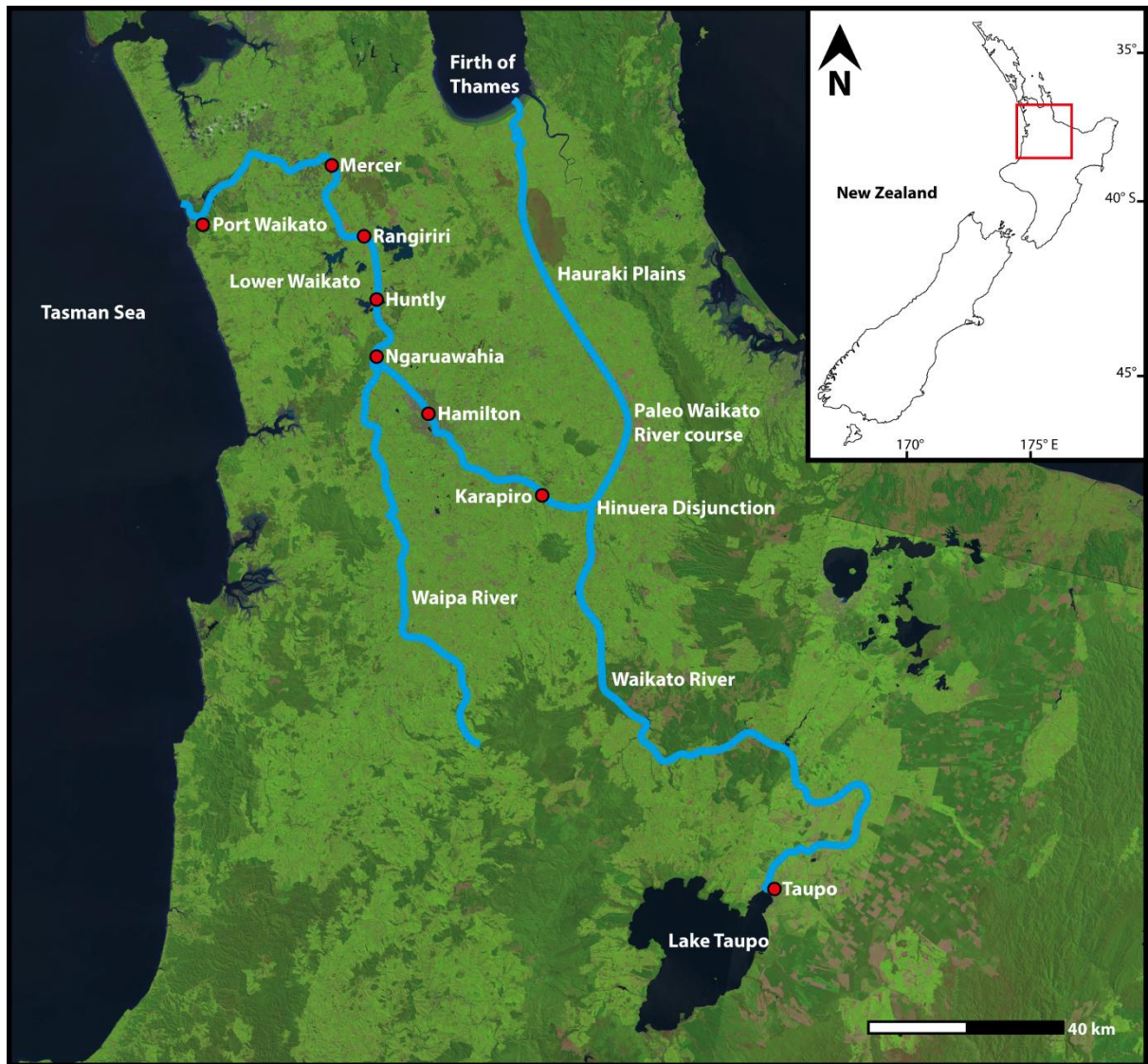


Figure 1.6: Waikato River and Waipa River in central North Island, New Zealand. Paleo Waikato River course adapted from Manville & Wilson (2004). (Image Source: USGS).

### 1.3.2 Geological History of the Waikato River

Volcanic activity in the Taupo Volcanic Zone (TVZ) has had a strong influence on the course of the Waikato River throughout its history. Prior to the Oruanui eruption ( $25,360 \pm 160$  BP; Vandergoes *et al.*, 2013), the ancestral Waikato River flowed from ancestral Lake Huka in the centre of the North Island, north through the Hauraki Plains, towards the Firth of Thames (Figure 1.6; McCraw, 2011). The ancestral Waikato River debouched into the Pacific Ocean, seaward of Great Barrier Island, as sea level was more than 100 m lower than present (Manville & Wilson, 2004; Williams, 2017), whereas the Waipa River originated at headwaters in the greywacke rocks of the Rangitoto Range and continued down to its mouth at Port Waikato (Williams, 2017). The Taupo Volcano's Oruanui eruption destroyed Lake Huka and formed the northern

half of Lake Taupo. Eruption debris blocked the outlet, causing the Lake's water level to rise, until erosion of the dam led to overflow and flooding of approximately 80 km<sup>3</sup> of water into the Waikato River (McCraw, 2011). The floodwaters carried large amounts of the volcanic sediment, and the Waikato River became a wide and shallow braided river (Manville & Wilson, 2004). At the Hinuera Disjunction, the Waikato River overtopped its divider with the Maungatautari gorge, to form its modern course through the Hamilton Basin towards Port Waikato (Manville & Wilson, 2004; McCraw, 2011). Volcanogenic alluvium, known as the Hinuera Formation, was deposited from the braided river in both the Hamilton Basin and Hauraki Plains, and comprises rhyolitic, pumiceous and ignimbritic sands and gravels (Hume *et al.*, 1975; Manville & Wilson, 2004). It is not known, whether the river suddenly avulsed towards the Hamilton Basin, or flowed along both courses simultaneously, with eventual abandonment of the channel through the Hauraki Plains, and establishment of its modern single-channel course through the Hamilton Basin to adjoin to the Waipa River at Ngaruawahia and debouch at Port Waikato (Manville & Wilson, 2004; McCraw, 2011).

The later, A.D. 232 (Hogg *et al.*, 2012) eruption from Lake Taupo produced a dam of pyroclastic material, blocking the Waikato River entirely (Manville, 2002). Dam collapse resulted in flooding of the lower catchment, carrying large volumes of volcanoclastic sediment, predominantly comprising pumice (Wo, 1994). These pumiceous deposits are the Taupo Pumice Alluvium, approximately 30 m thick, and make up the lowermost terraces in the Hamilton Basin (Lowe, 2010).

### **1.3.3 Anthropogenic Impacts on the Waikato River**

Settlement by Māori (~1280 AD) and Europeans (1642 AD) in New Zealand (Lowe, 2008), altered the Waikato River catchment area and disturbed its flow characteristics, primarily as a result of deforestation. Prior to human settlement, 85-90% of New Zealand was covered by native vegetation (Glade, 2003). Significant areas of land were deforested which resulted in an overall increase in river discharge. Wetlands and shallow lakes on the flood plain of the Lower Waikato River were drained, resulting in the larger flood flows due to loss of water storage (EW, 2008). The Lower Waikato Flood Protection Scheme was developed in the late 1950's to combat the increase in flood flow in the Lower Waikato River (EW, 2008). The scheme increased water

storage in the catchment by retaining Lake Waikare and the Whangamarino wetland, creating stopbanks, pump stations and flood gates, and narrowing the lower river (Fenton, 1989; EW, 2008).

Currently, approximately  $2,900 \text{ m}^3 \text{ s}^{-1}$  of water is allocated for use in the Waikato catchment (Brown, 2010). Almost all of this water is recycled back into the river, with approximately  $70 \text{ m}^3 \text{ s}^{-1}$  being consumed (e.g. for irrigation and city supply; Brown, 2010).

### **1.3.3.1 Hydroelectric Dams**

In the early- to mid-twentieth century, New Zealand began to develop hydroelectric power. Eight dams were constructed along the Waikato River between the 1930's and 1960's, from Lake Taupo through to Karapiro (Figure 1.6; EW, 2008).

Artificial lakes in the North Island trap 0.62 Mt of sediment per year, a large proportion of which is from hydropower reservoirs on the Waikato River (Hicks *et al.*, 2019).

Damming of the Waikato River has thus decreased sediment supply to the Lower Waikato, which has caused degradation of the river bed (Fenton, 1989).

### **1.3.3.2 Sand Extraction for Mining**

Sand extraction has been occurring in the Lower Waikato since the 1950's (Fenton, 1989; EW, 2008). The total volume of sand extracted from the Waikato River since the early 1950's to late 1980's was  $13 \times 10^6 \text{ m}^3$  (Fenton, 1989). Currently 1.2 Mt of sand is extracted from the Waikato North Head Mine Site per year (NZ Steel, 2020). Sand extraction has resulted in lower elevations of the river bed and water height, draining of wetlands, lowered lake levels adjacent to the river, and flooding in the region (Fenton, 1989; EW, 2008).

### **1.3.4 Weather and Climatic Setting**

Rainfall distribution in New Zealand is predominantly controlled by topography and the prevailing westerly winds (Brown, 2010). The greatest amount of rainfall in the Waikato River catchment occurs on the slopes of Mt Ruapehu with an annual average of

3, 200 mm (EW, 2008). The catchment experiences a mean annual rainfall of 1, 150 mm and 1, 120 mm at the Ruakura and Taupo recording stations, respectively (Brown, 2010). Long term rainfall trends are controlled by El Niño-Southern Oscillation cycles, as well as seasonal patterns, in which the largest amount of rain is experienced in July (winter) and the least amount of rain in February (summer) (Brown, 2010).

New Zealand is classified in the warm temperate, fully humid climate zone, Cfb, under the Köppen Climate Classification. New Zealand typically has no dry periods year-round, and has a warm summer, and for at least four months of the year, the temperature has a threshold value of 10 °C (Kottek *et al.*, 2006).

### **1.3.5 Sub-surface Geology of the Waikato River Catchment**

Underlying geology influences river flow through its varying infiltration characteristics (Brown, 2010). The catchment area of the Waikato River between Taupo and Karapiro is mostly composed of volcanic material such as pumice, ignimbrite, and volcanic ash (Brown, 2010). From Karapiro to Ngaruawahia the geology comprises pumiceous sands and gravel with some clay and peat (Fenton, 1989). From Ngaruawahia through to Port Waikato (the Lower Waikato zone), the underlying geology is dominated by Late Eocene-Oligocene sediments (Te Kuiti Group) in the west (Brown, 2010; Fenton, 1989), with peat and alluvial deposits in the low-lying areas (Fenton, 1989). Rainfall rapidly infiltrates volcanic material adding to groundwater stores, sustaining base flow, and reducing flood flows (Brown, 2010). Conversely, the Oligocene sediments have a smaller infiltration rate, making the Lower Waikato River more sensitive to rainfall, resulting in a lower base flow (especially in periods of low rainfall), and larger flood flows following periods of high rainfall (e.g. Figure 1.7; Fenton, 1989; Brown, 2010).

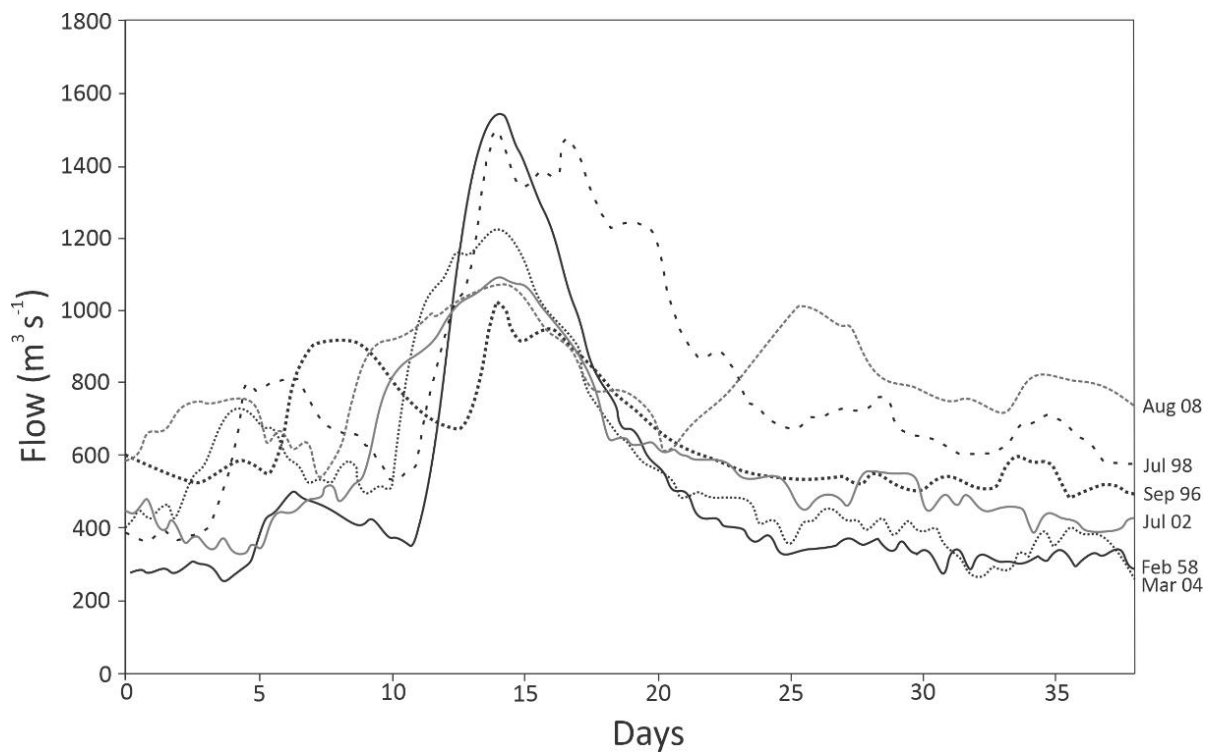


Figure 1.7: Hydrographs of the Waikato River's six largest flood peaks at Ngaruawahia (1958-2008). Modified from Brown (2010) after Mighty River Power (2001).

### 1.3.6 Sediment in the Waikato River

Suspended sediment is fine-grained sediment (silt and clay) that is held in suspension, and bedload is coarser-grained sediment that is not held in suspension and travels along the riverbed. Erosion of sediment from a catchment is the greatest source of suspended sediment to a river (Hughes, 2015), and disturbance of catchments by humans has likely increased the amount of suspended sediments in New Zealand rivers (Hughes, 2015). The main transport methods of sediment to the Waikato River are, hillslope erosion, mass movement and stream bank erosion (Hughes, 2015).

Bedload sediment in the Waikato River comprises poorly sorted coarse-grained pumiceous sands and gravels (Fenton, 1989; Wo, 1994). Bedload sedimentation rate in the Lower Waikato river bed is estimated to be  $2.8 \text{ mm yr}^{-1}$  since the Taupo eruptions (Fenton, 1989). Gravel dominates the river bed up to approximately 100 km from the river mouth, after which sand dominates (Wo, 1994). Bedload transport was estimated to be  $180,000 \text{ m}^3 \text{ yr}^{-1}$  between 1975 and 1989, which has most likely decreased as a result of sediment retention at Karapiro Dam (Fenton, 1989).



Environment Waikato (EW, 2008) studied the suspended sediment in the Waikato River and identified that the catchment area mostly comprises pasture (62%), planted forest (19%), and indigenous forest (10%). This study showed that the land under pasture is more susceptible to erosion than forested land. Exposed soil comprises 1% of the catchment and easily erodes during rainfall events. Approximately 40% of the total catchment area is susceptible to erosion (EW, 2008). Measured rates of erosion in the Lower Waikato showed some variability between 7-30 tonnes per hectare of topsoil on cropping land. Not all suspended sediment reaches the river mouth; some gets stored within the catchments, for example by floodplain or in-channel deposition, although there is insufficient data to quantify this (Hughes, 2015).

Sediment yield is the mass of sediment transported past a marker point in a river per unit time. Variations in sediment yield are mostly a factor of rainfall in the river catchment and corresponding changes in runoff, mean slope, land-cover and smaller factors including the underlying geology (Hughes, 2015). The mean annual suspended sediment yield of the Waikato River at Rangiriri, and in the Waipa River at Whatawhata are  $21 \text{ t km}^{-2} \text{ y}^{-1}$  and  $60 \text{ t km}^{-2} \text{ y}^{-1}$ , respectively (Hoyle *et al.*, 2012). More recently, Hicks *et al.* (2019) developed a hydrological model to estimate the suspended sediment load at the Waikato River mouth as  $0.38 \text{ Mt yr}^{-1}$ .

## **1.4 Geology of the Port Waikato Region**

The Port Waikato region overlies a sequence of Jurassic, Late Eocene-Oligocene strata, and unconsolidated Pleistocene sands (Figure 1.8; Barker *et al.*, 2016). Jurassic strata at Port Waikato include those of the Murihiku Terrane: Upper Puti Siltstone, Coleman Conglomerate, Waikorea Siltstone, and the Huriwai Formation (Challinor, 2001; Barker *et al.*, 2016). The Jurassic strata were folded between 142-99 Ma to form the Kawhia Syncline that plunges north-north-west, and is bordered by the Kawaroa Anticline to the west (Figure 1.8; Challinor, 2001; Barker *et al.*, 2016). The Waikato Fault trends north-northeast, downthrowing to the north, with an offset of 2.7 km at Port Waikato (Rodgers & Grant-Mackie, 1978). The Oligocene Te Kuiti Group unconformably overlies and is faulted against Jurassic strata, both of which are overlain by Early Miocene Waitemata Group and ultimately unconformably overlain by Pleistocene sands (Tripathi & Kamp, 2008; Kamp *et al.*, 2014; Barker *et al.*, 2016). The Te Kuiti Group comprises limestones, sandstones and conglomerates, formed by deposited marine sediment as

New Zealand was inundated by marine water, approximately 40 Ma (Kamp *et al.*, 2014). The Te Kuiti Group has since been uplifted, tilted approximately 4°, and eroded (Barker *et al.*, 2016). Cretaceous and Eocene rocks are not present at Port Waikato, due to an unconformity separating Jurassic strata from the Te Kuiti Group (Barker *et al.*, 2016).

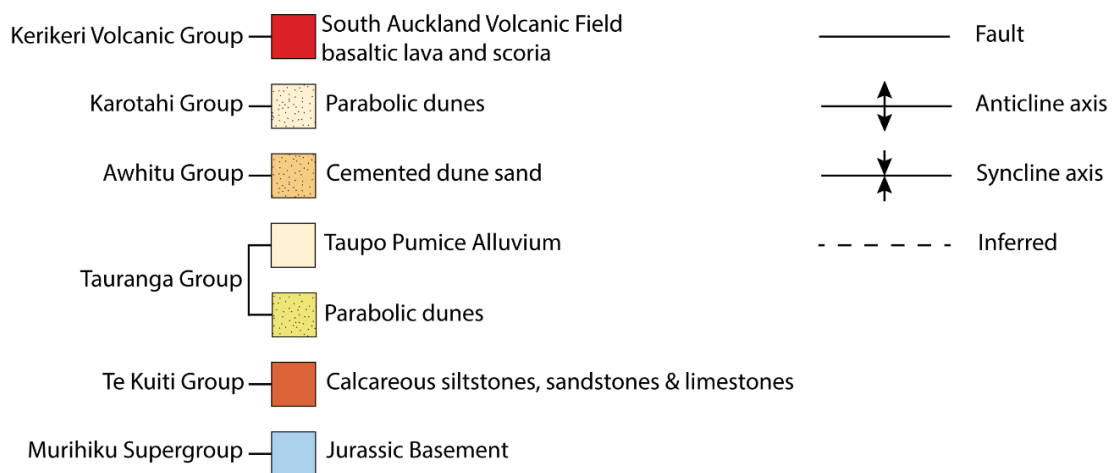
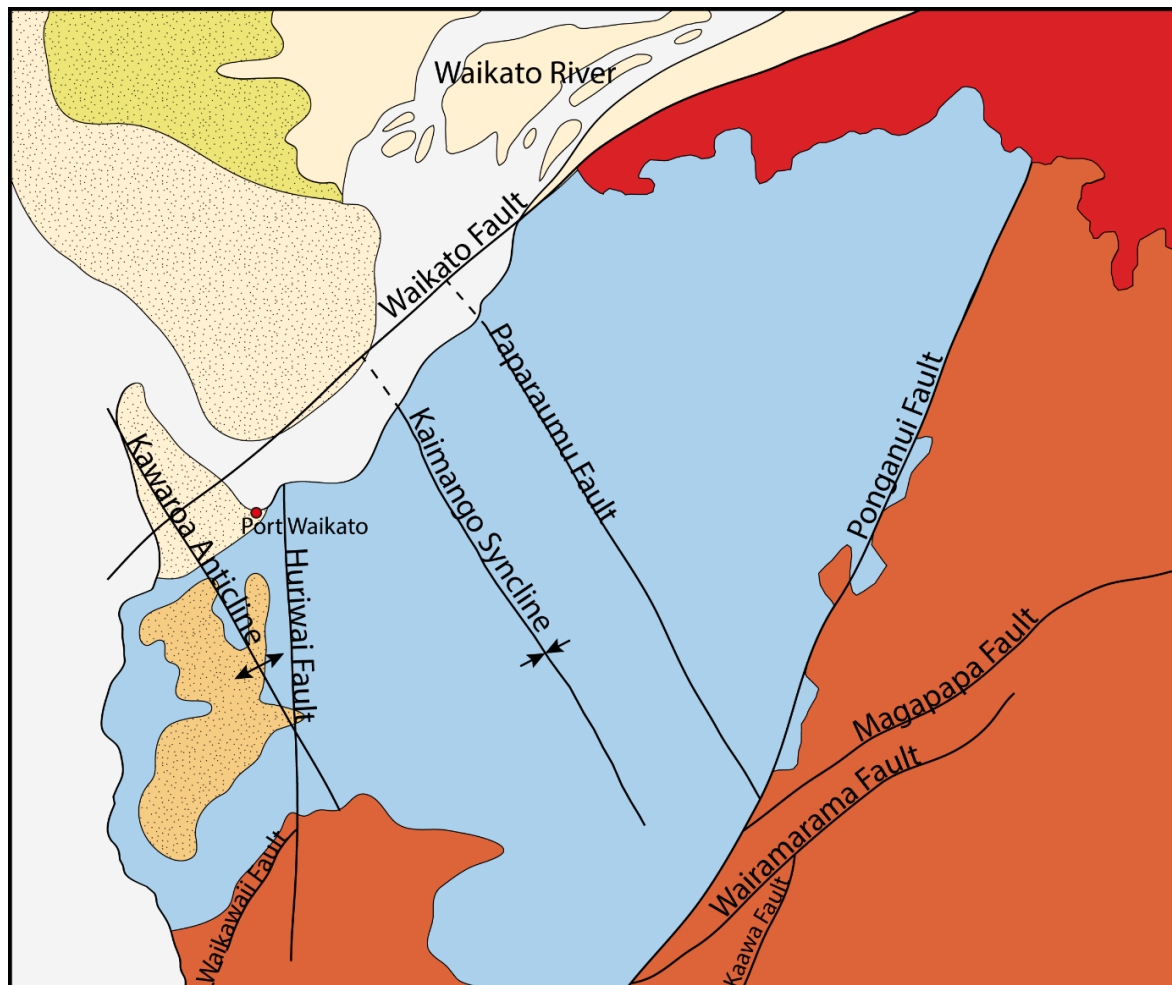


Figure 1.8: Geology and structural features of the Port Waikato region. Modified after Barker *et al.* (2016) and Edbrooke (2005).

## 1.5 The Coastal Setting of Port Waikato

### 1.5.1 Estuarine Classification in New Zealand

Pritchard (1967) developed a widely used oceanographic definition of an estuary as “*a semi-enclosed coastal body of water in which sea water is measurably diluted by fresh water derived from land drainage*”.

Estuarine classification in New Zealand is based on the oceanographic definition. Hume *et al.* (2007) created an estuarine classification system in New Zealand based on their definition of an estuary - a modification of Pritchard's (1967) definition. Thus, Hume *et al.* (2007) define an estuary as,

*a partially enclosed coastal body of water that is either permanently or periodically open to the sea in which the aquatic ecosystem is affected by the physical and chemical characteristics of both runoff from the land and inflow from the sea* (p. 908).

Hume *et al.* (2007) used this definition to classify every estuary in New Zealand; the Estuary Environment Classification (EEC) system. The EEC defines eight types of estuaries based on the following four levels: (1) regional climate and oceanic processes, (2) hydrodynamics (function of tides, freshwater discharge and ocean waves), (3) catchment processes (function of geology and landcover), and (4) local hydrodynamics in sub estuary (sediment deposition and erosion). Most of the estuaries on the west coast of the North Island are bar-built estuaries, with a sand bar or barrier-island, protecting the main estuary from the ocean (Mead & Moores, 2005).

The Waikato River mouth is classified under the EEC as a Category C estuary, a tidal river mouth (Hume *et al.*, 2007). Hume *et al.* (2007) describe that a tidal river mouth is dominated by river flow, where the volume of river flow is larger than the tidal volume. The main river channel is well flushed of saline water, although, a salt wedge can develop in which the freshwater discharging from the river flows above the saline seawater, representing a hypopycnal flow (Hume *et al.*, 2007).

## 1.5.2 Morphology of the Waikato River Mouth

Downstream of Mercer, the Waikato River develops into a meandering river, and the main channel bifurcates into several smaller channels (anastomosing) for approximately 10 km before entering the bay head delta. The bay head delta comprises elongated deposits, and is the widest part of the river mouth area, located approximately 6 km from the tidal inlet and extending 9 km inland (Jones & Hamilton, 2014).

Seaward of the bay head delta, is a central basin along a major river bend before a sand spit as the river turns northward (Figure 1.9). Sand spits and tidal inlets are common features on wave-dominated shorelines. The spit shelters the water behind from waves, helping to form a lower-energy central basin (Figures 1.4 & 1.9; Dalrymple *et al.*, 1992; Hume *et al.*, 1992). Sediments forming the sand spit at Port Waikato are derived from the south, as the littoral drift pattern (i.e. longshore current) travels north (Hume *et al.*, 1992). The intertidal portion of the sand spit is incised by smaller channels from the river, and on occasion cut all the way through. The entire tidal prism is forced to pass through the inlet, and so strong currents pass through it. Often in estuaries, tidal deltas form on either side of a tidal inlet by waves depositing sand in the main channel which is then redistributed by the tidal currents (Masselink *et al.*, 2011). The ebb (outgoing) currents transport sediment seaward to form an ebb-tidal delta on the seaward side of the inlet, and the flood currents transport the sediment landward to form a flood-tidal delta on the landward side of the inlet. However, at the Waikato River mouth, there are no ebb- or flood-tidal deltas present.

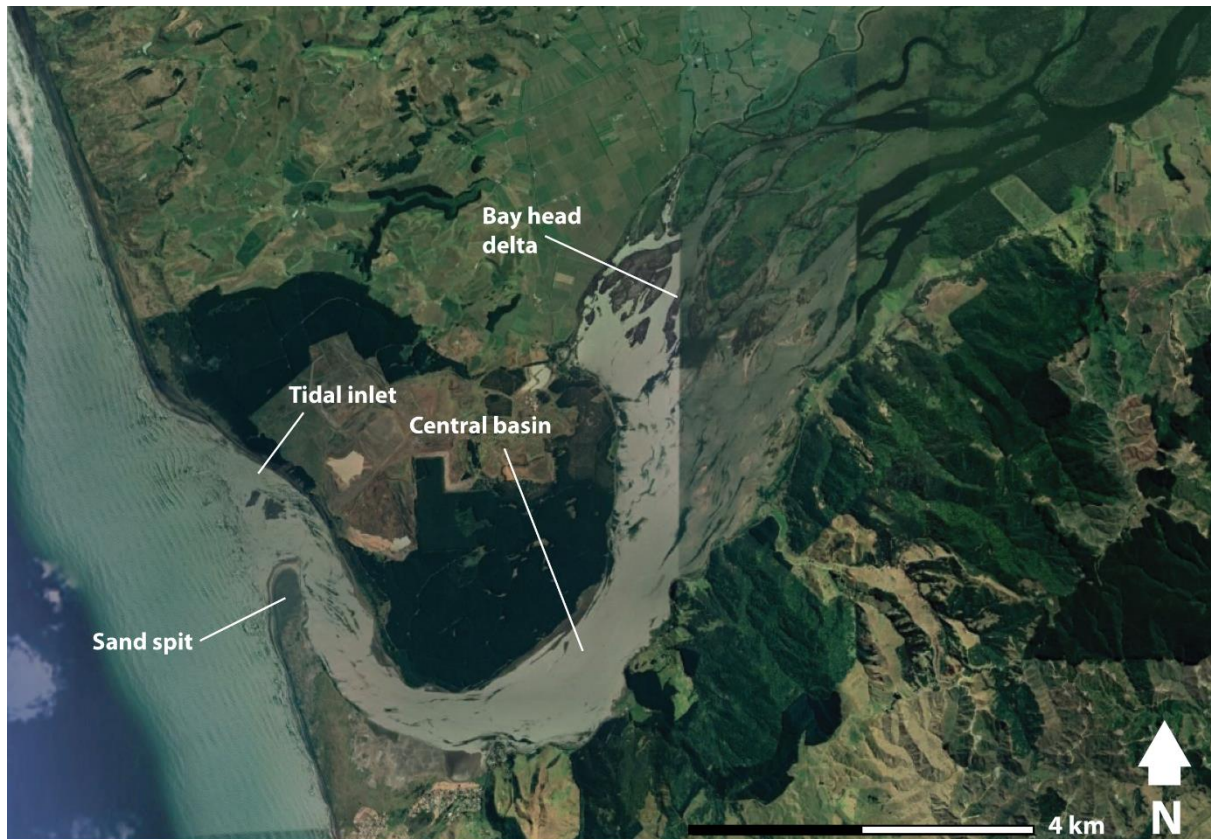


Figure 1.9: Morphological features of the Waikato River mouth. (Image Source: Google Earth, 2019).

### 1.5.3 Tides in Estuaries

Tides have the largest influence in the outer zone of an estuary. Tides are mostly controlled by gravitational and centrifugal forces caused by the moon and sun, thus there are two ‘tidal waves’ on the earth (Dalrymple, 2010b; Pinet, 2019). The flood tide is the incoming tidal wave, and increases water level, whereas the ebb tide is the outgoing tidal wave, and decreases water level (Dalrymple, 2010b). Spring tides and neap tides occur twice monthly, and respectively occur when the moon, earth and sun are in line with one another, and when the sun and moon are at right angles to one another. Spring tides produce a larger tidal range (difference between low and high tide) and stronger tidal currents, whereas neap tides produce a smaller tidal range and weaker tidal currents (Pinet, 2019).

Tidal current speeds change systematically, both over a tidal cycle and spring-neap cycles, and have a strong influence on tidal sedimentation. Current speeds of the standing tidal wave are at their slowest at high and low tide, and so, fine-grained sediment (mud) is typically deposited from suspension (Dalrymple, 2010b). Current

speeds are greatest during the middle of each ebb and flood tide, and fine sediment is resuspended or prevented from settling, leaving coarser (sandy/silty) sediment on the sea floor. These coarse layers have no internal structures if deposited from suspension, or can be cross-laminated if deposited during peak current speeds (Dalrymple, 2010b). These coarse and fine layers form alternating horizontal laminations that show the cyclic and systematic changes in tidal current speed (Dalrymple, 2010b).

### **1.5.3.1 Measured Tides at Port Waikato**

New Zealand has semidiurnal tides, where the period for one tidal cycle is slightly longer than 12 hours (Dalrymple, 2010b; Pinet, 2019). Tidal ranges in New Zealand estuaries (including the Waikato River mouth) are generally between 2 and 4 metres (Jones & Hamilton, 2014), and so are classified as mesotidal (Dalrymple, 2010b; Pinet, 2019).

At the Waikato River mouth the flood tide propagates up the river channel. The tidal prism is measured as  $35.637 \times 10^6 \text{ m}^3$ , and so the tide has a minor effect at Mercer during periods of low river flow (Jones & Hamilton, 2014; Greer *et al.*, 2016). The tidal influence is based upon measured water level, and from this the tidal limit is determined to occur at Mercer (Figure 1.6; approximately 35 km from the river mouth).

Salt water transported into the river mouth from the Tasman Sea with the rising tide reaches approximately 10 km inland from the tidal inlet during neap tides, and 13 km during spring tides (Jones & Hamilton, 2014). Jones and Hamilton (2014), used a CTD (conductivity, temperature, depth) probe to identify a significant variability in temperature and salinity, both laterally and longitudinally. Jones and Hamilton (2014) identified a distinct salt water wedge in the lower estuary, whereas upstream, there is little vertical variability in salinity, indicating that the water is well mixed.

### **1.5.4 Estuarine Sedimentation**

The interactions between fluvial and marine processes in estuarine environments lead to complexity in sedimentation. Estuaries act as basins for terrigenous sediment delivered by rivers, and marine sediment by the waves and tides (Mead & Moores, 2005; Semeniuk, 2016). Tides are a steady source of energy for sediments entering and exiting

an estuary, whereas waves cause resuspension of fine sediment which can then be delivered into an estuary by the incoming tide (Mead & Moores, 2005; Hume *et al.*, 2007). The energy of a flow decreases in the direction that it is travelling, resulting in both the volume and grain size of sediment to decrease with distance from the source of the flow (Dalrymple & Choi, 2007). Therefore, in general, the coarsest grains are located in the upper and lower estuary, and the finest grains in the central basin at the bedload of convergence (Figure 1.4; Mead & Moores, 2005; Dalrymple & Choi, 2007). The turbidity maximum zone (TMZ), occurs where freshwater and saltwater mix. At the TMZ, the volume of suspended sediment is greatest, and sedimentation is increased by flocculation, where fine particles (silt and clay) combine to increase in size and settle out of the water column (Mead & Moores, 2005; Dalrymple & Choi, 2007).

There is no sedimentation data for the Waikato River mouth, although other west coast estuaries in the North Island have been investigated. For example, 50-80% of sediment input to Raglan harbour (south of Port Waikato) is terrigenous (catchment) derived sediment (Mead & Moores, 2005). Mead and Moores (2005) state that river catchments deliver the most amount of sediment to estuaries in the Waikato Region.

## **1.6 Summary**

Both the longest river in the country and draining the largest catchment area in New Zealand, the Waikato River's course towards Port Waikato first began approximately 26 ka, as a result of the collapse of a pyroclastic dam at Lake Taupo. The Waikato River catchment is underlain by volcanic and Oligocene sediment, with the bedload being dominated by coarse pumiceous sands. Discharge of the Waikato River is strongly controlled by a series of dams between Taupo and Karapiro. Additionally, mining in the lower catchment resulted in a lowering of the riverbed and drainage of wetlands, with the result that the Lower Waikato is strongly susceptible to floods.

The geology of the Port Waikato region comprises Jurassic strata, Te Kuiti Group limestones, sandstones and conglomerates, and Pleistocene sands, each unconformably overlying the other. The region has been subject to faulting and folding, with Jurassic strata being folded to form the Kawhia Syncline flanked by the smaller Kawaroa Anticline and Kaimango Syncline, and the terrane bounding Waikato Fault striking almost parallel to the Waikato River as it nears the river mouth.

Under the EEC, the Waikato River mouth is classified as a tidal river mouth estuary. The river mouth area contains characteristic features of a wave-dominated estuary, with a sand spit barrier, and bay head delta; however, being the largest river in New Zealand, there is significant fluvial influence in the estuary. The hydrodynamics of the river mouth are dominated by river discharge, and has as tidal range of 2-4 metres. Little research has been undertaken about the Waikato River mouth, so interpreting data on the sedimentology, ichnology and hydrodynamics of the area will be extremely useful for providing baseline data and comparison to the river's already measured suspended sediment yields and discharge.



## 1.7 References

- Barker, S., Briggs, R. M., Kamp, P. J. J., & Hansen, R. J. (2016). *Field Guide to the Geology of Port Waikato*. Department of Earth and Ocean Sciences, University of Waikato (UoW), Hamilton, New Zealand. 61p.
- Bhattacharya, J. P. (2010). Deltas. In N. P. James & R. W. Dalrymple (Eds.), *Facies Models 4* (4 ed., pp. 233-264). St. John's, Newfoundland: Geological Association of Canada.
- Boyd, R., Dalrymple, R., & Zaitlin, B. A. (1992). Classification of clastic coastal depositional environments. *Sedimentary Geology*, 80(3), 139-150.
- Boyd, R. (2010). Transgressive wave-dominated coasts. In N. P. James & R. W. Dalrymple (Eds.), *Facies Models 4* (4 ed., pp. 265-294). St. John's, Newfoundland: Geological Association of Canada.
- Brown, E. J. (2010). Flow regime and water use. In K. J. Collier, D. P. Hamilton, W. N. Vant & C. Howard-Williams (Eds.), *The Waters of the Waikato*. University of Waikato, Hamilton, New Zealand: Environment Waikato and Centre for Biodiversity and Ecological Research.
- Challinor, A. B. (2001). Stratigraphy of Tithonian (Ohauan-Puarooan) marine beds near Port Waikato, New Zealand, and a redescription of *Belemnopsis Aucklandica* (Hochstetter). *New Zealand Journal of Geology and Geophysics*, 44, 219-242.
- Cooper, J. A. G. (1993). Sedimentation in a river dominated estuary. *Sedimentology*, 40(5), 979-1017.
- Dalrymple, R. W., Zaitlin, B. A., & Boyd, R. (1992). Estuarine facies models: Conceptual basis and stratigraphic implications. *Journal of Sedimentary Research*, 62(6), 1130-1146.
- Dalrymple, R. W., & Choi, K. (2007). Morphologic and facies trends through the fluvial-marine transition in tide-dominated depositional systems: A schematic framework for environmental and sequence-stratigraphic interpretation. *Earth-Science Reviews*, 81(3), 135-174.
- Dalrymple, R. W. (2010a). Interpreting sedimentary succession: Facies, facies analysis and facies models. In N. P. James & R. W. Dalrymple (Eds.), *Facies Models 4* (4 ed., pp. 3-18). St. John's, Newfoundland: Geological Association of Canada.
- Dalrymple, R. W. (2010b). Tidal depositional systems. In N. P. James & R. W. Dalrymple (Eds.), *Facies Models 4* (4 ed., pp. 201-232). St. John's, Newfoundland: Geological Association of Canada.
- Dashtgard, S. E., MacEachern, J. A., Frey, S. E., & Gingras, M. K. (2012). Tidal effects on the shoreface: Towards a conceptual framework. *Sedimentary Geology*, 279, 42-61.
- Dumas, S., & Arnott, R. W. C. (2006). Origin of hummocky and swaley cross-stratification— The controlling influence of unidirectional current strength and aggradation rate. *Geology*, 34(12), 1073-1076.

- Edbrooke, S. W. (Compiler) (2005). *Geology of the Waikato area: Scale 1:250,000: Lower Hutt*: Institute of Geological & Nuclear Sciences.
- Environment Waikato Regional Council (EW). (2008). *The Health of the Waikato River and Catchment: Information for the Guardians Establishment Committee*. Document No: 1288444. Waikato Regional Council, Hamilton, New Zealand. 63p. <https://www.waikatoregion.govt.nz/assets/WRC/Environment/Natural-Resources/rivers-and-streams/gecreport.pdf>.
- Fenton, J. A. (1989). *Sediment Transport, River Morphology and Bottom Sediments of the Lower Waikato River*. MSc thesis. University of Waikato, Hamilton, New Zealand.
- Galloway, W. (1975). Process framework for describing the morphologic and stratigraphic evolution of deltaic depositional system. *Society of Economic Paleontologists and Mineralogist (SEPM), Special Publication No. 31*, 127-156.
- Gingras, M. K., MacEachern, J. A., & Dashtgard, S. E. (2011). Process ichnology and the elucidation of physico-chemical stress. *Sedimentary Geology*, 237(3), 115-134.
- Glade, T. (2003). Landslide occurrence as a response to land use change: A review of evidence from New Zealand. *Catena*, 51, 297-314.
- Greer, D., Atkin, E., Mead, S., Haggitt, T., & O'Neill, S. (2016). *Mapping Residence Times in West Coast Estuaries of the Waikato Region*. Technical Report 2016/19. Waikato Regional Council, Hamilton, New Zealand. 288p. <https://www.waikatoregion.govt.nz/assets/WRC/Environment/Natural-Resources/rivers-and-streams/gecreport.pdf>.
- Heward, A. P. (1981). A review of wave-dominated clastic shoreline deposits. *Earth-Science Reviews*, 17(3), 223-276.
- Hicks, D. M., Semadeni-Davies, A., Haddadchi, A., Shankar, U., & Plew, D. (2019). *Updated Sediment Load Estimator for New Zealand*. Prepared for Ministry for the Environment, Report No: 2018341CH. National Institute of Water & Atmospheric Research Ltd, Christchurch, New Zealand. 190p.
- Hogg, A., Lowe, D. J., Palmer, J., Boswijk, G., & Ramsey, C. B. (2012). Revised calendar date for the Taupo eruption derived by 14C wiggle-matching using a New Zealand kauri 14C calibration data set. *The Holocene*, 22(4), 439-449.
- Hoyle, J., Hicks, M., & Roulston, H. (2012). *Sampled Suspended Sediment Yields from the Waikato Region*. Prepared for National Institute of Water and Atmospheric Research (NIWA). Technical Report 2012/01. Waikato Regional Council, Hamilton, New Zealand. 59p. <http://www.waikatoregion.govt.nz/services/publications/technical-reports/tr/tr201201>.
- Hughes, A. (2015). *Waikato River Suspended Sediment: Loads, Sources, and Sinks*. NIWA Client Report No: HAM2015-059. National Institute of Water & Atmospheric Research Ltd (NIWA), Hamilton, New Zealand. [https://www.waikatoregion.govt.nz/assets/PageFiles/37532/11%20-%20FINAL\\_](https://www.waikatoregion.govt.nz/assets/PageFiles/37532/11%20-%20FINAL_)

NIWA\_Waikato%20River%20Suspended%20Sediments%20-%20loads%20sources%20and%20sinks.pdf.

- Hume, T. M., Sherwood, A. M., & Nelson, C. S. (1975). Alluvial sedimentology of the Upper Pleistocene Hinuera Formation, Hamilton Basin, New Zealand. *Journal of the Royal Society of New Zealand*, 5(4), 421-462.
- Hume, T. M., Bell, R. G., de Lange, W. P., Healy, T. R., Hicks, D. M., & Kirk, R. M. (1992). Coastal oceanography and sedimentology in New Zealand, 1967–91. *New Zealand Journal of Marine and Freshwater Research*, 26(1), 1-36.
- Hume, T. M., Snelder, T., Weatherhead, M., & Liefing, R. (2007). A controlling factor approach to estuary classification. *Ocean & Coastal Management*, 50(11), 905-929.
- James, N. P., & Dalrymple, R. W. (2010). *Facies Models 4*. (4 ed.). St. John's, Newfoundland: Geological Association of Canada.
- Jones, H. F. E., & Hamilton, D. P. (2014). *Assessment of the Waikato River Estuary and Delta for Whitebait Habitat Management: Field survey, GIS Modelling and Hydrodynamic Modelling*. Prepared for Waikato Regional Council. Environmental Research Institute (ERI) Report No. 27, University of Waikato, Hamilton. 79p.
- Kamp, P. J. J., Tripathi, A. R. P., & Nelson, C. S. (2014). Paleogeography of Late Eocene to Earliest Miocene Te Kuiti Group, Central-Western North Island, New Zealand. *New Zealand Journal of Geology and Geophysics*, 57(2), 128-148.
- Kottek, M., Grieser, J., Beck, C., Rudolf, B., & Rubel, F. (2006). World Map of the Köppen-Geiger climate classification updated. *Meteorologische Zeitschrift*, 15(3), 259-263.
- La Croix, A. D., Dashtgard, S. E., Gingras, M. K., Hauck, T. E., & MacEachern, J. A. (2015). Bioturbation trends across the freshwater to brackish-water transition in rivers. *Palaeogeography, Palaeoclimatology, Palaeoecology*, 440, 66-77.
- Lowe, D. J. (2008) Polynesian settlement of New Zealand and the impacts of volcanism on early Maori society: An update. In D. J. Lowe (Ed.), *Guidebook for Pre-conference North Island Field Trip A1 'Ashes and Issues' (28-30 November, 2008)*. Australian and New Zealand 4th Joint Soils Conference, Massey University, Palmerston North (1-5 Dec. 2008): New Zealand Society of Soil Science, pp.142-147. ISBN 978-0-473-14476-0.
- Lowe, D. J. (2010). Introduction to the landscapes and soils of the Hamilton Basin. In: Lowe, D.J., Neall, V.E., Hedley, M., Clothier, B., & Mackay, A (Ed.), *Guidebook for Pre-conference North Island, New Zealand 'Volcanoes to Oceans' field tour (27- 30 July)*. 19th World Soils Congress, International Union of Soil Sciences, Brisbane. Soil and Earth Sciences Occasional Publication No. 3, Massey University, Palmerston North, pp.1.24-1.61.
- MacEachern, J. A., Pemberton, G. S., Gingras, M. K., & Bann, K. L. (2010). Ichnology and facies models. In N. P. James & R. W. Dalrymple (Eds.), *Facies Models 4* (4 ed., pp. 19-58). St. John's, Newfoundland: Geological Association of Canada.

- Manville, V. (2002). Sedimentary and geomorphic responses to ignimbrite emplacement: Readjustment of the Waikato River after the a.d. 181 Taupo Eruption, New Zealand. *The Journal of Geology*, 110(5), 519-541.
- Manville, V., & Wilson, C. J. N. (2004). The 26.5 ka Oruanui eruption, New Zealand: A review of the roles of volcanism and climate in the post - eruptive sedimentary response. *New Zealand Journal of Geology and Geophysics*, 47(3), 525-547.
- Masselink, G., Hughes, M., & Knight, J. (2011). *Introduction to Coastal Processes and Geomorphology*. (2nd ed.). New York, NY: Routledge
- McCraw, J. (2011). *The Wandering River: Landforms and Geological History of the Hamilton Basin*. Guidebook No. 16. Lower Hutt, New Zealand: Geoscience Society of New Zealand.
- Mead, S., & Moores, A. (2005). *Estuary Sedimentation: A Review of Estuarine Sedimentation in the Waikato Region*. Environment Waikato Technical Report Series 2005/13. ASR Ltd Marine Consulting and Research, Hamilton, New Zealand. <http://www.waikatoregion.govt.nz/services/publications/technical-reports/tr/tr200513>.
- Mulder, T., & Syvitski, J. P. M. (1995). Turbidity Currents Generated at River Mouths during Exceptional Discharges to the World Oceans. *The Journal of Geology*, 103(3), 285-299.
- Mulder, T., Syvitski, J. P. M., Migeon, S., Faugères, J.-C., & Savoye, B. (2003). Marine hyperpycnal flows: Initiation, behavior and related deposits. A review. *Marine and Petroleum Geology*, 20(6), 861-882.
- New Zealand Steel (NZ Steel). (2020). *Waikato North Head Mine Site*. Retrieved 31 January, 2020, from <https://www.nzsteel.co.nz/new-zealand-steel/the-story-of-steel/the-mining-operations/waikato-north-head-mine-site/>.
- Pinet, P. R. (2019). *Invitation to Oceanography*. (Eighth ed.). Burlington, MA: Jones & Bartlett Learning.
- Plint, A. G. (2010). Wave- and storm-dominated shoreline and shallow-marine systems. In N. P. James & R. W. Dalrymple (Eds.), *Facies Models 4* (4 ed., pp. 167-20). St John's, Newfoundland: Geological Association of Canada.
- Posamentier, H. W., & Walker, R. G. (2006). *Facies Models Revisited*. SEPM Society for Sedimentary Geology Special Publication.
- Potter, P. E. (1959). Facies model conference. *Science*, 129(3358), 1292-1294.
- Prothero, D. R., & Schwab, F. L. (2004). *Sedimentary Geology: An Introduction to Sedimentary Rocks and Stratigraphy*. (Vol. 1). New York, NY: W.H Freeman.
- Rodgers, K. A., & Grant-Mackie, J. A. (1978). *Aspects of the Geology of the Port Waikato Region: Compiled from Published and Unpublished Data and Ideas of Staff and Students of the Department of Geology, University of Auckland and Others*. Auckland: Department of Geology, University of Auckland.

- Semeniuk, V. (2016). Stratigraphy of estuaries. In M. J. Kennish (Ed.), *Encyclopedia of Estuaries* (pp. 623-648). Dordrecht: Springer Netherlands.
- Tripathi, A. R. P., & Kamp, P. J. J. (2008). *Timing of Initiation of Reverse Displacement on The Taranaki Fault, Northern Taranaki Basin: Constraints from the on land record (Oligocene Te Kuiti Group)*. [Conference Contribution]. Presented at the New Zealand Petroleum Conference, retrieved from <https://hdl.handle.net/10289/3758>.
- Vandergoes, M. J., Hogg, A. G., Lowe, D. J., Newnham, R. M., Denton, G. H., Southon, J., Barrell, D. J. A., Wilson, C. J. N., McGlone, M. S., Allan, A. S. R., Almond, P. C., Petchey, F., Dabell, K., Dieffenbacher-Krall, A. C., & Blaauw, M. (2013). A revised age for the Kawakawa/Oruanui tephra, a key marker for the Last Glacial Maximum in New Zealand. *Quaternary Science Reviews*, 74, 195-201.
- Walker, R. G. (1979). *Facies Models*. (1 ed.). St. John's, Newfoundland: Geological Association of Canada.
- Walker, R. G. (1984). *Facies Models*. (2 ed.). St. John's, Newfoundland: Geological Association of Canada
- Walker, R. G., & James, N. P. (1992). *Facies Models: Response to Sea-level Change*. (3 ed.). St. John's, Newfoundland: Geological Association of Canada.
- Williams, P. W. (2017). Rivers and Their Landscapes. In P. W. Williams (Ed.), *New Zealand Landscape* (pp. 185-243). Elsevier.
- Wo, Y. G. (1994). *Reduction of Water and Bed Levels in the Lower Waikato River*. PhD thesis. University of Waikato, Hamilton, New Zealand.

# Chapter 2

## Process Sedimentology of the Waikato River Mouth, Port Waikato, New Zealand

---

### 2.1 Introduction

Nearshore and shallow marine depositional systems are well studied from a sedimentological and stratigraphical point of view. Depositional processes determine the geometry and connectivity of sand bodies, which are important for the exploitation of hydrocarbons (Ainsworth *et al.*, 2011), groundwater (Kostic *et al.*, 2005), and carbon storage (La Croix *et al.*, 2019b). In siliciclastic shallow marine environments, deposition of sediment is controlled by the interplay between fluvial and marine (e.g. tides, waves, longshore currents) processes. Physico-chemical variability, caused by these interactions, affect sedimentation patterns and the distribution of burrowing infauna (Dashtgard, 2011).

Sedimentological facies models (Galloway, 1975; Boyd *et al.*, 1992) have been created to describe how depositional processes in nearshore and shallow marine settings are recorded in the sedimentary record. However, facies models serve as a norm for comparison and may not capture the short-term (hours to days) complexity of dynamically changing processes in mixed-energy environments (Rossi & Steel, 2016). More recent developments in sedimentological facies models by Ainsworth *et al.* (2011) focus on using depositional processes as recorded in sedimentary (and biogenic) structures to predict geomorphology in coastal settings. Their models rely on process-response linkages and require that all processes are equally recorded in the sediments. Given that modern sedimentary environments are used widely as analogues for the rock record (Gingras *et al.*, 1999; Smith *et al.*, 2009; Dashtgard *et al.*, 2012a; La Croix *et al.*, 2019a) it is reasonable to test the extent to which processes can be inferred from deposits. The details of preservation potential of physical processes on short timescales in modern sedimentary environments needs to be examined in order to improve the ways analogues are applied to interpret Earth's past sedimentary environments and processes.

Although, published studies of modern nearshore and shallow marine environments are increasingly available, only a few of these (e.g., Ayranci *et al.*, 2012; Fricke *et al.*, 2017; Gugliotta *et al.*, 2017; Ayranci & Dashtgard, 2020; Choi *et al.*, 2020) link quantified measurements of hydrodynamic processes to the sedimentological and ichnological character of the deposits. The aim of this study is, therefore, to examine whether depositional processes recorded using oceanographic instrumentation can be linked to the corresponding sedimentary deposits, and to determine whether the sedimentary record is biased towards certain processes operating at specific timeframes. These aims will be addressed by comparing sediment cores with real-time oceanographic measurements of the physical and chemical properties of water, in order to delineate sediment-water interactions.

The sedimentology and ichnology of the lower Waikato River is poorly constrained. There are few published studies that document the hydrodynamics near the Waikato River mouth (e.g. Jones & Hamilton, 2014). Sedimentological data from Port Waikato, focuses on iron sand deposits occurring at the Waikato North Head Mine Site (Brathwaite *et al.*, 2017; Brathwaite *et al.*, 2020). Other research has examined fluvial sedimentation upstream of the reach of tidal influence (Fenton, 1989; Wo, 1994). Due to the state of knowledge, and the relatively limited relevant historical data, an opportunity exists to examine the process-response sedimentology of the prominent intertidal barrier sand spit at the Waikato River mouth, over which river flow, tides, and waves interact.

### **2.1.1 Sedimentology and Ichnology of Barriers and Mouth Bars**

As a river enters a body of water, it becomes unconfined and its velocity decreases, depositing its coarsest grains to form mouth bars (Wright, 1977; Fielding *et al.*, 2005; Olariu & Bhattacharya, 2006). Mouth bars are progradational, and form in river- (Olariu & Bhattacharya, 2006), wave- (Zurbuchen *et al.*, 2020) and tide-dominated deltas (Hori *et al.*, 2002), and lacustrine deltas (Tye & Coleman, 1989; Olariu *et al.*, 2012). The size and shape of mouth bars are mostly controlled by the river: large river mouth systems may have mouth bars a few kilometres long and wide (Tye, 2004; Bhattacharya, 2010). The resulting bar shape is influenced by processes acting on the coastline, such that mouth bars in tide-dominated deltas are reworked and elongated across-shore to form

tidal bars (Dalrymple & Choi, 2007). Wave-dominated deltas have elongated and reworked mouth bars orientated along-shore, and may lead to the formation of barriers and sand spits (Bhattacharya & Giosan, 2003; Warrick, 2020). Additionally, mouth bars formed on tectonically active and wave-dominated coastlines, with a high sediment yield and dynamic processes at the mouth (e.g. west coast New Zealand), have aggradational and elongated mouth bars (Warrick, 2020). Mouth bar deposits are typically formed from parallel-laminated beds and massive or cross-bedded fine sand interbedded with silt to very fine sand, and *Rosselia* and proximal *Phycosiphon* Ichnofacies (Olariu & Bhattacharya, 2006; Maceachern & Bann, 2020).

Barriers form on wave-dominated coastlines, separating river mouths and lagoons from the open ocean. There are a range of types and terminology of barriers including barrier islands, barrier bars, sand spits, back barriers, tidal bars, strand plains, and delta fronts (Mulhern *et al.*, 2019). They are often transgressive, although are also known to form on prograding deltas (e.g. Bhattacharya & Giosan, 2003). Barriers are formed from sediment transported along a coastline by longshore currents (Mulhern *et al.*, 2019; Fruergaard *et al.*, 2020), and continue to elongate, extending up to tens of kilometres downdrift (Mulhern *et al.*, 2019). A tidal inlet may cut through a barrier when the wave processes are not strong enough, and its size is determined by the tidal prism (Boyd, 2010). Barrier geomorphology is influenced by the interactions of waves and tides, storms, sediment supply, and geological setting (Fruergaard *et al.*, 2020), and barriers in mixed-energy environments are often low-lying, merging into tidal flats (Boyd, 2010). Barrier deposits are formed from low angle cross-bedded and parallel laminated sand, with *Psilonichnus* and *Skolithos* Ichnofacies in the subaerial and subaqueous parts, respectively (Hauck *et al.*, 2009; Boyd, 2010). However, if the barrier is subjected to strong currents and wave action, these ichnological signatures are often destroyed (Hauck *et al.*, 2009).

## **2.2 Study Area**

### **2.2.1 Waikato River, New Zealand**

The Waikato River is 425 km long and drains a catchment of 14,260 km<sup>2</sup> on the North Island of New Zealand (Manville, 2002; Williams, 2017). The river drains mountainous terrain of the Taupo Volcanic Zone and passes through the lowlands of the Hamilton



Basin and Lower Waikato Region, to debouch into the Tasman Sea at Port Waikato (Figure 2.1; Brown, 2010; Williams, 2017). The Waipa River is the largest tributary to the Waikato River, with a catchment area of 3,060 km<sup>2</sup>, and joins the Waikato River at Ngaruawahia (Figure 2.1; Manville, 2002; Williams, 2017).

The Waikato River has an average annual discharge of approximately 600 m<sup>3</sup> s<sup>-1</sup>, and minimum and maximum discharges of 200 m<sup>3</sup> s<sup>-1</sup> and 800 m<sup>3</sup> s<sup>-1</sup>, respectively (Jones & Hamilton, 2014). Flow characteristics in the river are controlled, in part, by dams which also cause storage of approximately 0.62 Mt of sediment per year in artificial lakes adjacent to the dams (Hicks *et al.*, 2019). Bedload carried by the river is gravel-dominated up to approximately 100 km from the mouth, downstream of which the bedload transitions to being sand-dominated (Wo, 1994). The Waikato River yields an estimated 0.38 Mt yr<sup>-1</sup> of suspended sediment (Hicks *et al.*, 2019).

### **2.2.1.1 Waikato River Mouth, Port Waikato, New Zealand**

At Port Waikato, tides are semidiurnal, with an average tidal range of 2.2 m (Greer *et al.*, 2016), and a tidal prism that is 35.637 x 10<sup>6</sup> m<sup>3</sup> (Jones & Hamilton, 2014; Greer *et al.*, 2016). The tide influences river flow as far upstream as Mercer (Figure 2.1; approximately 35 km from the mouth). Marine water is transported into the river mouth as a saltwater wedge from the Tasman Sea with the rising tide. The salt wedge reaches approximately 10 km inland from the entrance during neap tides and 13 km during spring tides, although, during high river flow conditions it is limited close to the river mouth (Jones & Hamilton, 2014).

At the seaward terminus of the Waikato River, a major sand spit has been built, of which the intertidal portion is the focus of this paper, and will be referred to as the sand spit for the remainder of the thesis. The sand spit is approximately 0.5 km wide and 1 km long (Figure 2.1). Over the last ~60 years, historical imagery shows that the entire sand spit has migrated northwards due to longshore drift (Figure 2.2).

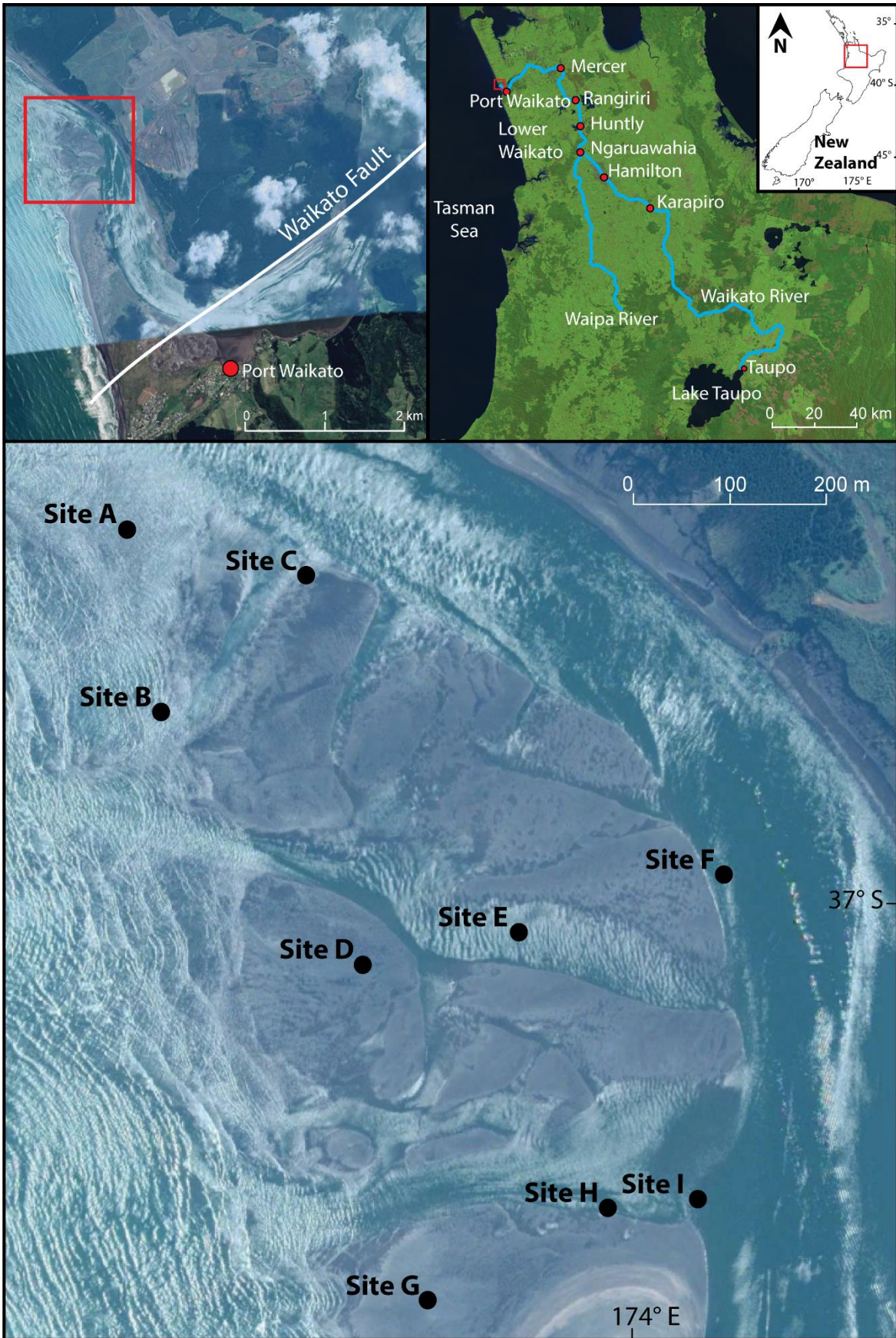


Figure 2.1: Site locations in the field area at the Waikato River mouth, Port Waikato, New Zealand. (Image Source: USGS and Google Earth).

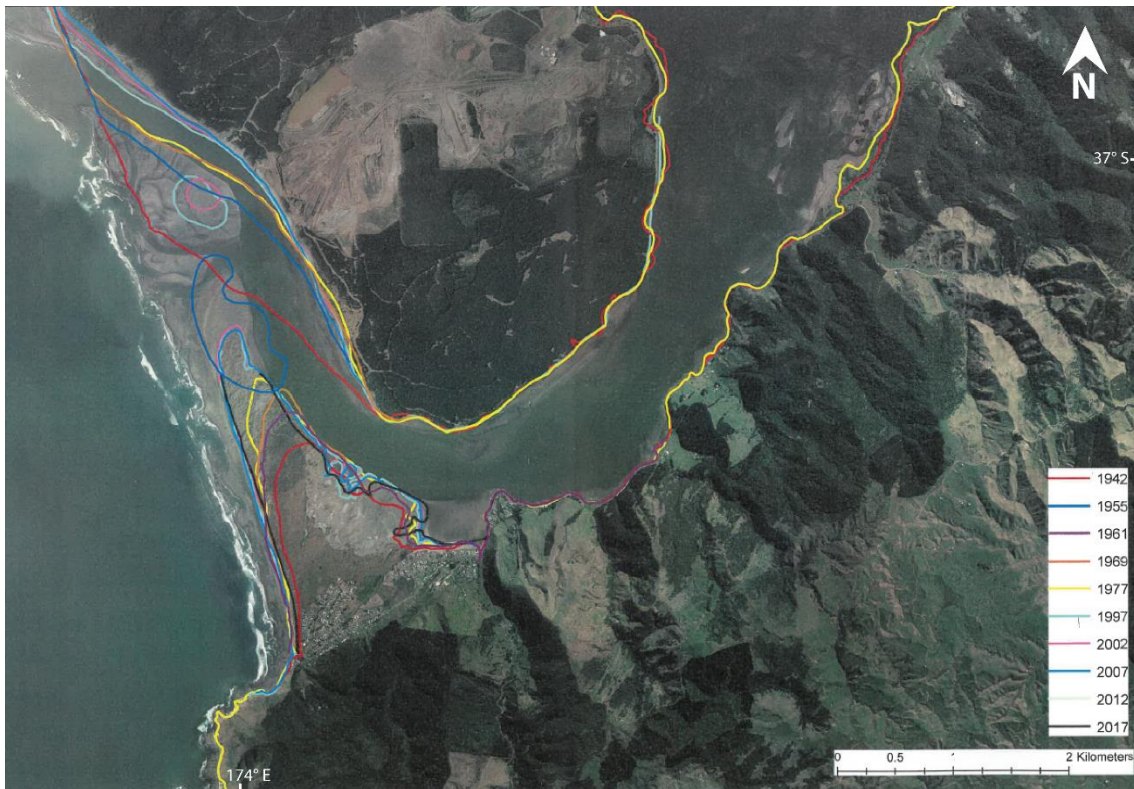


Figure 2.2: Air photo of Waikato River mouth in 2012. Colour outlines show the changes in position of the shoreline and sand spit between 1942 and 2017. Modified from WRC (2018).

## 2.3 Methods

Sedimentological and oceanographic data were collected from the intertidal portion of the sand spit at Port Waikato over nine days (15<sup>th</sup> to 23<sup>rd</sup>) in January 2020. Four datasets were collected: (1) surface and channel sediment samples, (2) bathymetry and topography surveys, (3) vibracores, and (4) oceanographic parameters from instruments. Table 2.1 summarises the vibracores and oceanographic instruments that were deployed at each of the sample sites. Figure 2.3 shows examples of the research instruments used for data collection and analysis.

Table 2.1: Vibracores and oceanographic instruments deployed at each site. All hydrodynamic instruments also had additional optical backscatter sensors (OBS); Nortek instruments were paired with Campbell Scientific OBS3+ sensors and the RBR instruments were paired with Seapoint turbidity sensors.

Site Name	Vibracore	Instrument	
Site A	Core 1		
Site B	Core 2		
Site C	Core 3	Acoustic Velocimeter (Nortek Vector; ADV)	
Site D	Core 4	Acoustic Doppler Current Profiler (Nortek Aquadopp; ADCP)	Conductivity-Temperature-Depth sensor (RBR Concerto)
Site E	Core 5	Nortek Aquadopp	RBR logger
Site F	Core 6	Nortek Aquadopp	RBR Concerto
Site G	Core 7		
Site H	Core 8	Nortek Vector	
Site I	Core 9		

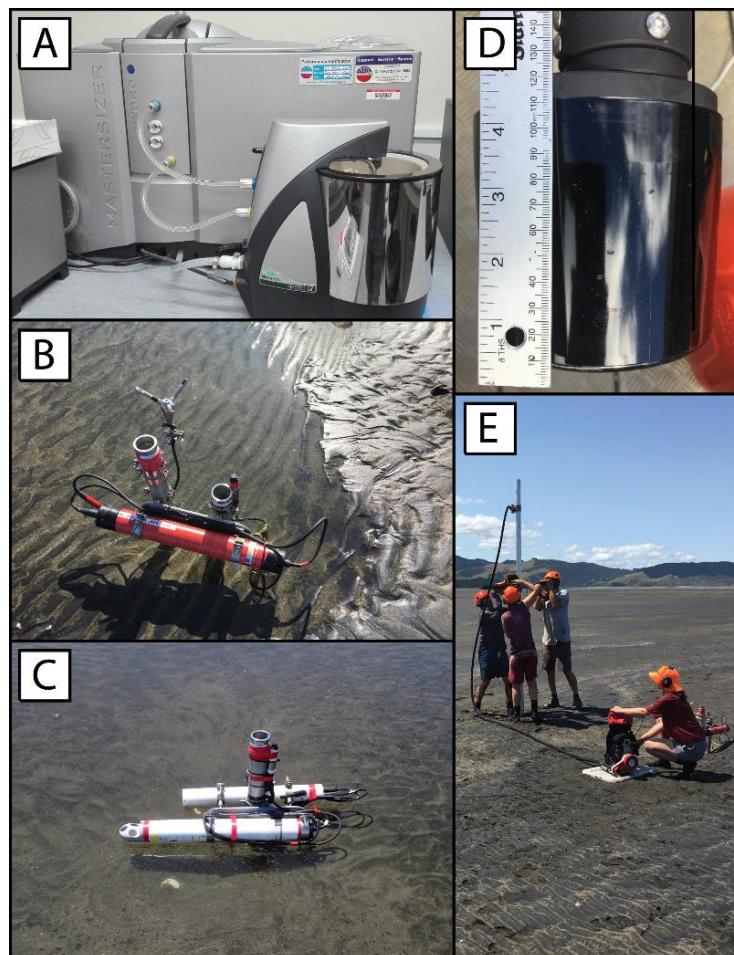


Figure 2.3: Photos of research equipment: (A) Mastersizer® particle-size analyser used for grain size analysis of surface and channel sediment samples, (B) Site C: Nortek Vector, with velocity sensor mounted on the left pipe and Optical back scatter (OBS; turbidity) sensor on the right, (C) Site E: Nortek Aquadopp in front, and RBR Concerto behind. OBS sensors attached to the pipe, (D) echosounder used for the bathymetry survey of the river channel, (E) Vibracore collecting core sample.

### **2.3.1 Sediment Samples**

Seventeen surface sediment samples (upper ca. 5 cm) from the sand spit were collected using five transects spaced 150-350 m apart. Each transect consisted of one to five samples ranging from 25-340 m apart.

Sediment samples from the river channel were collected along seven transects, ranging from 100-400 m apart. Each transect comprised two to four samples, spaced at 50-200 m intervals, totalling 21 samples. The channel transects extended from the riverward side of the spit into the thalweg of the channel and as far towards the far (eastern) bank as possible. Channel samples were acquired using a Ponar Grab Sampler, and water depth and time were recorded with each sample. Grain size of the sediment samples was analysed using a Mastersizer® laser diffraction particle-size analyser. Samples were not pre-treated with hydrogen peroxide to remove organics, as no difference was found on a test sample. GRADISTAT was used to determine the statistical parameters of the grain size distributions (Blott & Pye, 2001). The Wentworth grain size scale was used to classify mean grain sizes calculated in GRADISTAT using the Folk and Ward method (Appendix A; Folk & Ward, 1957).

### **2.3.2 Topography & Bathymetry Survey**

Topography and channel bathymetry surveys were conducted to map the elevations of the sand spit and adjacent river channel. The topographic survey employed a corrected network of Real Time Kinematic (RTK) Global Positioning System (GPS) measurements that were collected using a backpack mounted unit. Measurements were obtained every 1 m along the sand spit, which was walked out during low tide on January 19<sup>th</sup> and 20<sup>th</sup>. The accuracy of measurements was verified by two fixed RTK base stations. The bathymetry survey was conducted using single-beam sonar mounted to University of Waikato's research vessel Maki. The sonar was also calibrated to the RTK base stations. Bathymetry data was calibrated to Global Navigation Satellite System (GNSS) height and echo sounder depth below the research vessel in order to calculate seabed elevation (Appendix B). All topography and bathymetry data were georeferenced to the NZGD 2000 New Zealand Transverse Mercator projected coordinate system in the Mount Eden Circuit, and New Zealand vertical datum 2016 (NZVD2016).

### 2.3.3 Oceanographic Instruments

Oceanographic instruments were deployed at five locations on the sand spit in order to capture any potential across- or along-spit variability (Figure 2.1). Acoustic Doppler Current Profilers (2 MHz Nortek Aquadopps) continuously recorded a profile of velocity at 1 Hz with vertical resolution of 25 mm. Acoustic Doppler Velocimeters (Nortek Vectors) recorded continuous point measurements of velocities at 8 Hz. Conductivity-temperature-depth (CTD) sensors (RBR Concertos) provided CTD data at 6 Hz. All instruments were paired with optical backscatter sensors (Campbell Scientific OBS3+ for Nortek instruments and Seapoint Turbidity sensors for RBR instruments), ranging in height from 10-40 cm above the bed, which sampled at the same rate as the other parameters. One further RBR pressure logger (RBR logger) with two OBSs attached was deployed. Instrument parameters and sampling schemes are summarised in Table 2.2 and Appendix C.

*Table 2.2: Oceanographic instrumentation deployed in the field, with information regarding the deployment location and inbuilt sensors.*

<b>Instrument</b>	<b>Sensors</b>
Nortek Vectors	Flow velocity and direction, pressure, and turbidity
Nortek Aquadopps	Flow velocity and direction, pressure, and turbidity
RBR Concertos	Depth, conductivity, temperature, salinity, pressure, sea pressure, specific conductivity, and turbidity
RBR logger	Depth, 2x turbidity, and sea pressure

RBR Ltd.'s Ruskin software was used for deploying, downloading, and displaying all the Concerto instrument data. Data was exported to text files, and then imported into MATLAB® for reading and processing. The only processing required for Concertos was to remove data from times during which the instruments were exposed.

Data processing for both the Nortek Aquadopps (ADCPs) and Vectors (ADV) included: (1) rotating into east, north, and up coordinates; (2) calculating moving averages; and (3) removing data when the sensors were out of the water. ADCP's had high back scatter counts, indicating good quality data, so no other adjustments were required. However, for the single point ADV measurements, low quality data (correlations <50) were removed. The data was also despiked (using a simple velocity threshold).

As it was not possible to safely collect in-situ water samples during the experiment (owing to substantial wave breaking over the spit), a laboratory calibration of the OBS sensors to determine suspended sediment concentration from the turbidity measurements was undertaken using sediment samples from the sand spit (consisting primarily of 0.265 mm diameter sized particles). However, applying the calibration curve to the turbidity data recorded in-situ, led to very unrealistic concentrations ( $>>10$  grams per litre). It is possible that the sediment in suspension in the field area is a combination of smaller mud sized grains ( $<0.0625$  mm) from the river, and sand-sized particles, which would account for this discrepancy. Therefore, we use the OBS data as a qualitative broad indication of the suspended sediment concentrations, rather than precise measurements of the volume.

#### **2.3.4 Vibracore**

Nine vibracores were collected on the sand spit (Figure 2.1). Cores were collected in 5 m long, 7.62 cm (outer) diameter pipe (1 mm thick) and stored in a refrigerator at 4 °C to preserve moisture. The core lengths, and their depth beneath the surface were measured in the field. Core lengths presented in this thesis represent compacted lengths and not original bed thicknesses. On average cores were compacted by 30%.

In the lab, cores were cut in half longitudinally. One half of the core was x-rayed and logged in detail (Appendices D & E), while the other was preserved for future study. Facies analysis was undertaken and focused on grain size, primary physical sedimentary structures, as well as bioturbation.

## 2.4 Results

### 2.4.1 Hydrodynamic Processes

The Waikato River mouth is variably influenced by river flow, waves and tides, throughout the tidal cycle. Oceanographic instruments record how hydrodynamic and physico-chemical processes differ across and along the sand spit.

#### Salinity

Salinity was measured at Sites D and F. At both sites, salinity varies between 30-35 psu, depending on tidal height (Figures 3a & 7a, Appendix C). Salinity remains stable through most of the high tide period at both sites. However, occasionally, a salinity minimum occurs down to 25 psu in the early- to mid-ebb tide, when flow velocities are slowest.

#### Temperature

Temperature was measured at Sites D, E, and F (Figures 3a, 4a, 6a & 7a, Appendix C). The water temperature across the site ranges between 18-22 °C, depending on timing throughout the day. Water temperature is consistent, varying by 1-2 °C over the inundated period, with warming during the day, and cooling overnight.

#### Turbidity

Turbidity was measured across all the instrument sites (Figures 1-8, Appendix C). For clarity, only turbidity from the Nortek instruments are described. Across all sites, turbidity consistently reaches a minimum at early ebb tide, and maximum at the start and end of the inundated period. Minimum turbidity reaches down to 0 counts, and maximum up to 4 counts. Additional features to note are that at Sites D and H, an additional turbidity peak occurs at high tide. These are up to 1 count at Site D, and 2 counts at Site H. At Site E, turbidity is lower than the other sites, with maximum turbidity occurring only for a short period of time, and turbidity of 0 counts occupying much of the inundated period for most days. Also, turbidity does not reach 0 counts at any point at Site H.



### Wave Height

At Sites C, E and F, water depth and wave heights are on average 1 m and reach a maximum of 1.5 m (Figures 1b, 4c & 6c, Appendix C). Site D wave heights are on average 1.5 m (Figure 2, Appendix C). Site H's ADV was situated in a channel and had recorded wave heights up to 2 m (Figure 8b, Appendix C).

### Flow Velocity and Direction

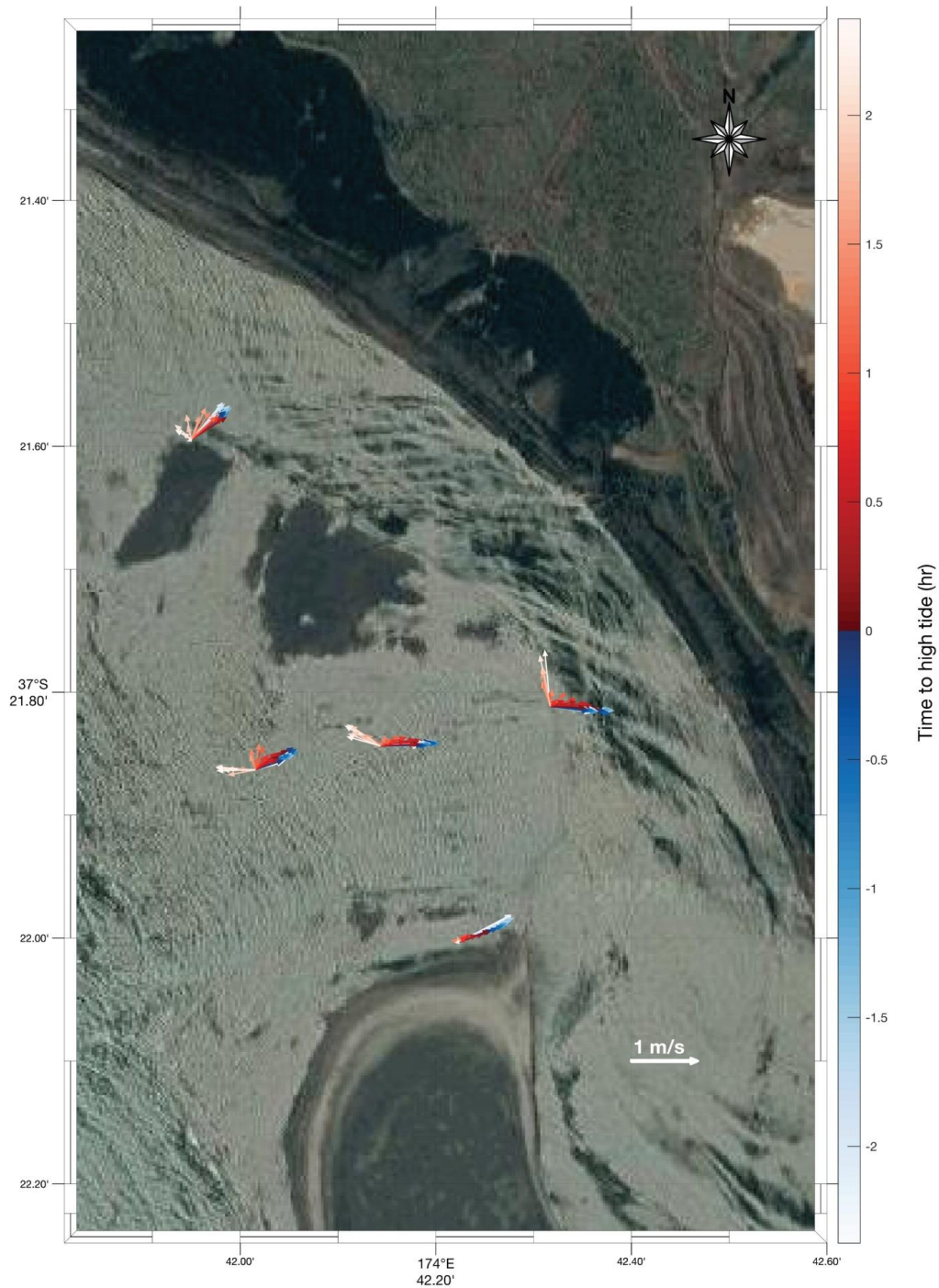
Horizontal velocity measurements are used to describe the overall flow velocity. Across the sites, maximum velocity occurs during the late flood tide, and minimum velocity during the early- to mid-ebb tide. At Sites C and E, velocity ranges from 0 m/s to 1 m/s (Figures 1b & 4c, Appendix C). However, at Site C, minimum velocity occurs towards the late ebb tide (Figure 1b, Appendix C). At Sites D, F and H, flow velocity varies between 0.2-0.9 m/s, 0-1 m/s, and 0-1.1 m/s, respectively (Figures 2c, 6c, & 8b, Appendix C).

There are multi directional currents in the study area, orientated east-west across the spit, and north along the spit, parallel to river flow. These current velocities depend upon timing of the tidal cycle, where east-west current velocities are dominant one hour either side of high tide, and, north to north-west current velocities increase at least 1.5-2 hours either side of high tide, and dominate during the ebb (falling) tide (Figure 2.4). As measured by the ADVs and ADCPs, east orientated flow velocities are fastest at the field site, reaching a maximum of 0.5 m/s at Sites C and D, and 1 m/s at Site E, F and H. West orientated flow velocities reach a maximum of 0.8 m/s at Sites D and E, 0.5 m/s at Sites F and H, and 0.2 m/s at Site C. North orientated flow velocity reaches a maximum of 0.5 m/s at Sites C, D and H, 0.3 m/s at Site E, and 0.2 m/s at Site F. Lastly, south orientated flows are smallest and occurring occasionally during the flood tide, and recorded at Site F and H at 0.2 m/s (Table 2.3).

*Table 2.3: East, west, north and south orientated flow velocity at each site recorded by the ADVs and ADCPs.*

<b>Site</b>	<b>East velocity (m/s)</b>	<b>West velocity (m/s)</b>	<b>North velocity (m/s)</b>	<b>South velocity (m/s)</b>
C	0.5	0.2	0.5	0
D	0.5	0.8	0.5	0
E	1	0.8	0.3	0
F	1	0.5	0.2	0.2
H	1	0.5	0.5	0.2

East-west minimum and maximum flow velocities coincide with the horizontal flow velocities at each site. During the flood tide, east orientated flow velocities are high, and north orientated speeds are negligible. North and west flow velocities increase with the ebb tide, following the flow velocity minimum at the mid-ebb tide, with the exception of Site C, where north orientated flows gradually decrease in speed over the inundated period.



*Figure 2.4: Flow velocity and direction across two tides, recorded from ADCPs and ADVs. Colour represents time relative to high tide, and length of arrow denotes flow velocity. Each arrow shows averages over 15 minutes.*

## **2.4.2 Topography and Bathymetry of the Waikato River Mouth**

The elevation of the sand spit and adjacent river channel relative to New Zealand vertical datum 2016, are shown in Figure 2.5. River channel depth ranges between 0.7 m and 13.8 m, and is shallowest along the banks of the river and deepest in the centre (i.e. the thalweg). The centre of the channel generally is between 6 m and 8.9 m deep, although a deeper depression in the centre of the study area reaches a maximum depth of between 9 m and 13.8 m deep. However, the channel is very energetic and dynamic (Jones & Hamilton, 2014), and it is anticipated that channel depth fluctuates through time due to large and mobile sand waves.

The elevation of the intertidal portions of the sand spit ranges between -2 m and 0 m. With higher elevations on the small surveyed portion of the subaerial part (Figure 2.5). The variation in elevation is due to the complex topography produced by channels and dunes.

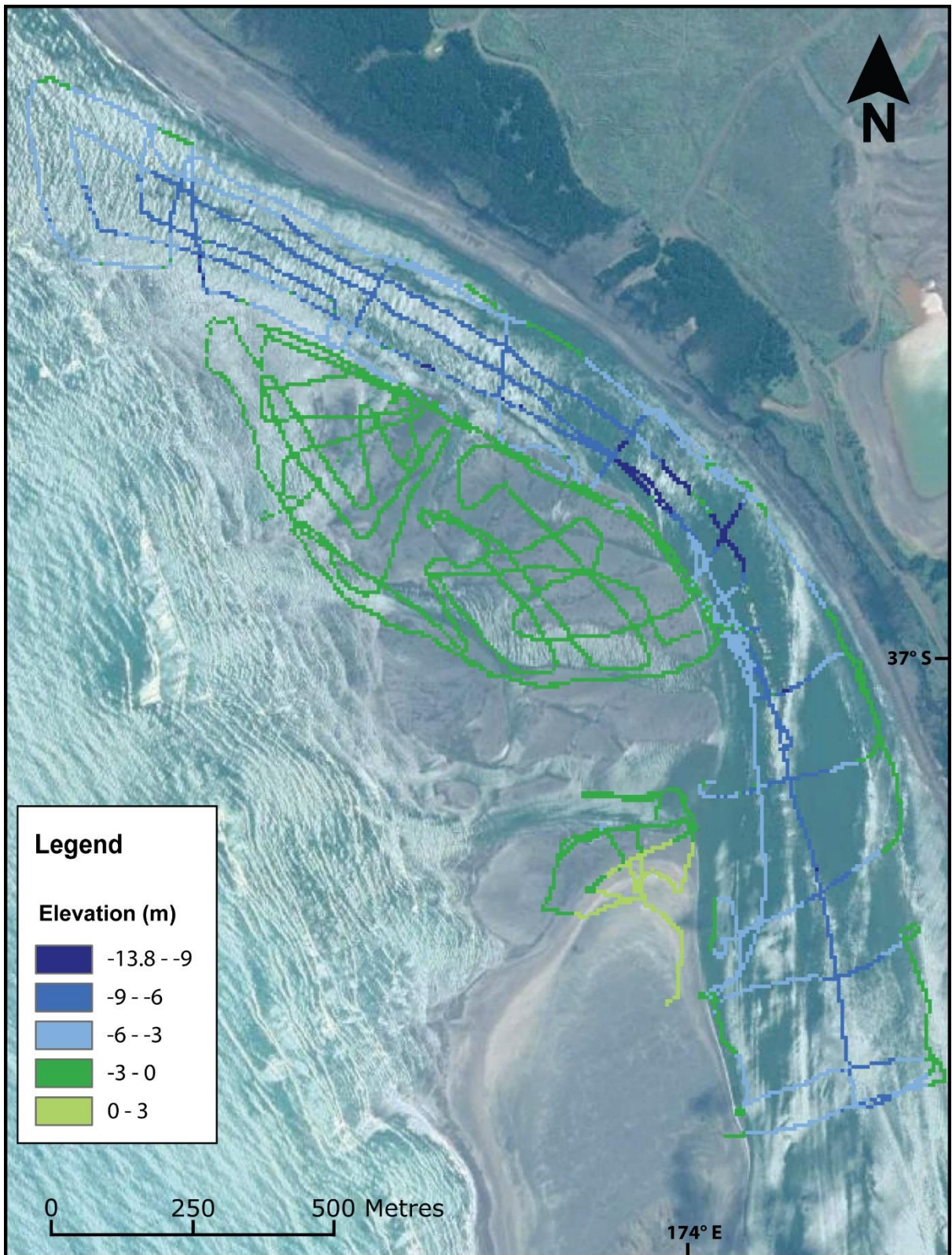


Figure 2.5: Elevation of study area; topography of sand spit, and bathymetry of the Waikato River channel.



### **2.4.3.1 Facies Descriptions and Interpretations**

Four facies were identified in the 9 cores (Figure 2.7). These are: (1) planar tabular to trough cross-bedded sand, (2) wave- to combined-flow ripple laminated sand, (3) planar parallel laminated sand, and (4) structureless to crudely cross-bedded sand, without shells (4a), or with shells (4b).

#### **F1: Planar tabular to trough cross-bedded sand**

Facies 1 consists of planar tabular to trough cross-bedded fine-grained sand with sporadically distributed shell fragments. Individual laminae range from 1-15 mm in thickness, whereas beds range up to approximately 30 cm thick, with gradational or sharp undulatory lower contacts. Coarse sand and pebble layers are scattered throughout the facies but tend to be discontinuous. Bioturbation is absent (bioturbation intensity [BI] 0; Taylor & Goldring, 1993). Facies 1 is interpreted to be deposited by quasi-steady unidirectional currents, as 3D dunes migrate across the sand spit.

#### **F2: Wave- to combined-flow ripple laminated sand**

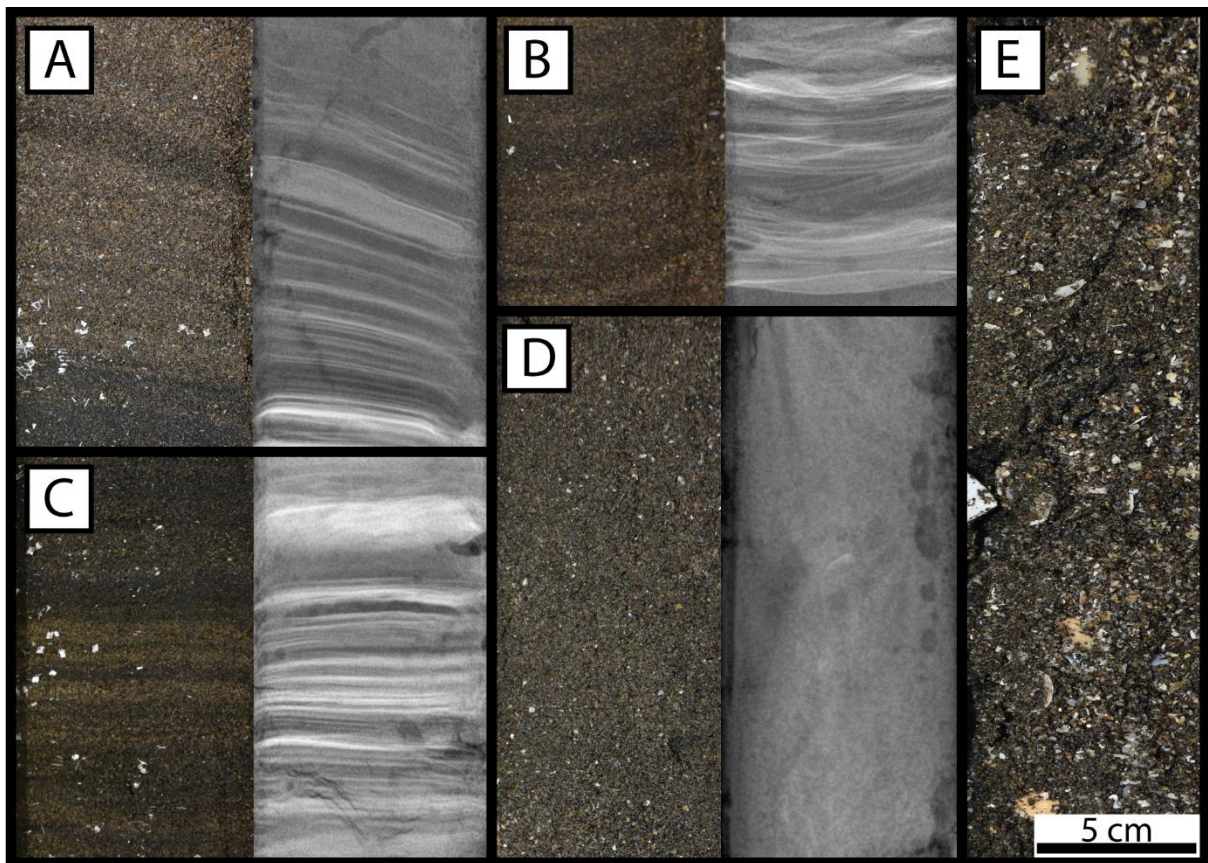
Facies 2 consists of wave-ripple laminated fine-grained sand. Beds range approximately between 5 cm to 10 cm thick, and individual laminae range from 1-3 mm in thickness, and have gradational or sharp undulatory lower contacts. Scattered coarse sand and pebble layers. Bioturbation is absent (BI 0). Scattered shell fragments occur, ranging in size from sand-sized to centimetre scale. Facies 2 is interpreted to be deposited by oscillatory (wave) processes or waves modified by unidirectional currents, as 2D or 3D ripples migrate across the sand spit.

#### **F3: Planar parallel laminated sand**

Facies 3 is composed of planar parallel laminated fine-grained sand. Internal lamination ranges from 1-3 mm thick, is horizontal to very low angle, beds vary approximately 10-20 cm thick, and have sharp lower contacts. Coarse sand and pebble layers occur sporadically. Bioturbation is absent (BI 0). Scattered shell fragments occur, ranging in size from sand-sized to centimetre scale. Facies 3 is interpreted to be deposited from high flow velocities.

F4: Structureless to crudely cross-bedded sand

Facies 4 is structureless to crudely cross-bedded sand. The sand is fine- to medium-grained with shell fragments scattered throughout. Beds range from 20 cm to 100 cm thick, with either gradational or sharp lower contacts. Crude cross-beds and current rippled beds are decimetre scale with gradational lower contacts. Structureless sand comprises predominantly no internal bedding or structures, with rare crude planar tabular or trough cross-stratification at varying scales with individual laminae approximately 1-5 mm thick. Bioturbation is absent (BI 0). Occasional micro fractures and overturning structures. F4a has scattered shell fragments, ranging in size from sand to pebble. F4b is a shelly structureless sand, with a large volume of shell fragments. Both F4a and F4b to be deposits of rapidly decelerating flow (0-0.06 m/s).



*Figure 2.7: Facies characteristics of selected intervals: (A) Facies 1, trough cross-bedded sand, in core 3, (B) facies 2, wave-ripple laminated sand in core 3, (C) facies 3, planar laminated sand, in core 3, (D) facies 4a structureless sand, in core 8, and (E) facies 4b shelly structureless sand, in core 9.*

### 2.4.3.2 Surface Bedforms

Sedimentary structures observed in core are the direct result of bedforms migrating across the depositional surface of the sand spit, which were observed at low tide. Bedforms observed include wave- and combined-flow ripples and dunes, as well as planar bedding. Dunes produced by combined-flow, show asymmetric stoss and lee sides, are generally onshore directed, and range in height from 10 cm to 30 cm (Figure 2.8A). Wave-produced dunes have a more symmetrical appearance, and their heights range from 10 cm to 20 cm (Figure 2.8B). Wave- and combined-flow ripples were also observed on the surface of the spit. Combined-flow ripples are distinguished from current ripples by their asymmetric shape and rounded crests (Figure 2.8C; Dumas *et al.*, 2005). Combined-flow ripples and dunes, and symmetrical ripples were observed at Sites D-H. Sites A, B, and C, are different from the rest of the sand spit because they are comparatively flat, with planar bedding, and wave ripples on the surface (Figure 2.8D).

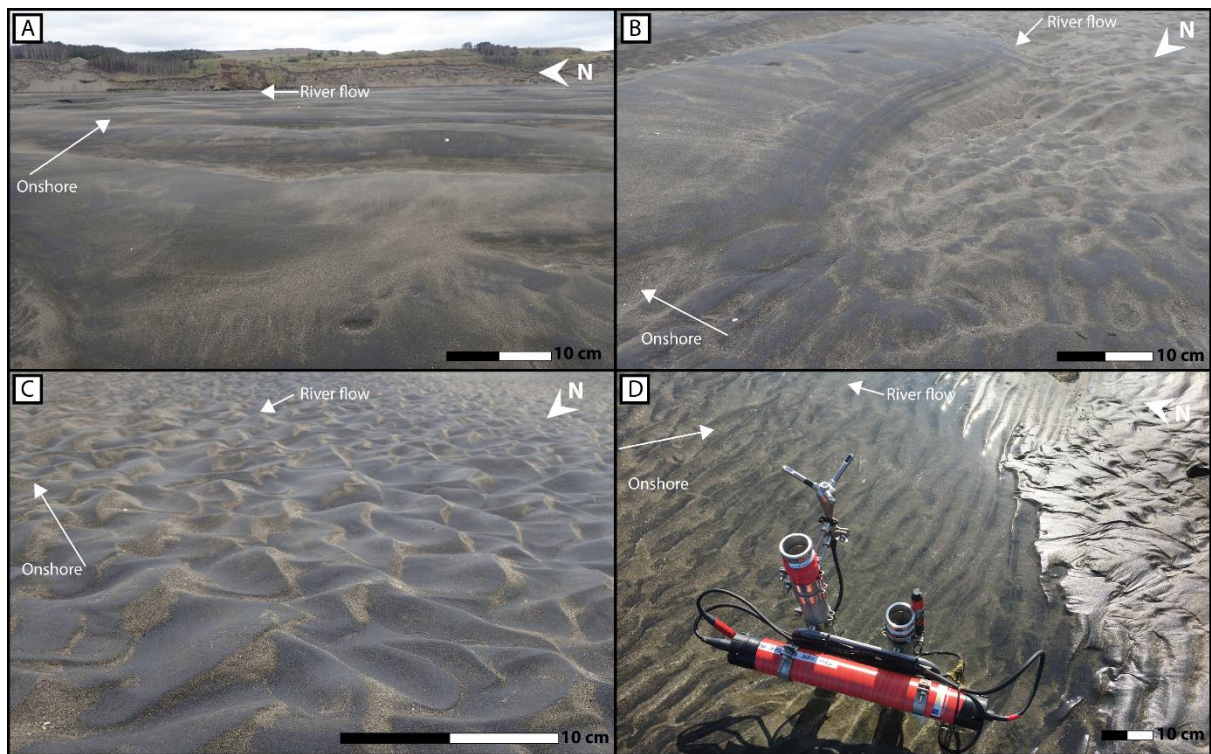


Figure 2.8: Bedforms visible on the surface of the sand spit: (A) Combined-flow dunes located between Sites E and F. Photo facing east; (B) Symmetrical, Wave dunes at Site D. Photo facing south-east; (C) Combined-flow ripples at Site E. Photo facing north east; and (D) Wave ripples at Site C. Photo facing east.



### 2.4.3.3 Cross-Sections

Stratigraphic cross-sections of cores from each transect are displayed in Figure 2.9. A large proportion of the cores comprise structureless sand, with cores 3 and 6, having the best preservation of sedimentary structures. Shelly structureless sand (F4b) is only present in cores 8 and 9, closest to the subaerial portion of the sand spit. Planar laminated sand is observed in cores 1, 2 and 6, and trough cross-bedded sand in cores 3, 5 and 6. Lastly, wave-ripple laminated sand has poor preservation potential, and is only evident in core 3.

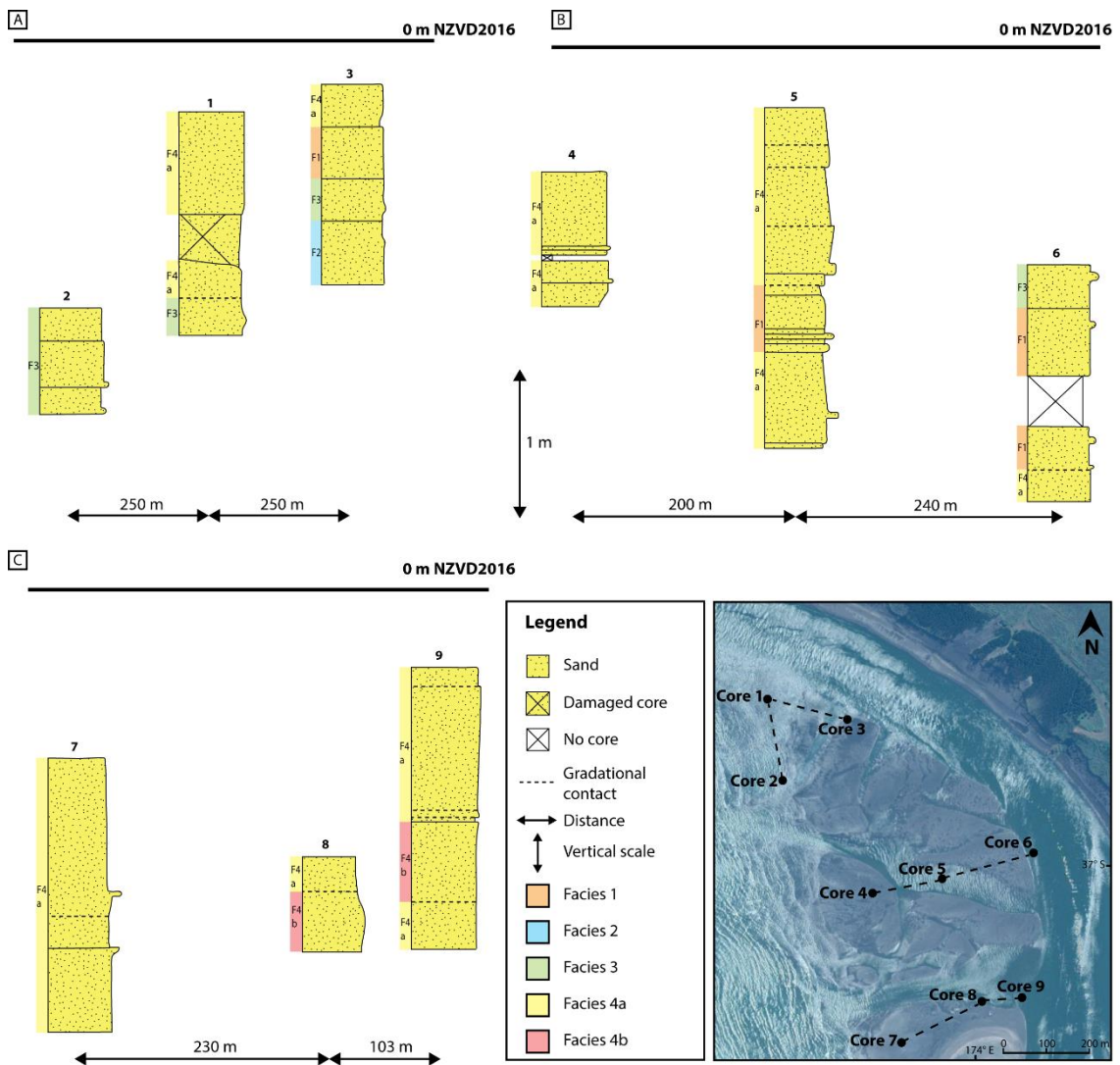


Figure 2.9: Vibracore cross-sections for (A) Cores 1-3, (B) Cores 4-6, and (C) Cores 7-9. NZVD2016 0 m elevation is used as the datum, although it is noted that the datum occurs above the cores since cores are intertidal. Inset map shows core locations in study area.

## 2.5 Discussion

### 2.5.1 Process Sedimentology at the River Mouth

The timing of sediment erosion, transport and deposition is determined by grain size, flow velocity and water depth. Sediment grain sizes observed in cores ranges from very fine (0.062 mm) to coarse (1 mm) sand. Although, most of the sediment is between fine (0.125 mm) and lower medium (0.5 mm) sand. Due to this range in grain sizes, both transport and deposition can occur simultaneously on the spit (Figure 2.10)

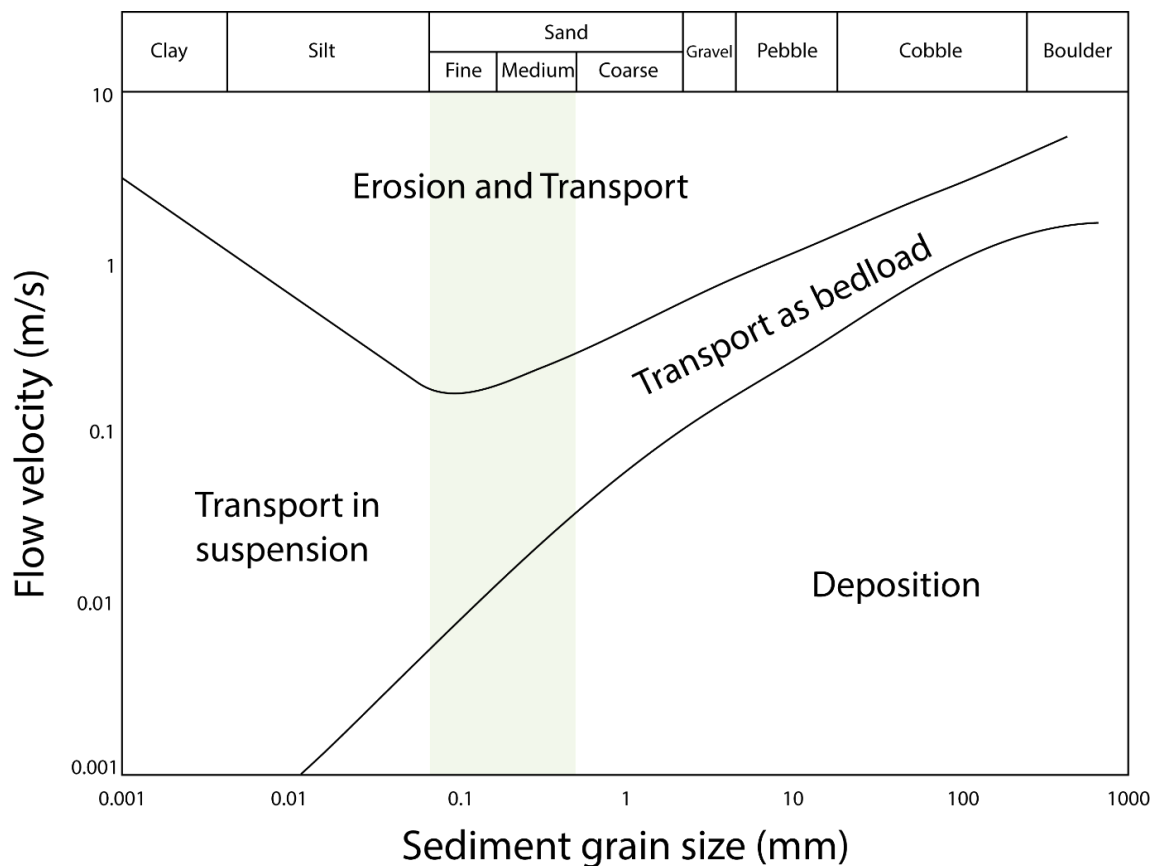


Figure 2.10: Hjulstrom diagram, showing sediment erosion, transport, and deposition as a function of flow velocity and sediment grain size. There is no assumed water depth. The range of grain sizes present on the sand spit are highlighted in green. Modified after Hjulstrom (1935).

Deposition of fine sand and lower medium sand occurs at velocities less than 0.02 m/s and 0.06 m/s respectively (Figure 2.10). Similarly, fine and lower medium sand are eroded at velocities larger than 0.2 m/s and 0.4 m/s respectively (Figure 2.10). Through an assessment of horizontal flow velocity at several sites over a week-long period, the sedimentary response throughout the tidal cycle was identified (Figure 2.11).

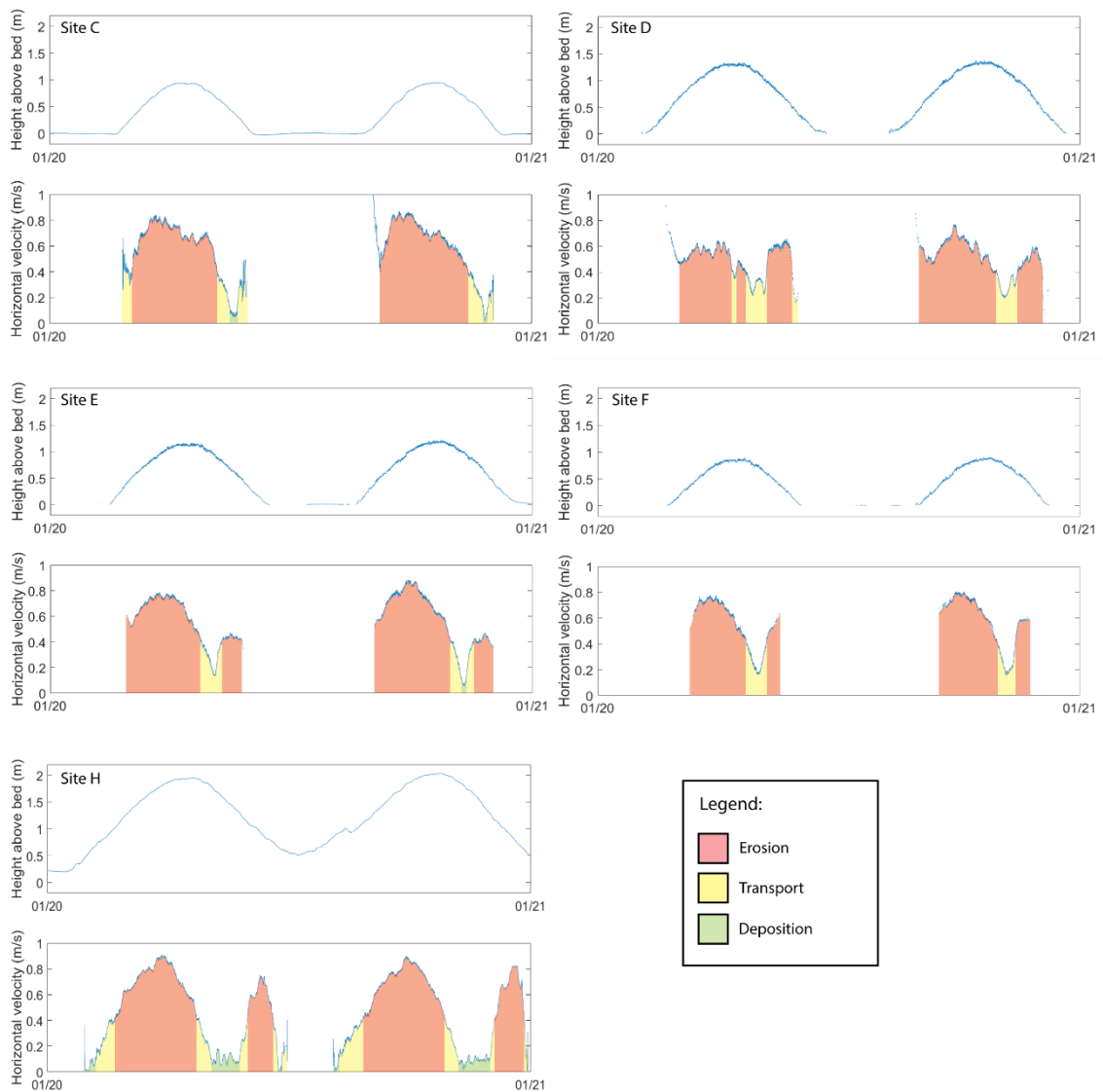


Figure 2.11: Horizontal flow velocities at Sites C, D, E, F, and H, recorded over a 24 hr period; from 12 am 20th to 12 am 21st January 2020. With erosion at flow velocities faster than 0.4 m/s, transport between 0.06-0.4 m/s, and deposition at flow velocities slower than 0.06 m/s.

Horizontal flow velocity changes systematically over a tidal cycle in a similar manner regardless of what site is considered. The interaction between river flow and tides leads to strong asymmetry between the flood and ebb tide, where minimum flow velocity occurs during the mid-ebb tide. Velocity data at Site H was obtained from a semi-permanent channel, thus the flow velocity is slightly exaggerated in comparison to the other sites. Across the sites, flow velocity in the early-ebb tide reaches up to approximately 0.4-0.6 m/s, and reaches a maximum of 0.8-1 m/s by the mid- to late-flood tide. Progressing on to the early-ebb tide, flow velocity slows back down to approximately 0.4-0.6 m/s. The flow conditions during the flood tide and early-ebb tide facilitate sediment erosion and transport (Figure 2.11). Minimum flow velocity ranging from 0 m/s to 0.3 m/s occurs in the early- to mid-ebb tide; although flow velocities of

less than 0.6 m/s are required for sediment deposition, which does not often occur across the sites (e.g. Sites D & F, Figure 2.11). Following the mid-ebb tide, flow velocity increases as the ebb tide progresses, reaching a maximum of 0.4-0.6 m/s, again facilitating erosion and transport of sediment (Figure 2.11).

Interestingly, the cores consist of mostly structureless sediment (F4a & F4b, Figure 2.9), produced from deposition of suspended sediment during low flow velocities in the early- to mid-ebb tide (Figure 2.11; Figures 1-8, Appendix C). Despite being a very small to negligible portion of the tidal cycle, a large volume of sediment is rapidly deposited during these low flow velocities.

When flow velocity exceeds the threshold for sediment entrainment, the sediment is eroded and transported, producing bedforms. These bedforms migrate across a depositional surface, and it is this migration that produces sedimentary structures recorded in the stratigraphic record (Prothero & Schwab, 2004). Flow velocity, grain size and water depth conditions on the sand spit facilitate the formation of bedforms over almost all of the inundated period (Figure 2.11). Hence, the sedimentary bedforms and their corresponding structures represent changes in flow velocity over the tidal cycle. These include wave- and combined-flow ripples and dunes, and planar bedding.

The conditions required for the development of bedforms are often described by bed-stability phase diagrams. Sedimentary bedforms produced by unidirectional currents, are conceptualised as being a function of water depth, flow velocity and grain size (Southard, 1991; Van Den Berg & Van Gelder, 1993), or alternatively, as a function of grain size and bed shear stress (Southard & Boguchwal, 1990). Bed-stability phase diagrams have also been developed for oscillatory (wave) flows, where the bedforms are described as a function of the oscillation period and maximum orbital velocity (Southard, 1991). However, probably most importantly, and therefore the most researched, are bedforms developed by combined unidirectional and oscillatory flows (i.e., 'combined flows'; Arnott & Southard, 1990; Southard, 1991; Dumas *et al.*, 2005; Kleinhans, 2005; Perillo *et al.*, 2014). Combined-flow bedforms, are best described as a function of the unidirectional velocity and oscillatory velocity (Figure 2.12), or by various mobility parameters (e.g. current velocity, shear stress and grain shear stress; Kleinhans, 2005).

The bed-stability phase diagram provides a guide to predicting the bedforms expected to develop on the sand spit based on the flow parameters measured with ADVs and ADCPs (Figure 2.12). To test whether all depositional processes occurring at the Waikato River mouth are recorded by the sediment, calculated unidirectional and maximum orbital velocities are plotted on the bed-stability phase diagram (Figure 2.1.2). Unidirectional current velocities were calculated by averaging the east-west and north-south current velocities over 15-minute time windows. To estimate a representative maximum orbital velocity for the waves over each 15-minute period, the pressure signal was first band-pass filtered to remove high and low frequency motions (leaving those between 3 s and 12.5 s periods). An upcrossing analysis of the filtered pressure signal was undertaken to identify each individual wave and the maximum velocity found for every single wave. Then the mean over the 15-minute window of these maximum values was used as the maximum orbital in Figure 2.12.

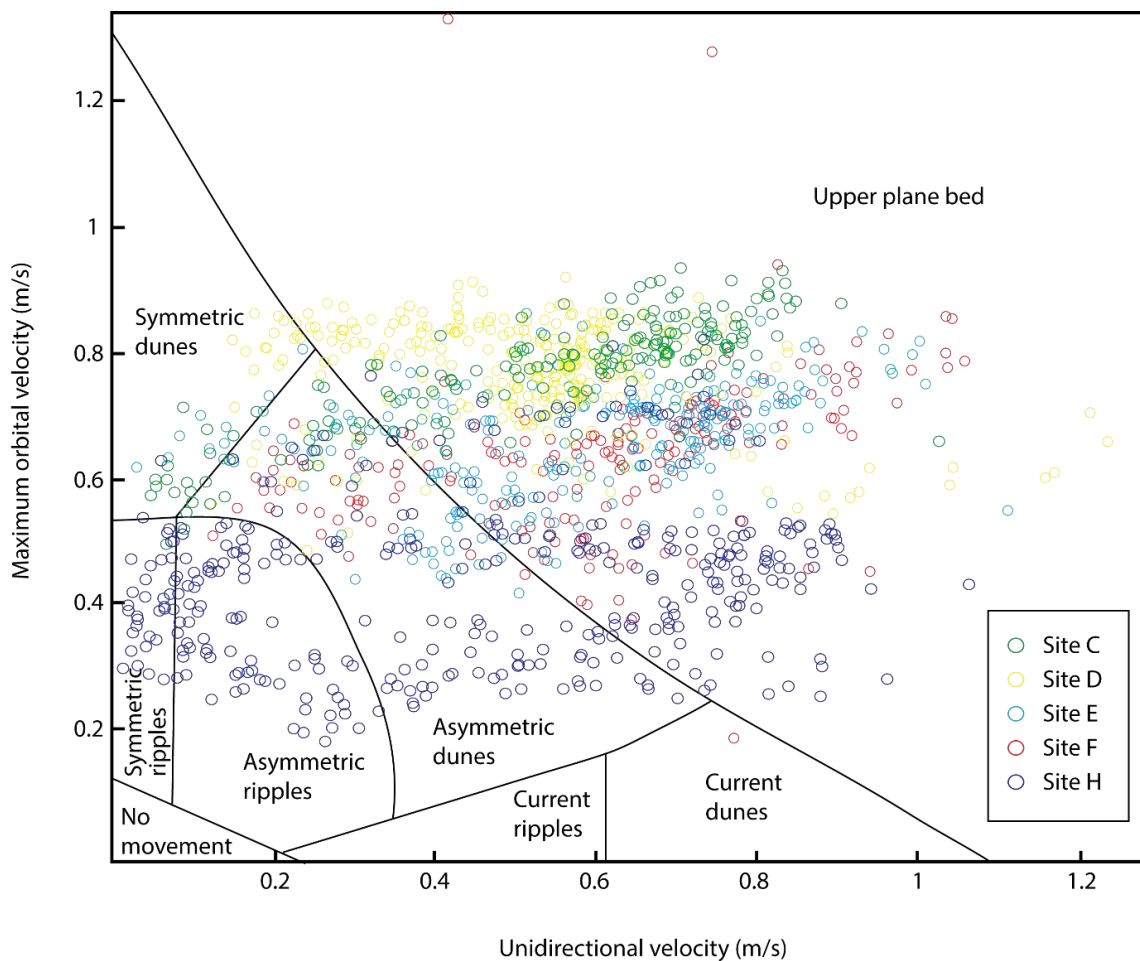


Figure 2.12: Sedimentary bedforms development in combined flow conditions, as a function of unidirectional flow velocity and orbital flow velocity. Assuming an average grain size of 0.25 mm diameter (upper fine sand). Overlain with data recorded from each site, where green is Site C, yellow is Site D, light blue is Site E, red is Site F, and dark blue is Site H. Modified after Perillo et al. (2014).

Maximum orbital (wave) and unidirectional (fluvial) current velocities range between 0.2-1 m/s and 0-1 m/s, facilitating the development of symmetrical (wave) and asymmetric (combined-flow) ripples and dunes, and planar bedding on the sand spit (Figure 2.12). Much of the orbital and unidirectional current velocities are greater than 0.6 m/s (Figure 2.12), leading to the regular development of planar bedding, which is consistent with the frequency of planar lamination in core (Figure 2.9).

Planar tabular to trough cross-bedded sands are preserved in core at Sites C, E, and F (Figures 2.7 & 2.9), and are the products of migrating wave- and combined-flow dunes on the surface, such as those observed at Sites E-H (Figure 2.8A & B). Orbital and unidirectional current velocity conditions required for the development of wave and combined-flow dunes are met for much of the inundated period at all sites (Figure 2.12).

Wave- to combined-flow ripple laminated sand is preserved in core at Site C (Figures 2.7 & 2.9), and are the product of migrating wave- and combined-flow ripples, such as those observed on the surface at Sites A-C and Sites D-H, respectively (Figure 2.8C & D). The development of ripples are measured mostly at Site H (Figure 2.12, dark blue), as the ADV was submerged in deep enough water (>40 cm) to capture the flow conditions, when the tidal height was low. Therefore, it is expected that flow velocity conditions for ripples do occur at all sites, but they were not captured by the other ADV and ADCPs.

## **2.5.2 Relative Importance of River Flow, Waves and Tides**

Combined sedimentological and hydrodynamic data forms a comprehensive data set to discuss the relative influence and interactions between depositional processes at the Waikato River mouth. Bed-stability phase diagrams provide insight to the bedforms developing under various flow velocity, grain size and water depth conditions. Across all sites, the sand spit experiences interacting wave and fluvial currents, producing wave- and combined-flow ripples and dunes, and planar bedding (Figure 2.12). These bedforms are matched to their corresponding structures in core, showing that these bedforms were also present in the past (Figures 2.7 & 2.9). Although, not all bedforms and structures are observed on the surface and in core, respectively across the sites. Sites A-C are comparatively flat with only planar bedding and wave ripples on the surface (Figure 2.8D), most likely due to erosion during high flow conditions, followed

by wave ripples developing as the water level drops with the end of the ebb tide. Being at the northern portion of the sand spit (Figure 2.1), Sites A-C are more influenced by wave processes, shown by their lack of combined-flow ripples and dunes (Figures 2.8 & 2.9). Whereas, dunes were observed on the surface at Sites D-H (Figure 2.8A & B), and of these sites, wave influence was strongest to the west at Site D (Figure 2.8B). Combined-flow dunes were more often observed on the bed with distance towards the east (landward), closer to the river (Figures 2.1 & 2.8A).

In contrast to the presence of wave ripples and dunes, there is no evidence in core or on the surface, for fluvial current ripples or dunes. The lack of fluvial signatures suggests that waves have a greater influence in the field area. When unidirectional current velocities are less than 0.2 m/s, orbital current velocity can reach up to 0.8 m/s (Figure 2.12); supporting that the river mouth is wave-dominated. Furthermore, there is a lack of tidal signatures (i.e., herringbone cross-stratification, tidal mud drapes etc.) in the sedimentary record, suggesting that tides have the smallest influence in the field area. Although, tides have a direct control on sediment deposition, by raising and lowering water level, allowing for the movement of waves and river flow over the sand spit (Dashtgard *et al.*, 2012b).

Waves appear to be the dominant depositional process at the Waikato River mouth. Combined river flow and waves facilitate sediment erosion, transport and re-working, and the tidal height determines their efficacy.

### **2.5.3 Implications for the Global Rock Record**

Nearshore, shallow marine, and river mouth settings display complex interactions between river flow, waves, and tides. Several classifications exist to describe these sedimentary environments: (1) Geomorphic classification (e.g. Hume *et al.*, 2007), used by oceanographers and coastal planners to describe the overall shape of the coastline (i.e. snapshot in time); (2) sedimentological and stratigraphic classification (e.g., Boyd *et al.*, 1992), describing sedimentological character by (inferred) depositional process; and (3) process-based classification (e.g., Ainsworth *et al.*, 2011), that builds on 2, but aims to capture the complexity of various depositional processes and the record in the stratigraphy.

The process-based classification of Ainsworth *et al.* (2011) is currently most used within the sedimentology literature (e.g. Longhitano *et al.*, 2012; Vakarelov *et al.*, 2012), which uses the preserved sedimentary structures to infer the depositional processes occurring in the environment. From inferring the depositional processes, the depositional environments can be classified using a three-part ranking of dominance, influence and affect. Which is ultimately used to model the geometry and morphology of geobodies in subsurface reservoirs, such as petroleum storage units.

However, the extent to which processes can be inferred from deposits is not yet clear (Rossi & Steel, 2016), which restricts our ability to use modern sedimentary environments as analogues to interpret the rock record. In river mouth settings, erosional and depositional processes vary on timescales from minutes, to hours, to days. These processes culminate to form the sedimentological signature which is the time-average of these interacting processes. The Waikato River mouth is used in this study to test the applicability of the process-based classification by plotting the sedimentological dataset, and combined sedimentological and hydrodynamic datasets (Figure 2.13).

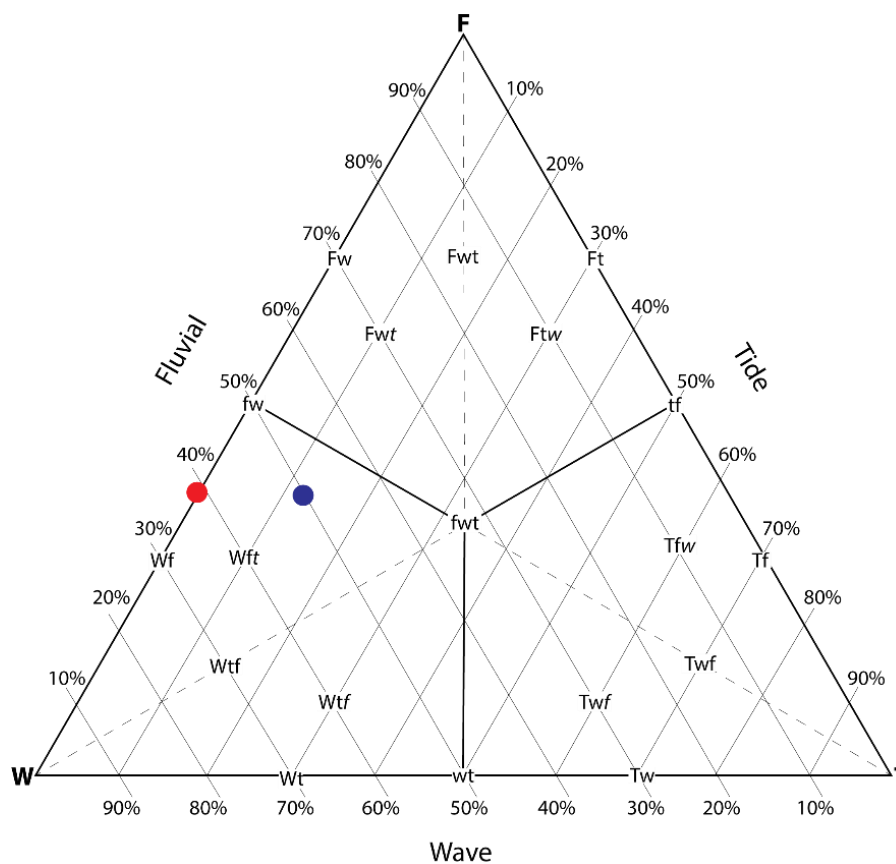


Figure 2.13: Process based classification modified after Ainsworth *et al.* (2011), with the Waikato River mouth plotted using the sedimentological dataset in red, and combined sedimentological and hydrodynamic datasets in blue.



Despite the Waikato River mouth being situated in a setting subject to strong waves and tides, the depositional record appears to be biased against the tidal signature. By investigating only the sedimentological data, the effect of tides in the setting would go unrecognised. Correspondingly, the Waikato River mouth would be classified as wave dominated and fluvially influenced (Wf; Figure 2.13). Importantly, however is the fact that by combining sedimentological and hydrodynamic data, the tidal signature is clearly identified, and the river mouth is classified as a wave dominated, fluvially influence and tidally affected (Wft; Figure 2.13).

The process-based framework by Ainsworth *et al.* (2011) best describes mixed-influence environments from a sedimentological and stratigraphic standpoint. However, these results highlight the difficulty in interpreting the presence and strength of depositional processes in similar mixed-energy environments within the rock record globally, because not all depositional processes may be recorded by the sediments. These results present implications towards applied aspects of this research, in predicting sand body geometries of subsurface water or petroleum reservoirs. The geomorphology of depositional environments is strongly controlled by the relative influence of river flow, waves and tides (Ainsworth *et al.*, 2011), and in order to capture the geometries of these geobodies, the full range of depositional processes needs to be understood.

## **2.6 Conclusions**

The Waikato River mouth is subject to the interactions of river flow, waves and tides. The combinations of river flow and tides leads to strong asymmetry between flood and ebb flow velocities. Fast flow velocities exist throughout most of the inundated period, facilitating erosion and transportation of sediment, producing sedimentary bedforms. However, the sedimentary record comprises mostly structureless sediment; a small to negligible portion of the tidal cycle. Additionally, the sedimentary structures present in core are inherently biased against the tidal signature, despite the tide having a direct control of sediment on the sand spit.

The results of this study demonstrate that depositional processes can be recorded using oceanographic instrumentation and linked to the corresponding sedimentary deposits. Erosional and depositional processes vary in river-mouth environments on time scales ranging from minutes, to hours, to days, and these processes culminate to form the

sedimentological signature. Not all processes are preserved by the sediments, and as a result, depositional processes may go unrecognised in the rock record in other mixed-energy environments. These results have important implications to applied use of this aspect of research, in modelling the morphology and connectivity of geobodies in subsurface reservoirs. Highlighting the need for using modern environments as analogues for the rock record, in which paired sedimentological and hydrodynamic data are a valuable tool for identifying all the depositional processes occurring within a mixed-influence environment.

## 2.7 References

- Ainsworth, R. B., Vakarelov, B. K., & Nanson, R. A. (2011). Dynamic spatial and temporal prediction of changes in depositional processes on clastic shorelines: Toward improved subsurface uncertainty reduction and management. *AAPG Bulletin*, 95(2), 267-297.
- Arnott, R. W., & Southard, J. B. (1990). Exploratory flow-duct experiments on combined-flow bed configurations, and some implications for interpreting storm-event stratification. *Journal of Sedimentary Research*, 60(2), 211-219.
- Ayranci, K., Lintern, D. G., Hill, P. R., & Dashtgard, S. E. (2012). Tide-supported gravity flows on the upper delta front, Fraser River delta, Canada. *Marine Geology*, 326-328, 166-170.
- Ayranci, K., & Dashtgard, S. E. (2020). Deep-water renewal events; Insights into deep water sediment transport mechanisms. *Scientific Reports*, 10(1), 6139.
- Bhattacharya, J., & Giosan, L. (2003). Wave-influenced deltas: Geomorphological implications for facies reconstruction. *Sedimentology*, 50, 187-210.
- Bhattacharya, J. P. (2010). Deltas. In N. P. James & R. W. Dalrymple (Eds.), *Facies Models 4* (4 ed., pp. 233-264). St. John's, Newfoundland: Geological Association of Canada.
- Blott, S. J., & Pye, K. (2001). GRADISTAT: A grain size distribution and statistics package for the analysis of unconsolidated sediments. *Earth Surface Processes and Landforms*, 26(11), 1237-1248.
- Boyd, R., Dalrymple, R., & Zaitlin, B. A. (1992). Classification of clastic coastal depositional environments. *Sedimentary Geology*, 80(3), 139-150.
- Boyd, R. (2010). Transgressive wave-dominated coasts. In N. P. James & R. W. Dalrymple (Eds.), *Facies Models 4* (4 ed., pp. 265-294). St John's, Newfoundland: Geological Association of Canada.
- Brathwaite, R. L., Gazley, M. F., & Christie, A. B. (2017). Provenance of titanomagnetite in ironsands on the west coast of the North Island, New Zealand. *Journal of Geochemical Exploration*, 178, 23-34.
- Brathwaite, R. L., Christie, A. B., & Gazley, M. F. (2020). Stratigraphy, provenance and localisation of the titanomagnetite placer at Waikato North Head, South Auckland, New Zealand. *Mineralium Deposita*.
- Brown, E. J. (2010). Flow regime and water use. In K. J. Collier, D. P. Hamilton, W. N. Vant & C. Howard-Williams (Eds.), *The Waters of the Waikato*. University of Waikato, Hamilton, New Zealand: Environment Waikato and Centre for Biodiversity and Ecological Research.
- Choi, K., Kim, D., & Jo, J. (2020). Morphodynamic evolution of the macrotidal Sittaung River estuary, Myanmar: Tidal versus seasonal controls. *Marine Geology*, 430, 106-367.
- Dalrymple, R. W., & Choi, K. (2007). Morphologic and facies trends through the fluvial-marine transition in tide-dominated depositional systems: A schematic

- framework for environmental and sequence-stratigraphic interpretation. *Earth-Science Reviews*, 81(3), 135-174.
- Dashtgard, S. E. (2011). Linking invertebrate burrow distributions (neochronology) to physicochemical stresses on a sandy tidal flat: Implications for the rock record. *Sedimentology*, 58(6), 1303-1325.
- Dashtgard, S., Venditti, J., Hill, P., Sisulak, C., Johnson, S., & La Croix, A. (2012a). Sedimentation across the tidal-fluvial transition in the Lower Fraser River, Canada. *The Sedimentary Record*, 10, 4-9.
- Dashtgard, S. E., MacEachern, J. A., Frey, S. E., & Gingras, M. K. (2012b). Tidal effects on the shoreface: Towards a conceptual framework. *Sedimentary Geology*, 279, 42-61.
- Dumas, S., Arnott, R. W. C., & Southard, J. B. (2005). Experiments on oscillatory-flow and combined-flow bed forms: Implications for interpreting parts of the shallow-marine sedimentary record. *Journal of Sedimentary Research*, 75(3), 501-513.
- Fenton, J. A. (1989). *Sediment Transport, River Morphology and Bottom Sediments of the Lower Waikato River*. MSc thesis. University of Waikato, Hamilton, New Zealand.
- Fielding, C. R., Trueman, J. D., & Alexander, J. (2005). Sharp-based, flood-dominated mouth bar sands from the Burdekin River delta of Northeastern Australia: Extending the spectrum of mouth-bar facies, geometry, and stacking patterns. *Journal of Sedimentary Research*, 75(1), 55-66.
- Folk, R. L., & Ward, W. C. (1957). Brazos River bar: A study in the significance of grain size parameters. *Journal of Sedimentary Research*, 27(1), 3-26.
- Fricke, A. T., Nittrouer, C. A., Ogston, A. S., Nowacki, D. J., Asp, N. E., Souza Filho, P. W. M., da Silva, M. S., & Jalowska, A. M. (2017). River tributaries as sediment sinks: Processes operating where the Tapajós and Xingu rivers meet the Amazon tidal river. *Sedimentology*, 64(6), 1731-1753.
- Fruergaard, M., Tessier, B., Poirier, C., Mouazé, D., Weill, P., & Noël, S. (2020). Depositional controls on a hypertidal barrier-spit system architecture and evolution, Pointe du Banc spit, north-western France. *Sedimentology*, 67(1), 502-533.
- Galloway, W. (1975). Process framework for describing the morphologic and stratigraphic evolution of deltaic depositional system. *Society of Economic Paleontologists and Mineralogist (SEPM), Special Publication No. 31*, 127-156.
- Gingras, M. K., Pemberton, S. G., Saunders, T., & Clifton, H. E. (1999). The ichnology of modern and Pleistocene brackish-water deposits at Willapa Bay, Washington: Variability in estuarine settings. *Palaios*, 14(4), 352-374.
- Greer, D., Atkin, E., Mead, S., Haggitt, T., & O'Neill, S. (2016). *Mapping Residence Times in West Coast Estuaries of the Waikato Region*. Technical Report 2016/19. Waikato Regional Council, Hamilton, New Zealand. 288p. <https://www.waikatoregion.govt.nz/assets/WRC/Environment/Natural-Resources/rivers-and-streams/gecreport.pdf>.

- Gugliotta, M., Saito, Y., Nguyen, V. L., Ta, T. K. O., Nakashima, R., Tamura, T., Uehara, K., Katsuki, K., & Yamamoto, S. (2017). Process regime, salinity, morphological, and sedimentary trends along the fluvial to marine transition zone of the mixed-energy Mekong River delta, Vietnam. *Continental Shelf Research*, 147, 7-26.
- Hauck, T., Dashtgard, S., Pemberton, G., & Gingras, M. (2009). Brackish-water ichnological trends in a microtidal barrier Island-embayment system, Kouchibouguac National Park, New Brunswick, Canada. *Palaios*, 24, 478-496.
- Hicks, D. M., Semadeni-Davies, A., Haddadchi, A., Shankar, U., & Plew, D. (2019). *Updated Sediment Load Estimator for New Zealand*. Prepared for Ministry for the Environment, Report No: 2018341CH. National Institute of Water & Atmospheric Research Ltd, Christchurch, New Zealand. 190p.
- Hjulstrom, F. (1935). *Studies of the Morphological Activity of Rivers as Illustrated by the River Fyris*. Uppsala: Almqvist & Wiksells.
- Hori, K., Saito, Y., Zhao, Q., & Wang, P. (2002). Architecture and evolution of the tide-dominated Changjiang (Yangtze) River delta, China. *Sedimentary Geology*, 146(3), 249-264.
- Hume, T. M., Snelder, T., Weatherhead, M., & Liefing, R. (2007). A controlling factor approach to estuary classification. *Ocean & Coastal Management*, 50(11), 905-929.
- Jones, H. F. E., & Hamilton, D. P. (2014). *Assessment of the Waikato River Estuary and Delta for Whitebait Habitat Management: Field Survey, GIS Modelling and Hydrodynamic Modelling*. Prepared for Waikato Regional Council. Environmental Research Institute (ERI) Report No. 27, University of Waikato, Hamilton. 79p.
- Kleinhaus, M. (2005). Phase diagrams of bed states in steady, unsteady, oscillatory and mixed flows. In L. C. Van Rijn (Ed.), *Sandpit Project* (pp. 1-16). Amsterdam: Aqua Publications.
- Kostic, B., Becht, A., & Aigner, T. (2005). 3-D sedimentary architecture of a Quaternary gravel delta (SW-Germany): Implications for hydrostratigraphy. *Sedimentary Geology*, 181(3), 147-171.
- La Croix, A. D., Dashtgard, S. E., & MacEachern, J. A. (2019a). Using a modern analogue to interpret depositional position in ancient fluvial-tidal channels: Example from the McMurray Formation, Canada. *Geoscience Frontiers*.
- La Croix, A. D., Wang, J., He, J., Hannaford, C., Bianchi, V., Esterle, J., & Undershultz, J. R. (2019b). Widespread nearshore and shallow marine deposition within the Lower Jurassic Precipice Sandstone and Evergreen Formation in the Surat Basin, Australia. *Marine and Petroleum Geology*, 109, 760-790.
- Longhitano, S. G., Mellere, D., Steel, R. J., & Ainsworth, R. B. (2012). Tidal depositional systems in the rock record: A review and new insights. *Sedimentary Geology*, 279, 2-22.

- Maceachern, J. A., & Bann, K. L. (2020). The Phycosiphon ichnofacies and the Rosselia ichnofacies: Two new ichnofacies for marine deltaic environments. *Journal of Sedimentary Research*, 90(8), 855-886.
- Manville, V. (2002). Sedimentary and geomorphic responses to ignimbrite emplacement: Readjustment of the Waikato River after the a.d. 181 Taupo Eruption, New Zealand. *The Journal of Geology*, 110(5), 519-541.
- Mulhern, J. S., Johnson, C. L., & Martin, J. M. (2019). Modern to ancient barrier island dimensional comparisons: Implications for analog selection and paleomorphodynamics. *Frontiers in Earth Science*, 7(109).
- Olariu, C., & Bhattacharya, J. (2006). Terminal distributary channels and delta front architecture of river-dominated delta systems. *Journal of Sedimentary Research*, 76, 212-233.
- Olariu, C., Bhattacharya, J. P., Leybourne, M. I., Boss, S. K., & Stern, R. J. (2012). Interplay between river discharge and topography of the basin floor in a hyperpycnal lacustrine delta. *Sedimentology*, 59(2), 704-728.
- Perillo, M. M., Best, J. L., & García, M. H. (2014). A new phase diagram for combined-flow bedforms. *Journal of Sedimentary Research*, 84(4), 301-313.
- Prothero, D. R., & Schwab, F. L. (2004). *Sedimentary Geology: An Introduction to Sedimentary Rocks and Stratigraphy*. (Vol. 1). New York, NY: W.H Freeman.
- Rossi, V. M., & Steel, R. J. (2016). The role of tidal, wave and river currents in the evolution of mixed-energy deltas: Example from the Lajas Formation (Argentina). *Sedimentology*, 63(4), 824-864.
- Smith, D. G., Hubbard, S. M., Leckie, D. A., & Fustic, M. (2009). Counter point bar deposits: Lithofacies and reservoir significance in the meandering modern Peace River and ancient McMurray Formation, Alberta, Canada. *Sedimentology*, 56(6), 1655-1669.
- Southard, J. B., & Boguchwal, L. A. (1990). Bed configurations in steady unidirectional water flows. Part 2. Synthesis of flume data. *Journal of Sedimentary Petrology*, 60(5), 658-679.
- Southard, J. B. (1991). Experimental determination of bed-form stability. *Annual Review of Earth and Planetary Sciences*, 19(1), 423-455.
- Taylor, A. M., & Goldring, R. (1993). Description and analysis of bioturbation and ichnofabric. *Journal of the Geological Society*, 150(1), 141-148.
- Tye, R. S., & Coleman, J. M. (1989). Evolution of Atchafalaya lacustrine deltas, south-central Louisiana. *Sedimentary Geology*, 65(1), 95-112.
- Tye, R. S. (2004). Geomorphology: An approach to determining subsurface reservoir dimensions. *American Association of Petroleum Geologists Bulletin*, 88(8), 1123-1147.
- Vakarelov, B. K., Ainsworth, R. B., & MacEachern, J. A. (2012). Recognition of wave-dominated, tide-influenced shoreline systems in the rock record: Variations from a microtidal shoreline model. *Sedimentary Geology*, 279, 23-41.

- Van Den Berg, J. H., & Van Gelder, A. (1993). A new bedform stability diagram, with emphasis on the transition of ripples to plane bed in flows over fine sand and silt. *Special Publications of the International Association of Sedimentologists*, 17, 11-21.
- Waikato Regional Council (WRC). (2018). *Aerial Photography - Historic Aerial Photographs*. Sourced from Retroleans and licensed by Land Information New Zealand (LINZ).
- Warrick, J. A. (2020). Littoral sediment from rivers: Patterns, rates and processes of river mouth morphodynamics. *Frontiers in Earth Science*, 8(355).
- Williams, P. W. (2017). Rivers and their landscapes. In P. W. Williams (Ed.), *New Zealand Landscape* (pp. 185-243). Elsevier.
- Wo, Y. G. (1994). *Reduction of Water and Bed Levels in the Lower Waikato River*. PhD thesis. University of Waikato, Hamilton, New Zealand.
- Wright, L. D. (1977). Sediment transport and deposition at river mouths: A synthesis. *GSA Bulletin*, 88(6), 857-868.
- Zurbuchen, J., Simms, A. R., Warrick, J. A., Miller, I. M., & Ritchie, A. (2020). A model for the growth and development of wave-dominated deltas fed by small mountainous rivers: Insights from the Elwha River delta, Washington. *Sedimentology*, 67(5), 2310-2331.

# Chapter 3

## Conclusions

---

A detailed hydrodynamic and sedimentology study was conducted on the intertidal portion of the sand spit at the mouth of the Waikato River, North Island, New Zealand. The main objective of the research was to test if the hydrodynamic processes could be linked to their sedimentological response in a mixed-influence (i.e., tides, river flow, waves) river mouth. By directly recording hydrodynamic processes and co-locating these to a robust sedimentological dataset of cores and surface samples, the hypothesis was that it is possible to interpret the controls on sedimentation and preservation over a tidal cycle, on a mixed-influence environment. This information has relevant applications to sedimentology, stratigraphy, and petroleum geology, by directly linking processes to bedforms in a complex wave-dominated coastline with a strong fluvial input. The results are an important step towards understanding how geoscientists can best use the present to interpret the past, and therefore, better unravel the complexities that make the rock record difficult to understand. One potential example of a use-case for this research is to predict sand body geometry in subsurface reservoirs of similar depositional affinity that are water or petroleum storage units (Purvis *et al.*, 2002), or for carbon storage to mitigate climate change (Holloway, 1997; Baines & Worden, 2004; Armitage *et al.*, 2010; La Croix *et al.*, 2019). This study is only one of the few recent pieces of research that links real-time hydrodynamic processes to associated sedimentary deposits (Ayranci *et al.*, 2012; Fricke *et al.*, 2017; Gugliotta *et al.*, 2017; Ayranci & Dashtgard, 2020; Choi *et al.*, 2020). Two questions were posed in chapter 1 and are re-stated with their conclusions outlined below.

- 1) *Can depositional processes be recorded using oceanographic instrumentation and linked to their corresponding sedimentary deposits?*

Being the longest river in New Zealand (Manville, 2002), the mouth of the Waikato River is subject to strong river flow, waves approaching from the west in the Tasman Sea, and tides have a mesotidal range (i.e., 2-4 m). Deployment of oceanographic instruments in an intertidal position on the sand spit recorded these hydrodynamic processes with a high fidelity. Wave heights were determined to be on average 1 m,



varying according to the level of tides, with seaward (east) directed flow reaching on average 1 m/s, and landward (west) directed flow reaching 0.8 m/s. Resultingly, there is a strong asymmetry between the flood tide and ebb tidal velocity and direction, and causing minimum flow velocity to occur in the early- to mid-ebb tide. Interactions between tides, waves and river flow produces multi-directional currents, orientated west, east, north, north-west and south.

Sedimentary bedforms and sedimentation patterns on the sand spit closely follow unidirectional and wave generated flows. Fast flow velocities during the flood and mid- to late-ebb tide, facilitate sediment erosion and transport, allowing for the formation of bedforms on the spit. Whereas minimum flow during the early- to mid-ebb tide result in the deposition of structureless sediment due to rapid fallout of sediment from the slows. Information on current velocities allow for the identification of the timing for erosion, transport and deposition of sediment, and the formation of sedimentary bedforms. Calculated orbital and unidirectional current velocities present that wave- and combined-flow ripples and dunes, and planar bedded sands develop on the spit, which were observed on the surface of the bed. The migrations of these bedforms produces sedimentary structures recorded in the stratigraphic record, and were observed in core.

2) *Is the sedimentary record biased towards certain processes operating at specific timeframes?*

It is well known that sedimentary structures are preserved signatures of the physical processes occurring at the time of deposition (Dalrymple, 2010). Combined-flow ripples and dunes, and planar bedded sand are produced from interacting river flow and waves. Whereas, wave ripples and dunes are produced by wave processes, with slight fluvial influence (Figure 2.12). Interestingly, despite being the mouth of a major river, there are no current ripples or dunes produced from river flow. Additionally, despite being situated in a setting subject to strong tides, the depositional record appears to be biased towards the wave and fluvial signature, and tides are subordinate. Tidal indications are manifest as rising and falling water levels, affecting current magnitude and velocity, but are not directly indicated in terms of “tidal” sedimentary structures (herringbone stratification, double mud drapes, etc.). Overall, not all of the processes operating through the full cycle were recorded in the sediments. Waves are important for sediment re-working, although it is not easy to attribute erosive surfaces to a specific time in the

cycle, perhaps most of the erosion occurs during the mid-flood tide when flow velocity is fastest (Figure 2.11). Whereas the early- to mid-ebb tide facilitates deposition due to minimum flow speeds less than 0.06 m/s. Ultimately, the sedimentary record in the sand spit at the mouth of the Waikato River shows that care must be taken in interpreting processes from their structures. In the context of the work of Ainsworth *et al.* (2011), the study area should be classified as Wft (Figure 3.1). However, the sedimentary structures and bedforms do not record the effect of tides, and so using only the sedimentary record, the river mouth would be classified as Wf. This difference in classification shows that the sedimentary record does not always capture all of the depositional processes in mixed-energy environments; which has implications for applied aspects of this research, modelling the morphology of coastlines in earths past and geobodies in subsurface reservoirs.

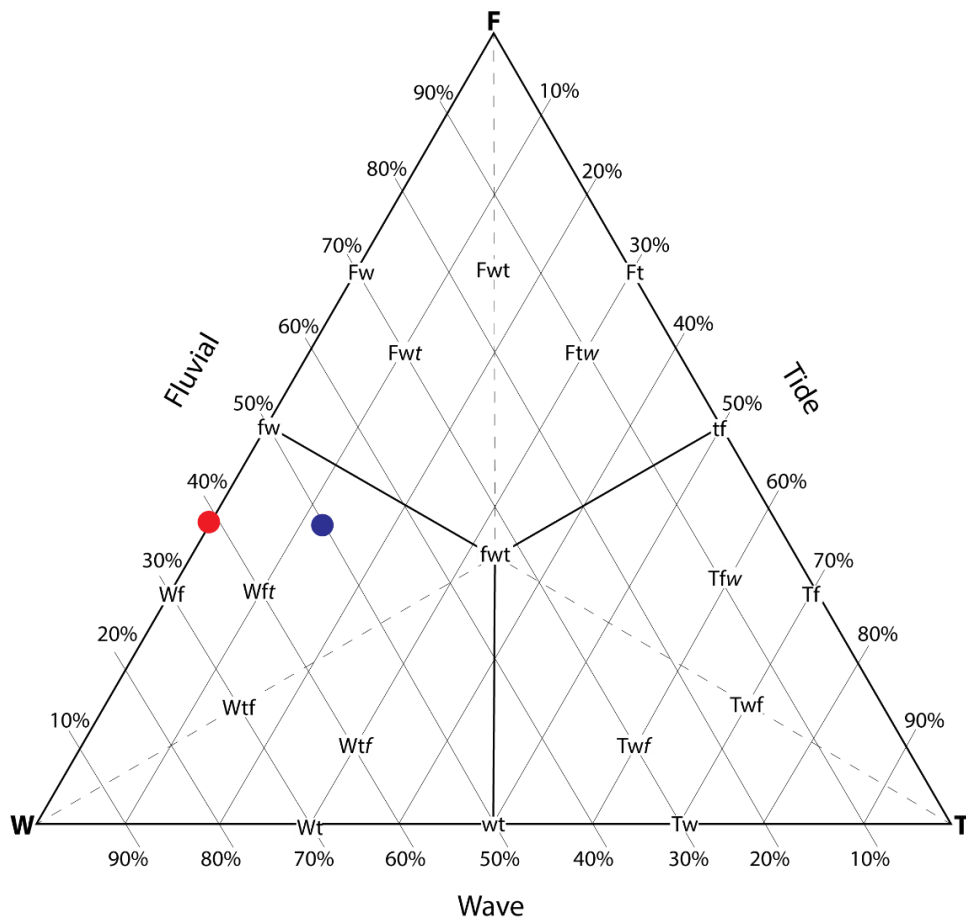


Figure 3.1: Waikato River mouth classified from Ainsworth *et al.* (2011). Classified as Wft using combined hydrodynamic and sedimentological dataset (blue), and Wf using only sedimentological data set (red).

In conclusion, this study has shown erosional and depositional processes vary in river mouth settings on time scales ranging from minutes, to hours, to days. Our ability to use

modern sedimentary environments as analogues to interpret the rock record is limited due to inferring dominant depositional processes from deposits. This is especially problematic because the sedimentological signature can be biased against tidal signature on a wave-dominated coastline with a large fluvial input. Highlighting the difficulty in interpreting physical processes in similar mixed-energy environments within the rock record. This study is one of a growing body of research into how mixed-influence depositional settings operate and are characterised (e.g. Bhattacharya & Giosan, 2003; Dashtgard *et al.*, 2012; Vakarelov *et al.*, 2012; Yang *et al.*, 2019). The results suggest that future research should involve: (1) vibracoring more of the spit to further investigate the sedimentary structures, (2) sampling box cores to identify biogenic structures (burrows) and potential infauna inhabiting the spit, and (3) investigating more areas of the river mouth to see how it fits into sedimentological classification (i.e. progradational or transgressive). Finally, this study adds an important time-series data set of process information for the Waikato River mouth, a location where regional erosion has been problematic and has impacted on the community (Dahm & Gibberd, 2019). Although, questions remain about the sand spits migration with long shore drift, and how the changing shoreline will affect the community. Under projected scenarios of climate change and associated level fluctuations the next step might be to examine longer term (e.g., seasonal, annual, interannual) trends in sedimentary processes and link these to deeper cores to look further back into the history of the area. This may lend clarity on how well short-term observations are useful for classifying sedimentary systems from their deposits.

### 3.1 References

- Ainsworth, R. B., Vakarelov, B. K., & Nanson, R. A. (2011). Dynamic spatial and temporal prediction of changes in depositional processes on clastic shorelines: Toward improved subsurface uncertainty reduction and management. *AAPG Bulletin*, 95(2), 267-297.
- Armitage, P. J., Worden, R. H., Faulkner, D. R., Aplin, A. C., Butcher, A. R., & Iliffe, J. (2010). Diagenetic and sedimentary controls on porosity in Lower Carboniferous fine-grained lithologies, Krechba field, Algeria: A petrological study of a caprock to a carbon capture site. *Marine and Petroleum Geology*, 27(7), 1395-1410.
- Ayranci, K., Lintern, D. G., Hill, P. R., & Dashtgard, S. E. (2012). Tide-supported gravity flows on the upper delta front, Fraser River delta, Canada. *Marine Geology*, 326-328, 166-170.
- Ayranci, K., & Dashtgard, S. E. (2020). Deep-water renewal events; Insights into deep water sediment transport mechanisms. *Scientific Reports*, 10(1), 6139.
- Baines, S. J., & Worden, R. H. (2004). Geological storage of carbon dioxide. *Geological Society Special Publication*, 233, 1-6.
- Bhattacharya, J., & Giosan, L. (2003). Wave-influenced deltas: Geomorphological implications for facies reconstruction. *Sedimentology*, 50, 187-210.
- Choi, K., Kim, D., & Jo, J. (2020). Morphodynamic evolution of the macrotidal Sittaung River estuary, Myanmar: Tidal versus seasonal controls. *Marine Geology*, 430, 106-367.
- Dahm, J., & Gibberd, B. (2019). *Waikato District Coastal Hazard Assessment*. Prepared for the Waikato District Council. Focus Report No. 19/130. Focus Resource Management Group.
- Dalrymple, R. W. (2010). Interpreting sedimentary successions: Facies, facies analysis and facies models. In N. P. James & R. W. Dalrymple (Eds.), *Facies Models 4* (4 ed.). St Johns, Newfoundland: Geological Association of Canada.
- Dashtgard, S., Venditti, J., Hill, P., Sisulak, C., Johnson, S., & La Croix, A. (2012). Sedimentation across the tidal-fluvial transition in the Lower Fraser River, Canada. *The Sedimentary Record*, 10, 4-9.
- Fricke, A. T., Nittrouer, C. A., Ogston, A. S., Nowacki, D. J., Asp, N. E., Souza Filho, P. W. M., da Silva, M. S., & Jalowska, A. M. (2017). River tributaries as sediment sinks: Processes operating where the Tapajós and Xingu rivers meet the Amazon tidal river. *Sedimentology*, 64(6), 1731-1753.
- Gugliotta, M., Saito, Y., Nguyen, V. L., Ta, T. K. O., Nakashima, R., Tamura, T., Uehara, K., Katsuki, K., & Yamamoto, S. (2017). Process regime, salinity, morphological, and sedimentary trends along the fluvial to marine transition zone of the mixed-energy Mekong River delta, Vietnam. *Continental Shelf Research*, 147, 7-26.

- Holloway, S. (1997). An overview of the underground disposal of carbon dioxide. *Energy Conversion and Management*, 38(SUPPL. 1), S193-S198.
- La Croix, A. D., Wang, J., He, J., Hannaford, C., Bianchi, V., Esterle, J., & Undershultz, J. R. (2019). Widespread nearshore and shallow marine deposition within the Lower Jurassic Precipice Sandstone and Evergreen Formation in the Surat Basin, Australia. *Marine and Petroleum Geology*, 109, 760-790.
- Manville, V. (2002). Sedimentary and geomorphic responses to ignimbrite emplacement: Readjustment of the Waikato River after the a.d. 181 Taupo Eruption, New Zealand. *The Journal of Geology*, 110(5), 519-541.
- Purvis, K., Kao, J., Flanagan, K., Henderson, J., & Duranti, D. (2002). Complex reservoir geometries in a deep water clastic sequence, Gryphon Field, UKCS: Injection structures, geological modelling and reservoir simulation. *Marine and Petroleum Geology*, 19(2), 161-179.
- Vakarelov, B. K., Ainsworth, R. B., & MacEachern, J. A. (2012). Recognition of wave-dominated, tide-influenced shoreline systems in the rock record: Variations from a microtidal shoreline model. *Sedimentary Geology*, 279, 23-41.
- Yang, B., Paik, S., Choi, Y., & Dalrymple, R. W. (2019). Sedimentology of a wave-dominated and tide-influenced deltaic system, upper Middle Miocene, southwestern Ulleung Basin, Korea. *Marine and Petroleum Geology*, 101, 78-89.

# Appendices

## Appendix A. Grainsize data

Summary grain size data used to produce the grain size map from Mastersizer® and GRADISTAT analysis of surface sediment (SS) and channel grab (GS) samples.

Table 1a: Mastersizer® data sheets showing proportion of sample within grain size bounds.

	Sample Name	SS1	SS2	SS3	SS4	SS5	SS6	SS7	SS8	SS9	SS10	SS11
	Measurement Date Time	17/02/2020	17/02/2020	17/02/2020	14/02/2020	14/02/2020	17/02/2020	14/02/2020	17/02/2020	17/02/2020	17/02/2020	17/02/2020
Grain size (um)	0.05	0.00	0.00	0.00	0.00	0.00	0.00	0.00	0.00	0.00	0.00	0.00
	0.06	0.00	0.00	0.00	0.00	0.00	0.00	0.00	0.00	0.00	0.00	0.00
	0.12	0.00	0.00	0.00	0.00	0.00	0.00	0.00	0.00	0.00	0.00	0.00
	0.24	0.00	0.00	0.00	0.00	0.00	0.00	0.00	0.00	0.00	0.00	0.00
	0.49	0.00	0.00	0.00	0.00	0.00	0.00	0.00	0.00	0.00	0.00	0.00
	0.98	0.00	0.00	0.00	0.00	0.00	0.00	0.00	0.00	0.00	0.00	0.00
	2	0.00	0.00	0.00	0.00	0.00	0.00	0.00	0.00	0.00	0.00	0.00
	3.9	0.00	0.00	0.00	0.00	0.00	0.00	0.00	0.00	0.00	0.00	0.00
	7.8	0.00	0.00	0.00	0.00	0.00	0.00	0.00	0.00	0.00	0.00	0.00
	15.6	0.00	0.00	0.00	0.00	0.00	0.00	0.00	0.00	0.00	0.00	0.00
	31	0.00	0.00	0.00	0.00	0.00	0.00	0.00	0.00	0.00	0.00	0.00
	37	0.00	0.00	0.00	0.00	0.00	0.00	0.00	0.00	0.00	0.00	0.00
	44	0.00	0.00	0.00	0.00	0.00	0.00	0.00	0.00	0.00	0.00	0.00
	53	0.00	0.00	0.00	0.00	0.00	0.00	0.00	0.00	0.00	0.00	0.00
	63	0.00	0.00	0.00	0.00	0.00	0.00	0.00	0.00	0.00	0.00	0.00
	74	0.01	0.02	0.02	0.00	0.01	0.01	0.00	0.00	0.01	0.25	0.00
	88	0.28	0.37	0.40	0.13	0.22	0.23	0.11	0.19	0.30	1.65	0.07
	105	1.61	1.71	1.92	1.08	1.41	1.44	1.05	1.33	1.44	4.41	0.67
	125	5.47	5.09	5.86	4.44	5.25	5.20	4.55	4.87	4.40	9.19	2.89
	149	10.53	9.28	10.64	9.33	10.61	10.27	9.78	9.64	8.18	13.47	6.31
	177	15.35	13.33	15.02	14.40	15.91	15.19	15.20	14.34	12.04	16.43	10.27
	210	19.08	16.94	18.32	18.89	20.04	19.09	19.73	18.28	15.92	17.55	14.84
	250	19.30	18.09	18.54	19.95	20.12	19.46	20.29	19.09	17.78	16.09	17.70
	300	13.18	13.48	12.86	14.20	13.37	13.37	13.86	13.64	14.00	10.20	14.79
	350	9.46	11.35	9.67	10.74	8.99	9.71	9.78	10.63	12.73	6.87	14.43
	420	4.32	6.52	4.78	5.19	3.66	4.50	4.31	5.49	8.00	2.98	9.79
	500	1.28	2.89	1.67	1.66	0.41	1.38	1.21	2.05	3.99	0.83	5.44
	590	0.13	0.83	0.29	0.00	0.00	0.16	0.11	0.41	1.19	0.07	2.37
	710	0.00	0.10	0.02	0.00	0.00	0.00	0.00	0.03	0.00	0.00	0.42
	840	0.00	0.00	0.00	0.00	0.00	0.00	0.00	0.00	0.00	0.00	0.00
	1000	0.00	0.00	0.00	0.00	0.00	0.00	0.00	0.00	0.00	0.00	0.00
	1190	0.00	0.00	0.00	0.00	0.00	0.00	0.00	0.00	0.00	0.00	0.00
	1410	0.00	0.00	0.00	0.00	0.00	0.00	0.00	0.00	0.00	0.00	0.00
1680	0.00	0.00	0.00	0.00	0.00	0.00	0.00	0.00	0.00	0.00	0.00	
2000	0.00	0.00	0.00	0.00	0.00	0.00	0.00	0.00	0.00	0.00	0.00	
2380	0.00	0.00	0.00	0.00	0.00	0.00	0.00	0.00	0.00	0.00	0.00	
2830	0.00	0.00	0.00	0.00	0.00	0.00	0.00	0.00	0.00	0.00	0.00	
3360	0.00	0.00	0.00	0.00	0.00	0.00	0.00	0.00	0.00	0.00	0.00	
Statistics	Dx (10)	157	159	154	164	159	159	164	161	164	135	177
	Dx (50)	245	258	245	254	243	247	249	253	271	220	292
	Dx (90)	382	423	390	393	369	385	382	400	445	356	482
	D [4,3]	259	277	261	268	254	261	263	269	289	235	313
	Kurtosis [3]	0.588	0.824	0.785	0.233	-0.003	0.613	0.579	0.8	0.239	0.769	0.461
	Skew [3]	0.822	0.921	0.891	0.735	0.64	0.832	0.809	0.897	0.779	0.897	0.847
	Laser Obscuration	9.58	10	9.94	11.6	9.73	10.49	11.4	10.2	9.84	10.74	10.3
	Weighted Residual	0.31	0.44	0.37	0.26	0.26	0.36	0.4	0.35	0.33	0.31	0.41
	Residual	0.35	0.47	0.41	0.29	0.31	0.39	0.44	0.38	0.36	0.34	0.44







Table 1b: GRADISTAT data sheets showing proportion of sample within grain size bounds.

**SAMPLE STATISTICS**

		<b>SS1</b>	<b>SS2</b>	<b>SS3</b>
ANALYST AND DATE:		Anya Podrumac, 4/15/2020	Anya Podrumac, 4/15/2020	Anya Podrumac, 4/15/2020
SAMPLE TYPE:		Unimodal, Moderately Well Sorted	Unimodal, Moderately Well Sorted	Unimodal, Moderately Well Sorted
TEXTURAL GROUP:		Sand	Sand	Sand
SEDIMENT NAME:		Moderately Well Sorted Fine Sand	Moderately Well Sorted Medium Sand	Moderately Well Sorted Fine Sand
FOLK AND WARD METHOD ( $\mu\text{m}$ )	MEAN ( $M_G$ ):	244.2	259.1	244.4
	SORTING ( $\sigma_G$ ):	1.417	1.470	1.441
	SKEWNESS ( $Sk_G$ ):	-0.006	0.006	0.001
	KURTOSIS ( $K_G$ ):	0.959	0.962	0.964
FOLK AND WARD METHOD (Description)	MEAN:	Fine Sand	Medium Sand	Fine Sand
	SORTING:	Moderately Well Sorted	Moderately Well Sorted	Moderately Well Sorted
	SKEWNESS:	Symmetrical	Symmetrical	Symmetrical
	KURTOSIS:	Mesokurtic	Mesokurtic	Mesokurtic
MODE ( $\mu\text{m}$ ):		230.0	275.0	230.0
$D_{10}$ ( $\mu\text{m}$ ):		155.5	157.0	153.4
$D_{50}$ ( $\mu\text{m}$ ):		244.7	258.4	244.9
$D_{90}$ ( $\mu\text{m}$ ):		386.8	423.8	395.1
$(D_{90} / D_{10})$ ( $\mu\text{m}$ ):		2.487	2.700	2.576
$(D_{90} - D_{10})$ ( $\mu\text{m}$ ):		231.3	266.9	241.7
$(D_{75} / D_{25})$ ( $\mu\text{m}$ ):		1.629	1.707	1.663
$(D_{75} - D_{25})$ ( $\mu\text{m}$ ):		120.5	139.5	126.0
$D_{10}$ ( $\phi$ ):		1.370	1.238	1.340
$D_{50}$ ( $\phi$ ):		2.031	1.953	2.030
$D_{90}$ ( $\phi$ ):		2.685	2.671	2.705
$(D_{90} / D_{10})$ ( $\phi$ ):		1.959	2.157	2.019
$(D_{90} - D_{10})$ ( $\phi$ ):		1.314	1.433	1.365
$(D_{75} / D_{25})$ ( $\phi$ ):		1.419	1.491	1.442
$(D_{75} - D_{25})$ ( $\phi$ ):		0.704	0.771	0.734
% GRAVEL:		0.0%	0.0%	0.0%
% SAND:		100.0%	100.0%	100.0%
% MUD:		0.0%	0.0%	0.0%
% V COARSE GRAVEL:		0.0%	0.0%	0.0%
% COARSE GRAVEL:		0.0%	0.0%	0.0%
% MEDIUM GRAVEL:		0.0%	0.0%	0.0%
% FINE GRAVEL:		0.0%	0.0%	0.0%
% V FINE GRAVEL:		0.0%	0.0%	0.0%
% V COARSE SAND:		0.0%	0.0%	0.0%
% COARSE SAND:		1.4%	3.8%	2.0%
% MEDIUM SAND:		46.3%	49.4%	45.8%
% FINE SAND:		50.4%	44.6%	49.8%
% V FINE SAND:		1.9%	2.1%	2.3%
% V COARSE SILT:		0.0%	0.0%	0.0%
% COARSE SILT:		0.0%	0.0%	0.0%
% MEDIUM SILT:		0.0%	0.0%	0.0%
% FINE SILT:		0.0%	0.0%	0.0%
% V FINE SILT:		0.0%	0.0%	0.0%
% CLAY:		0.0%	0.0%	0.0%

SS4	SS5	SS6	SS7	SS8
Anya Podrumac, 4/15/2020	Anya Podrumac, 4/15/2020	Anya Podrumac, 4/15/2020	Anya Podrumac, 4/15/2020	Anya Podrumac, 4/15/2020
Unimodal, Well Sorted	Unimodal, Well Sorted	Unimodal, Moderately Well Sorted	Unimodal, Well Sorted	Unimodal, Moderately Well Sorted
Sand	Sand	Sand	Sand	Sand
Well Sorted Medium Sand	Well Sorted Fine Sand	Moderately Well Sorted Fine Sand	Well Sorted Fine Sand	Moderately Well Sorted Medium Sand
253.9	242.0	246.4	248.9	254.1
1.411	1.393	1.415	1.394	1.434
0.002	-0.015	-0.002	0.002	0.015
0.955	0.955	0.960	0.953	0.963
Medium Sand	Fine Sand	Fine Sand	Fine Sand	Medium Sand
Well Sorted	Well Sorted	Moderately Well Sorted	Well Sorted	Moderately Well Sorted
Symmetrical	Symmetrical	Symmetrical	Symmetrical	Symmetrical
Mesokurtic	Mesokurtic	Mesokurtic	Mesokurtic	Mesokurtic
275.0	230.0	230.0	230.0	230.0
161.5	156.7	157.0	160.7	158.9
254.0	242.6	246.8	249.1	253.2
398.1	372.4	389.9	387.2	405.7
2.466	2.376	2.483	2.409	2.553
236.7	215.7	232.9	226.5	246.8
1.620	1.590	1.627	1.597	1.653
123.6	113.1	121.2	117.6	128.7
1.329	1.425	1.359	1.369	1.301
1.977	2.043	2.019	2.005	1.981
2.631	2.674	2.671	2.638	2.654
1.980	1.876	1.966	1.927	2.039
1.302	1.249	1.312	1.269	1.352
1.427	1.390	1.421	1.405	1.448
0.696	0.669	0.702	0.676	0.725
0.0%	0.0%	0.0%	0.0%	0.0%
100.0%	100.0%	100.0%	100.0%	100.0%
0.0%	0.0%	0.0%	0.0%	0.0%
0.0%	0.0%	0.0%	0.0%	0.0%
0.0%	0.0%	0.0%	0.0%	0.0%
0.0%	0.0%	0.0%	0.0%	0.0%
0.0%	0.0%	0.0%	0.0%	0.0%
0.0%	0.0%	0.0%	0.0%	0.0%
0.0%	0.0%	0.0%	0.0%	0.0%
0.0%	0.0%	0.0%	0.0%	0.0%
1.7%	0.4%	1.5%	1.3%	2.5%
50.1%	46.1%	47.0%	48.2%	48.9%
47.1%	51.8%	49.7%	49.3%	47.1%
1.2%	1.6%	1.7%	1.2%	1.5%
0.0%	0.0%	0.0%	0.0%	0.0%
0.0%	0.0%	0.0%	0.0%	0.0%
0.0%	0.0%	0.0%	0.0%	0.0%
0.0%	0.0%	0.0%	0.0%	0.0%
0.0%	0.0%	0.0%	0.0%	0.0%
0.0%	0.0%	0.0%	0.0%	0.0%
0.0%	0.0%	0.0%	0.0%	0.0%



SS14	SS15	SS16	SS17	GS1
Anya Podrumac, 4/15/2020	Anya Podrumac, 4/15/2020	Anya Podrumac, 4/15/2020	Anya Podrumac, 4/15/2020	Anya Podrumac, 4/15/2020
Unimodal, Moderately Well Sorted Sand	Unimodal, Moderately Well Sorted Sand	Unimodal, Moderately Well Sorted Sand	Unimodal, Well Sorted Sand	Unimodal, Moderately Well Sorted Sand
oderately Well Sorted Medium Sand	oderately Well Sorted Medium Sand	oderately Well Sorted Medium Sand	Well Sorted Fine Sand	oderately Well Sorted Medium Sand
289.4	275.4	328.8	242.2	264.7
1.443	1.421	1.489	1.365	1.462
0.005	0.004	0.014	0.005	-0.003
0.958	0.978	0.958	0.963	0.960
Medium Sand	Medium Sand	Medium Sand	Fine Sand	Medium Sand
Moderately Well Sorted	Moderately Well Sorted	Moderately Well Sorted	Well Sorted	Moderately Well Sorted
Symmetrical	Symmetrical	Symmetrical	Symmetrical	Symmetrical
Mesokurtic	Mesokurtic	Mesokurtic	Mesokurtic	Mesokurtic
275.0	275.0	325.0	230.0	275.0
181.2	176.7	196.8	160.3	160.8
289.1	275.0	328.1	241.9	264.5
468.5	432.9	553.4	360.5	430.4
2.585	2.450	2.812	2.248	2.677
287.3	256.2	356.6	200.1	269.7
1.670	1.611	1.742	1.541	1.691
150.3	132.3	185.1	105.1	140.2
1.094	1.208	0.854	1.472	1.216
1.790	1.863	1.608	2.047	1.919
2.464	2.500	2.345	2.641	2.637
2.253	2.070	2.748	1.794	2.168
1.370	1.293	1.492	1.169	1.421
1.522	1.453	1.666	1.359	1.491
0.740	0.688	0.800	0.624	0.758
0.0%	0.0%	0.0%	0.0%	0.0%
100.0%	100.0%	100.0%	100.0%	100.0%
0.0%	0.0%	0.0%	0.0%	0.0%
0.0%	0.0%	0.0%	0.0%	0.0%
0.0%	0.0%	0.0%	0.0%	0.0%
0.0%	0.0%	0.0%	0.0%	0.0%
0.0%	0.0%	0.0%	0.0%	0.0%
0.0%	0.0%	0.0%	0.0%	0.0%
0.0%	0.0%	0.0%	0.0%	0.0%
0.0%	0.0%	0.0%	0.0%	0.0%
6.5%	3.8%	15.0%	0.3%	3.9%
58.6%	56.7%	59.9%	45.7%	51.8%
34.4%	39.0%	25.0%	53.0%	42.6%
0.4%	0.5%	0.2%	1.0%	1.7%
0.0%	0.0%	0.0%	0.0%	0.0%
0.0%	0.0%	0.0%	0.0%	0.0%
0.0%	0.0%	0.0%	0.0%	0.0%
0.0%	0.0%	0.0%	0.0%	0.0%
0.0%	0.0%	0.0%	0.0%	0.0%
0.0%	0.0%	0.0%	0.0%	0.0%
0.0%	0.0%	0.0%	0.0%	0.0%
0.0%	0.0%	0.0%	0.0%	0.0%

GS2	GS3	GS4	GS5	GS6
Anya Podrumac, 4/15/2020	Anya Podrumac, 4/15/2020	Anya Podrumac, 4/15/2020	Anya Podrumac, 4/15/2020	Anya Podrumac, 4/15/2020
Unimodal, Well Sorted	Unimodal, Moderately Well Sorted	Unimodal, Moderately Well Sorted	Unimodal, Moderately Sorted	Unimodal, Moderately Well Sorted
Sand	Sand	Sand	Slightly Gravelly Sand	Sand
Well Sorted Fine Sand	Moderately Well Sorted Medium Sand	Moderately Well Sorted Medium Sand	Slightly Very Fine Gravelly Medium Sand	Moderately Well Sorted Medium Sand
249.2	391.8	371.6	409.7	332.5
1.350	1.566	1.442	1.635	1.540
-0.006	0.045	0.004	0.079	0.036
0.969	0.960	0.941	0.987	0.962
Fine Sand	Medium Sand	Medium Sand	Medium Sand	Medium Sand
Well Sorted	Moderately Well Sorted	Moderately Well Sorted	Moderately Sorted	Moderately Well Sorted
Symmetrical	Symmetrical	Symmetrical	Symmetrical	Symmetrical
Mesokurtic	Mesokurtic	Mesokurtic	Mesokurtic	Mesokurtic
230.0	385.0	385.0	385.0	325.0
168.4	222.1	230.2	223.3	191.9
249.7	387.2	371.6	401.6	329.7
368.0	707.2	589.7	795.6	583.2
2.185	3.184	2.562	3.563	3.040
199.6	485.1	359.5	572.3	391.4
1.514	1.867	1.673	1.956	1.824
104.2	247.3	193.0	277.8	202.6
1.442	0.500	0.762	0.330	0.778
2.001	1.369	1.428	1.316	1.601
2.570	2.170	2.119	2.163	2.382
1.782	4.343	2.781	6.556	3.062
1.128	1.671	1.357	1.833	1.604
1.351	1.991	1.701	2.187	1.750
0.598	0.901	0.742	0.968	0.867
0.0%	0.0%	0.0%	0.1%	0.0%
100.0%	100.0%	100.0%	100.0%	100.0%
0.0%	0.0%	0.0%	0.0%	0.0%
0.0%	0.0%	0.0%	0.0%	0.0%
0.0%	0.0%	0.0%	0.0%	0.0%
0.0%	0.0%	0.0%	0.0%	0.0%
0.0%	0.0%	0.0%	0.0%	0.0%
0.0%	0.0%	0.0%	0.1%	0.0%
0.0%	2.0%	0.0%	4.4%	0.4%
0.3%	27.1%	21.2%	28.7%	17.2%
49.6%	55.0%	64.6%	51.5%	56.3%
49.6%	15.9%	14.2%	15.3%	25.9%
0.5%	0.0%	0.0%	0.0%	0.3%
0.0%	0.0%	0.0%	0.0%	0.0%
0.0%	0.0%	0.0%	0.0%	0.0%
0.0%	0.0%	0.0%	0.0%	0.0%
0.0%	0.0%	0.0%	0.0%	0.0%
0.0%	0.0%	0.0%	0.0%	0.0%
0.0%	0.0%	0.0%	0.0%	0.0%
0.0%	0.0%	0.0%	0.0%	0.0%
0.0%	0.0%	0.0%	0.0%	0.0%



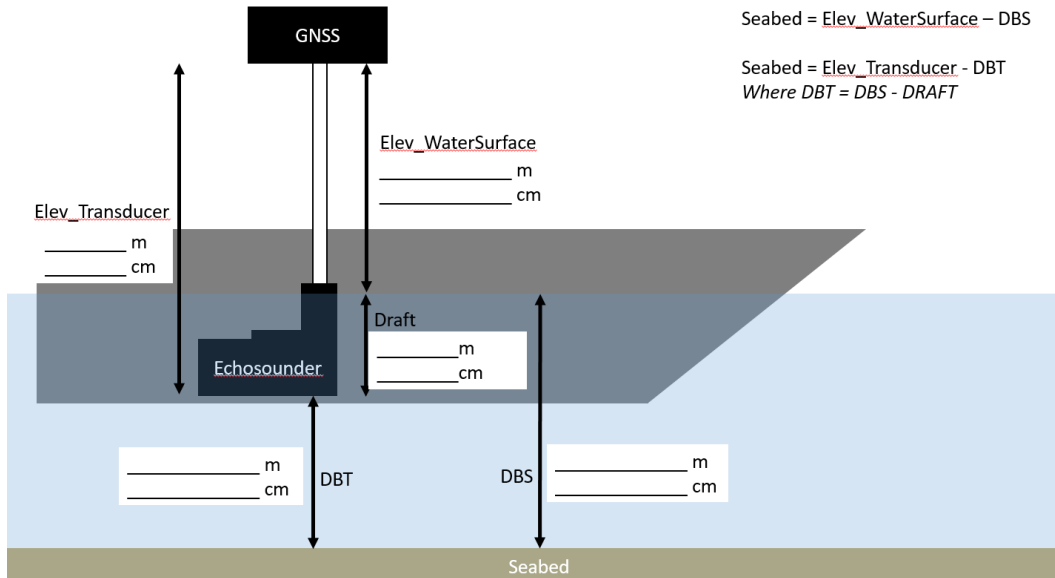


GS17	GS22	GS23	GS24
Anya Podrumac, 4/15/2020	Anya Podrumac, 4/15/2020	Anya Podrumac, 4/15/2020	Anya Podrumac, 4/15/2020
Unimodal, Moderately Well Sorted	Unimodal, Well Sorted	Unimodal, Moderately Sorted	Unimodal, Moderately Well Sorted
Sand	Sand	Slightly Gravelly Sand	Sand
Moderately Well Sorted Medium Sand	Well Sorted Fine Sand	Slightly Very Fine Gravelly Medium Sand	Moderately Well Sorted Medium Sand
349.5	211.7	358.1	316.6
1.515	1.400	1.663	1.487
0.026	-0.013	0.073	0.012
0.952	0.930	0.984	0.953
Medium Sand	Fine Sand	Medium Sand	Medium Sand
Moderately Well Sorted	Well Sorted	Moderately Sorted	Moderately Well Sorted
Symmetrical	Symmetrical	Symmetrical	Symmetrical
Mesokurtic	Mesokurtic	Mesokurtic	Mesokurtic
325.0	230.0	325.0	325.0
207.8	135.4	190.7	188.9
347.6	212.2	351.3	314.9
598.5	327.4	708.1	530.8
2.880	2.418	3.713	2.810
390.6	192.0	517.4	341.9
1.785	1.618	2.006	1.741
205.3	102.9	252.9	177.0
0.741	1.611	0.498	0.914
1.525	2.237	1.509	1.667
2.267	2.885	2.391	2.404
3.060	1.791	4.800	2.631
1.526	1.274	1.893	1.491
1.760	1.367	2.017	1.632
0.836	0.694	1.004	0.800
0.0%	0.0%	0.0%	0.0%
100.0%	100.0%	100.0%	100.0%
0.0%	0.0%	0.0%	0.0%
0.0%	0.0%	0.0%	0.0%
0.0%	0.0%	0.0%	0.0%
0.0%	0.0%	0.0%	0.0%
0.0%	0.0%	0.0%	0.0%
0.0%	0.0%	0.0%	0.0%
0.0%	0.0%	0.0%	0.0%
0.3%	0.0%	2.9%	0.0%
19.5%	0.0%	22.6%	12.6%
58.9%	31.8%	50.0%	58.9%
21.3%	62.6%	24.1%	28.2%
0.1%	5.6%	0.5%	0.3%
0.0%	0.0%	0.0%	0.0%
0.0%	0.0%	0.0%	0.0%
0.0%	0.0%	0.0%	0.0%
0.0%	0.0%	0.0%	0.0%
0.0%	0.0%	0.0%	0.0%

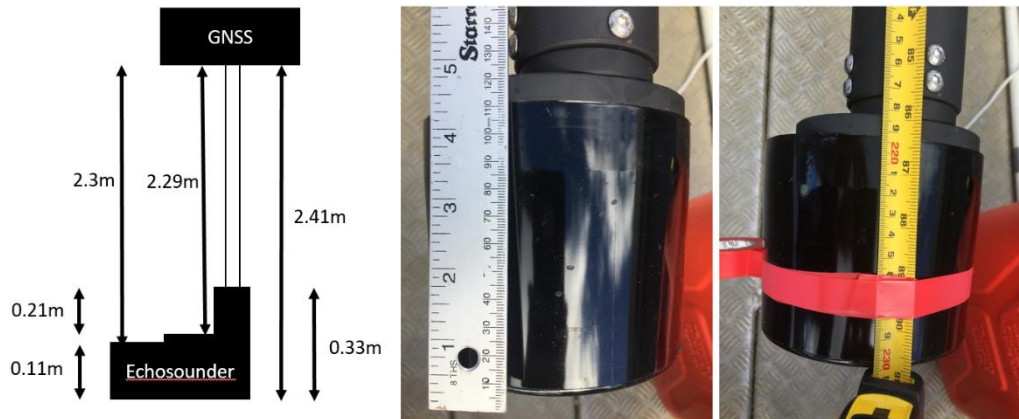


## Appendix B. Topography and Bathymetry

The sonar was also calibrated to the RTK base stations. Bathymetry data was calibrated to GNSS height and echo sounder depth below the research vessel in order to calculate seabed elevation



## ECHOSOUNDER



## Appendix C. Process Data from Oceanographic Instruments

Time series results of all parameters measured for each instrument. Table presents the order of appearance and figure numbers.

Site Name	Instruments	Figure No.
Site C	Nortek Vector	1
Site D	Nortek Aquadopp	2
Site D	RBR Concerto	3
Site E	Nortek Aquadopp	4
Site E	RBR Concerto	5
Site F	Nortek Aquadopp	6
Site F	RBR Concerto	7
Site H	Nortek Vector	8

Site C: Nortek Vector  
Figure 1a: Raw data.

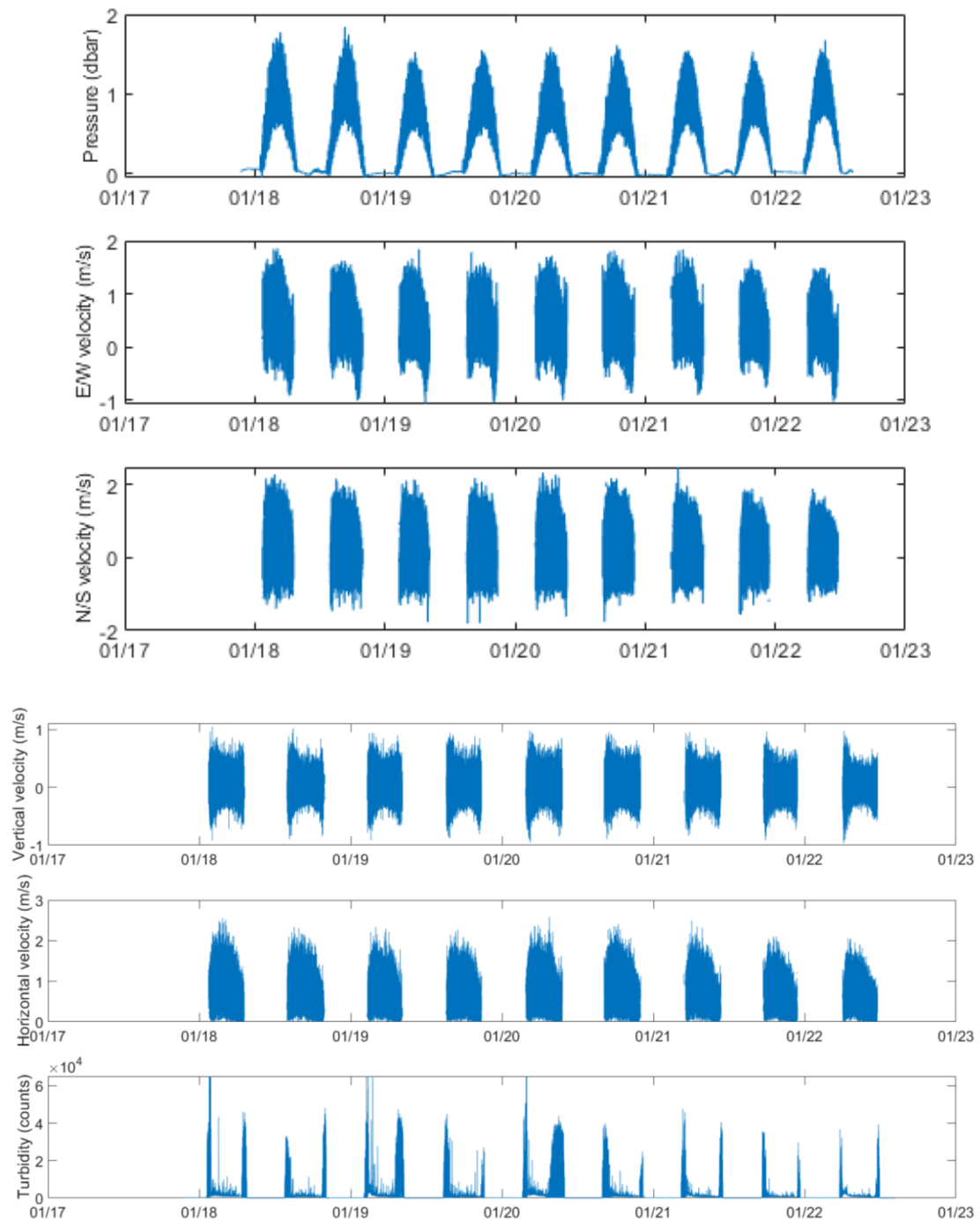
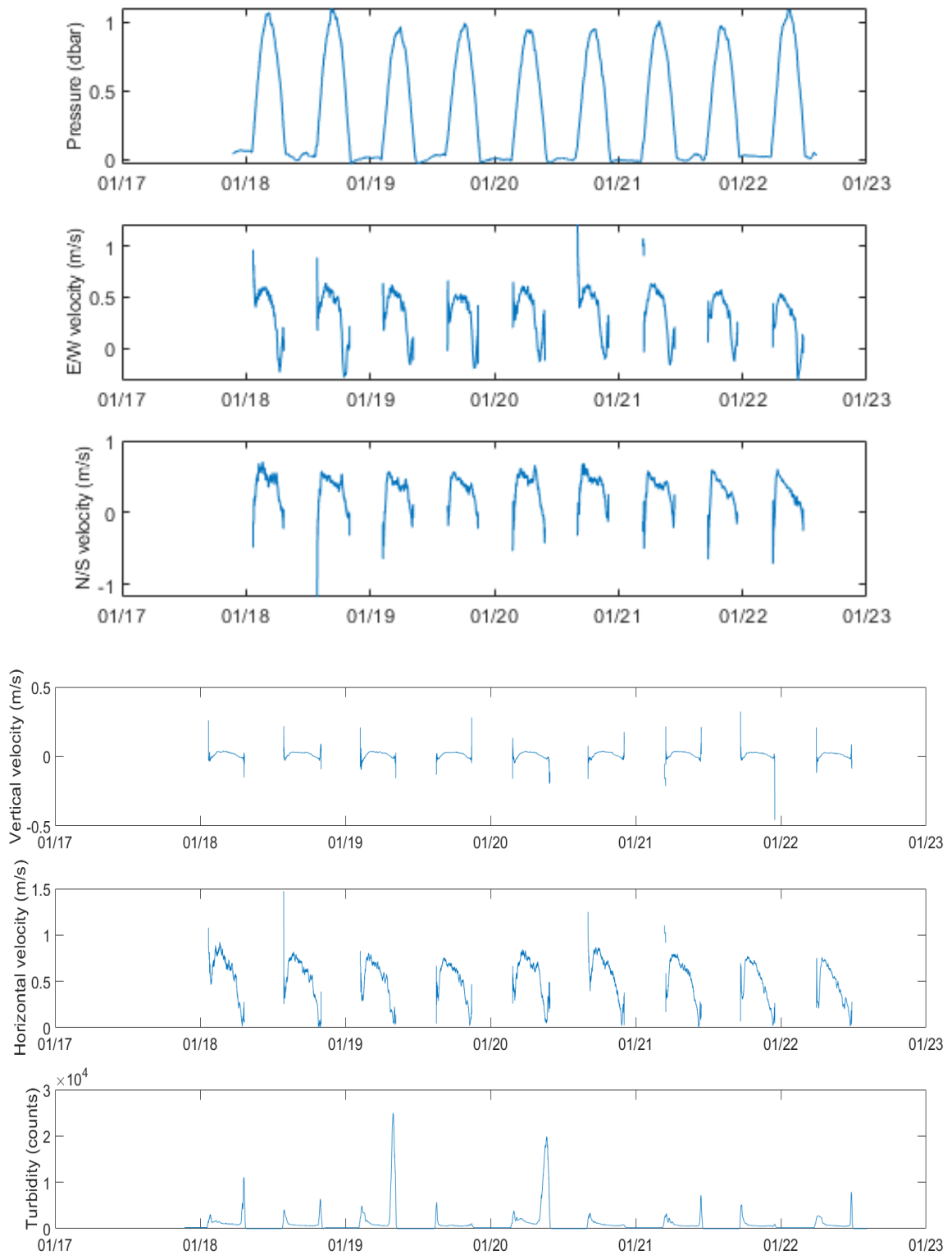


Figure 1b: Data averaged over 10 minutes



Site D: Nortek Aquadopp

Figure 2a: Raw Data.

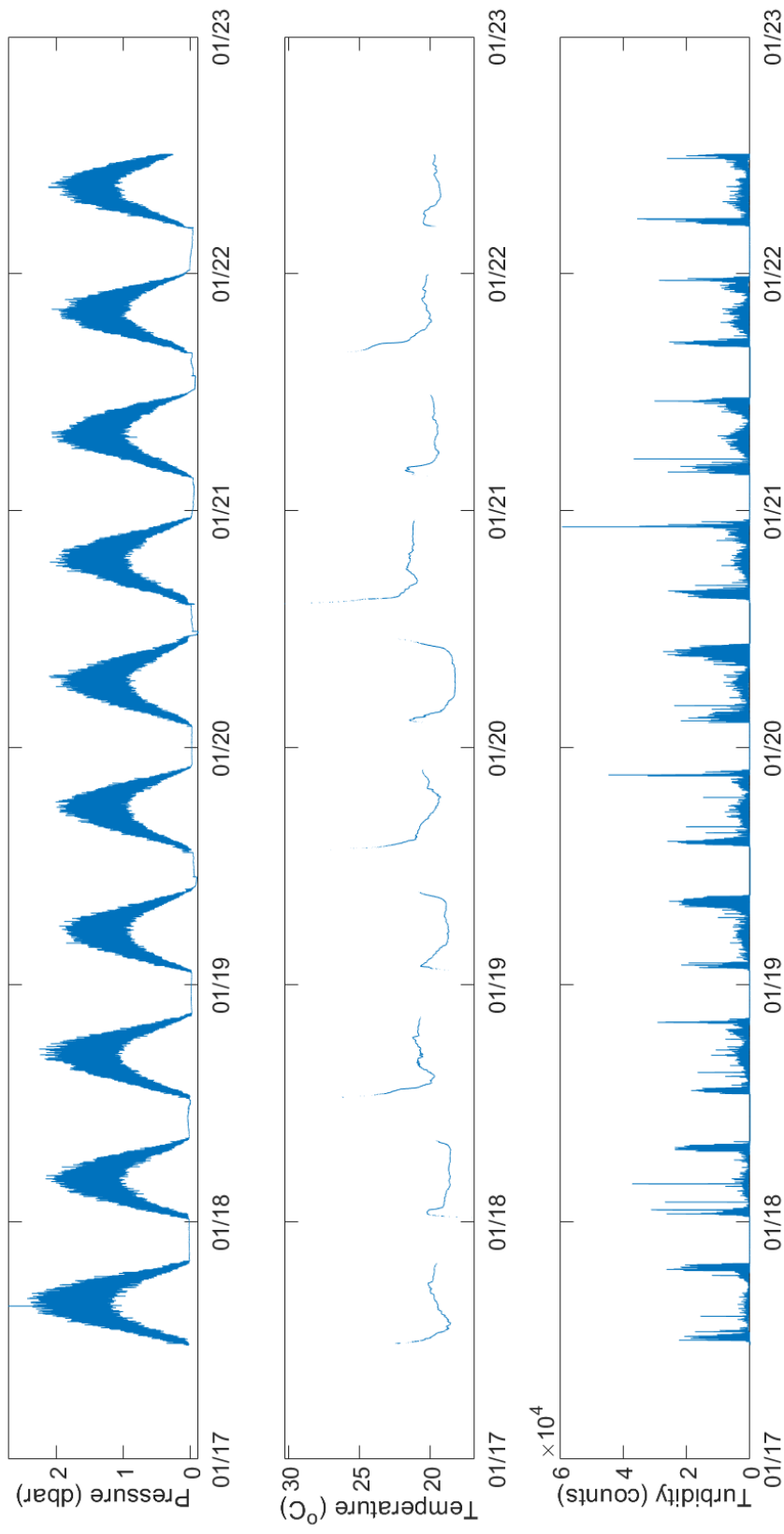


Figure 2b: Raw data

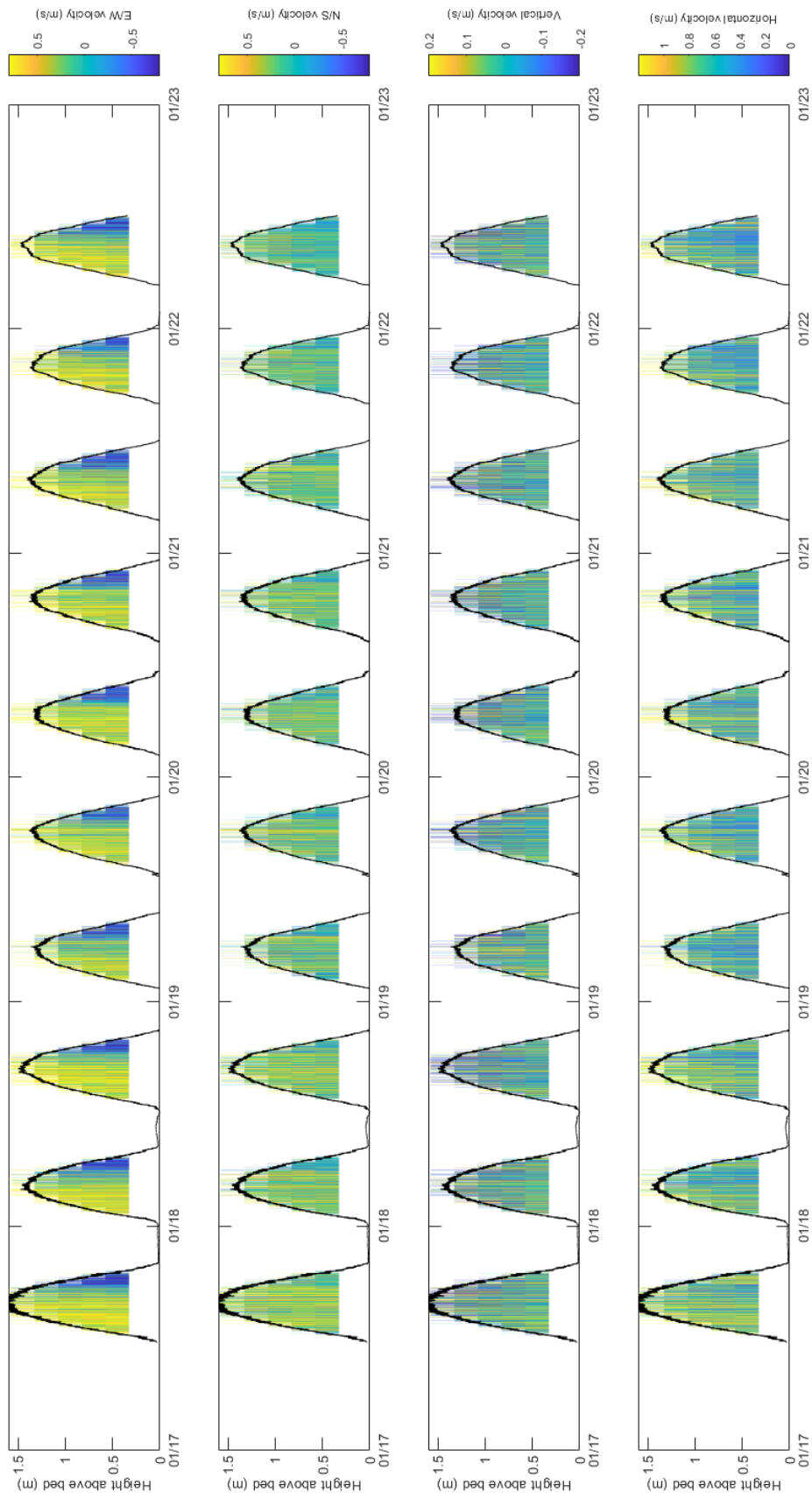
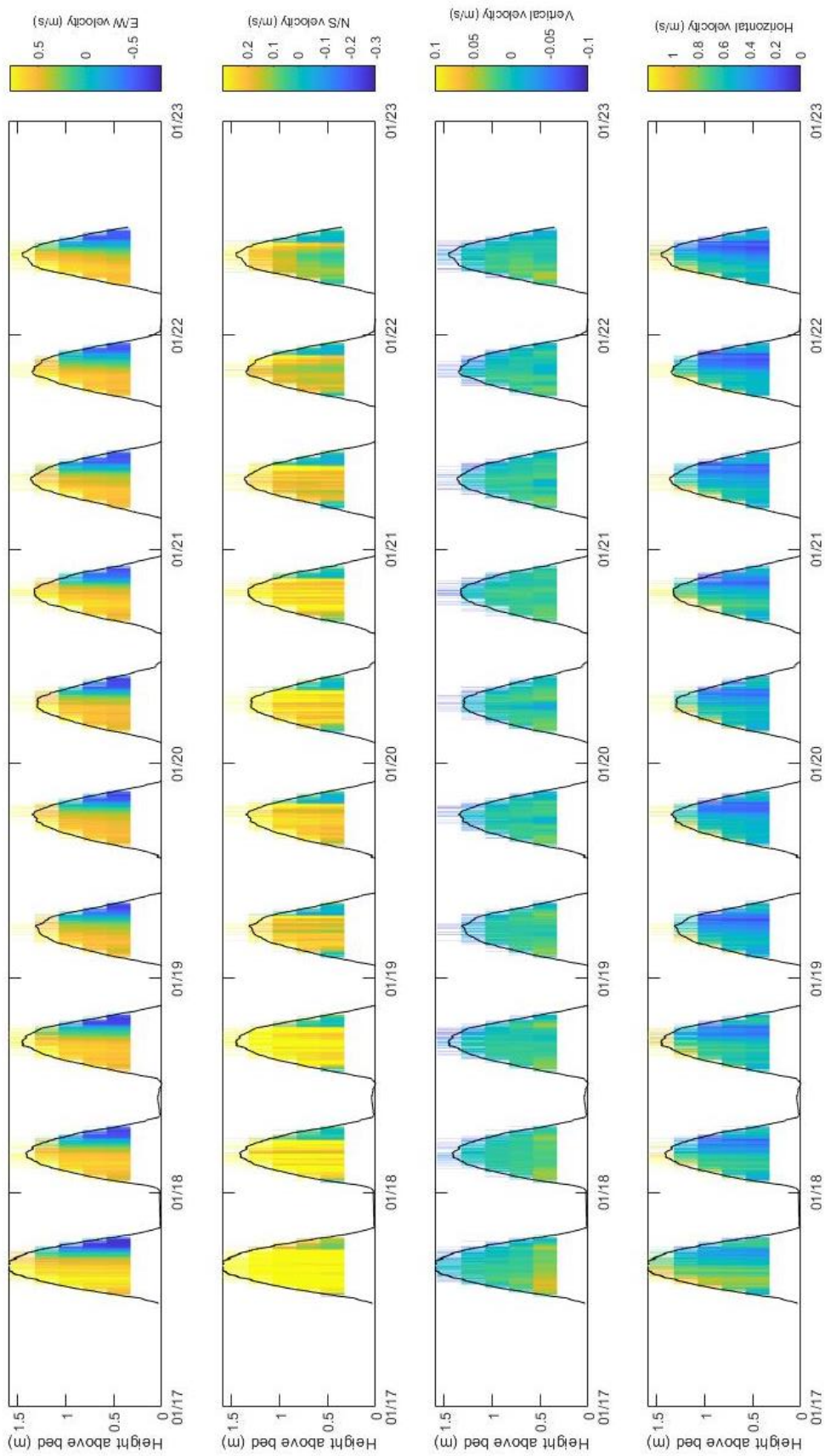


Figure 2c: Data averaged over 10 minutes



Site D: RBR Concerto

Figure 3a

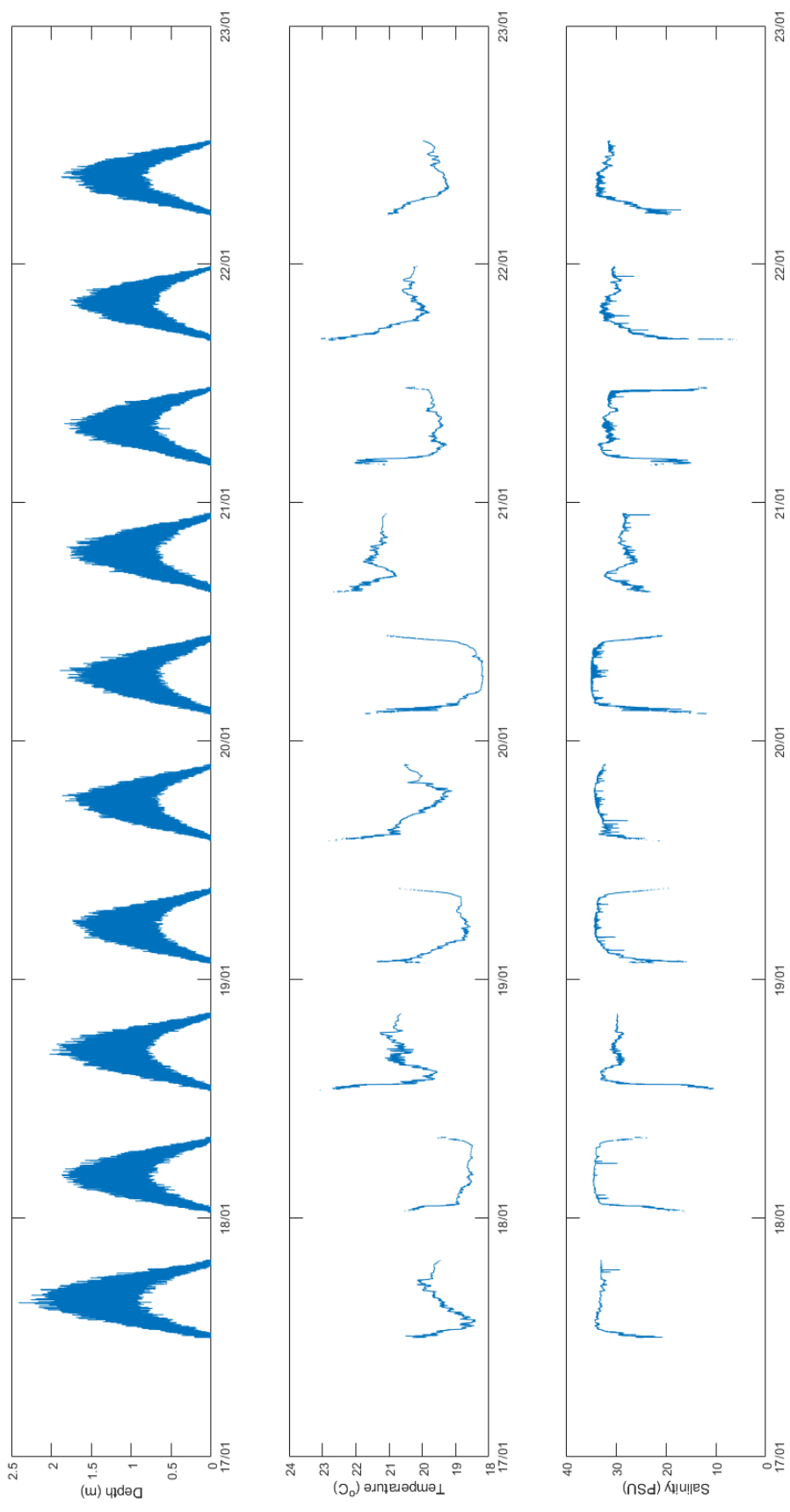




Figure 3b

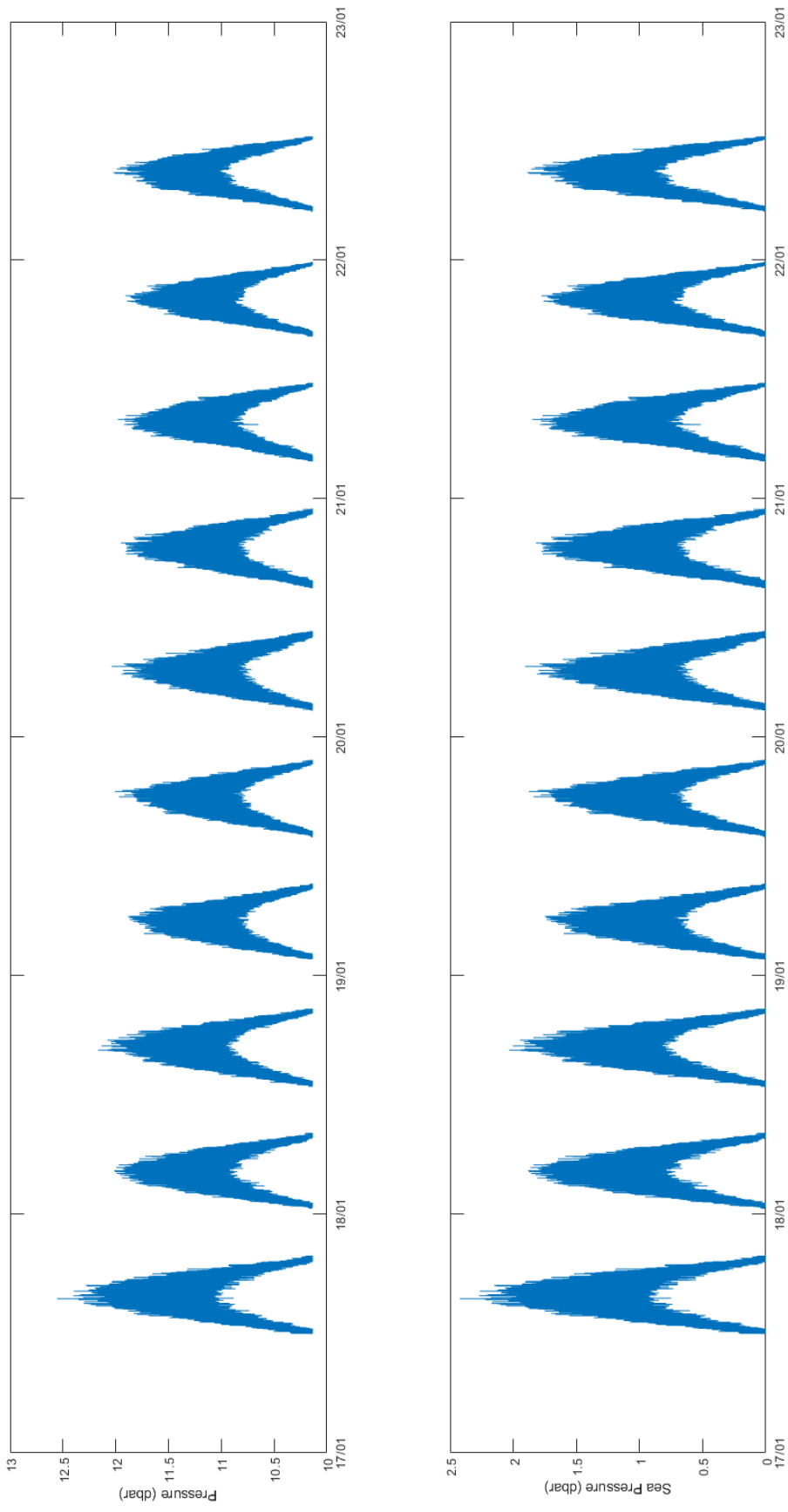
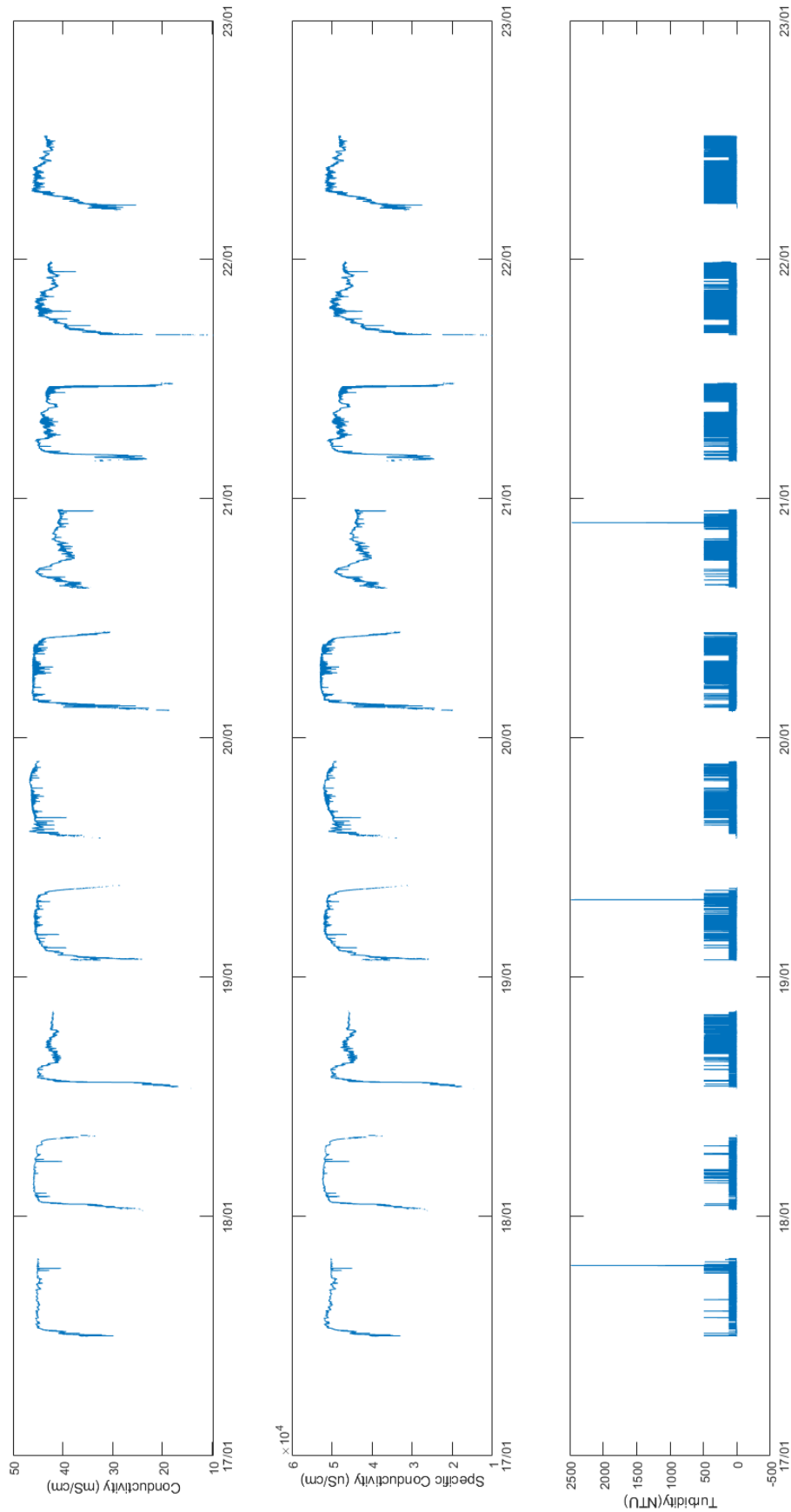


Figure 3c



Site E: Nortek Aquadopp

Figure 4a

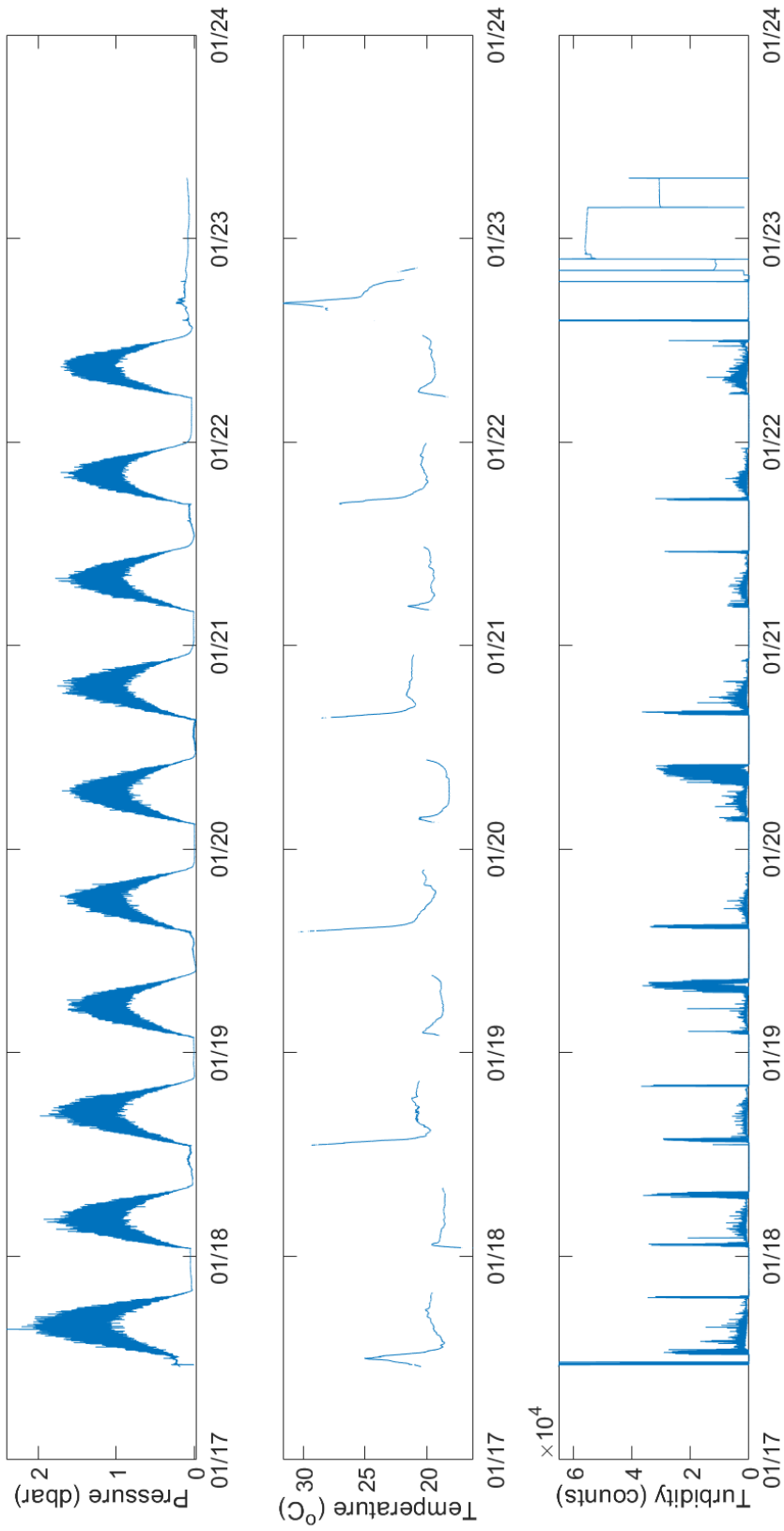


Figure 4b: Raw data

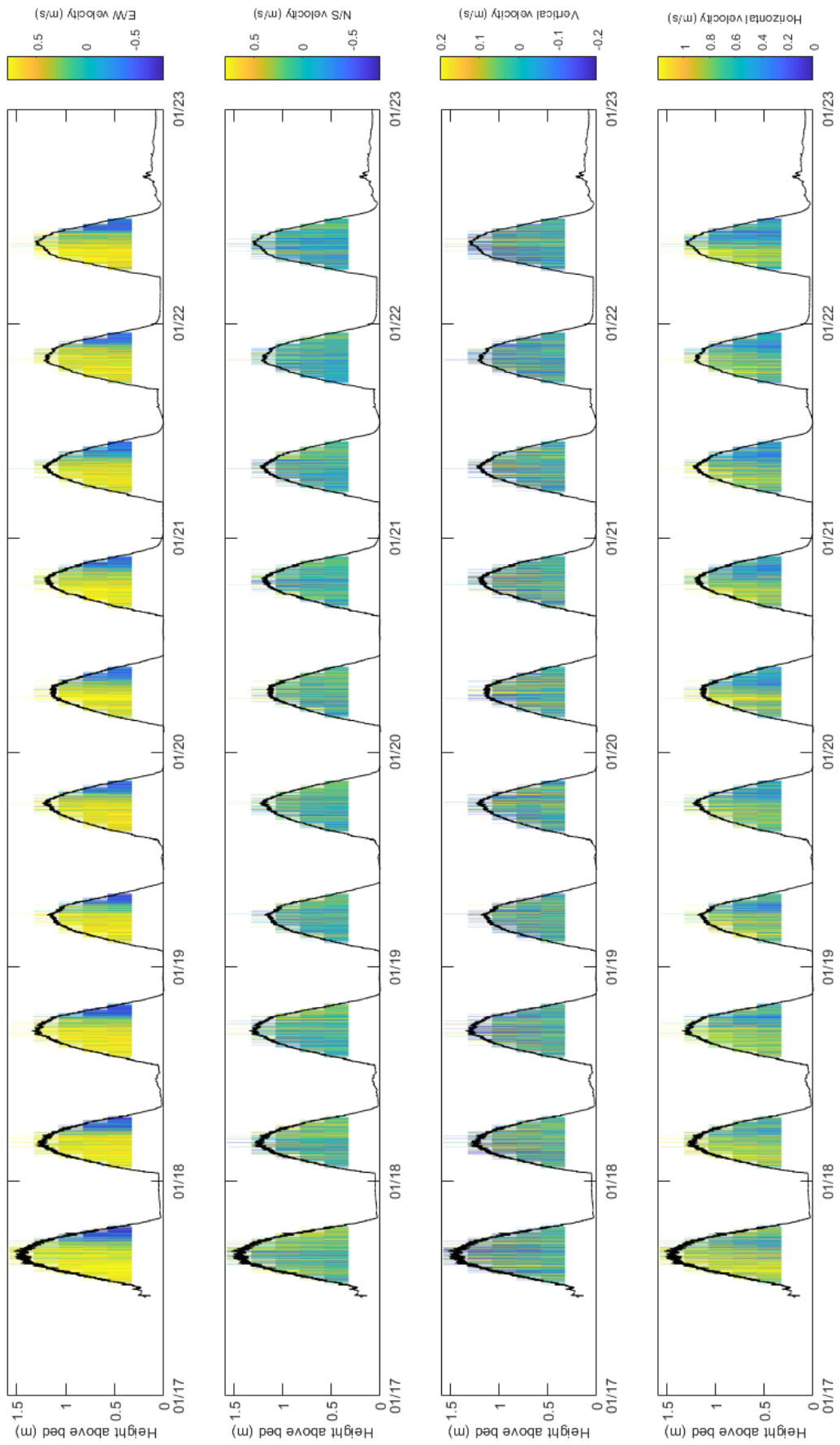
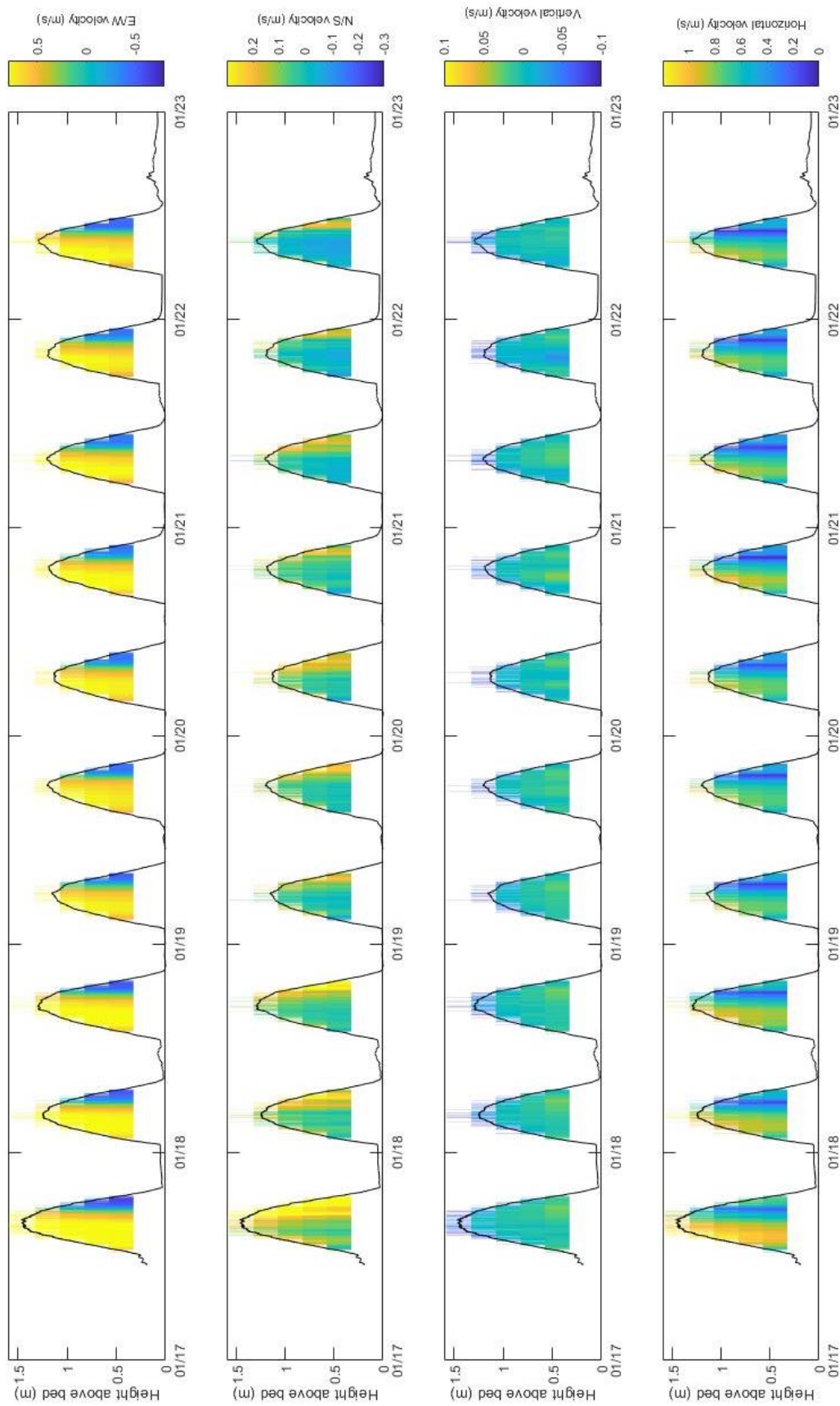


Figure 4c: Data averaged over 10 minutes



Site E: RBR Concerto (RBR logger)

Figure 5a

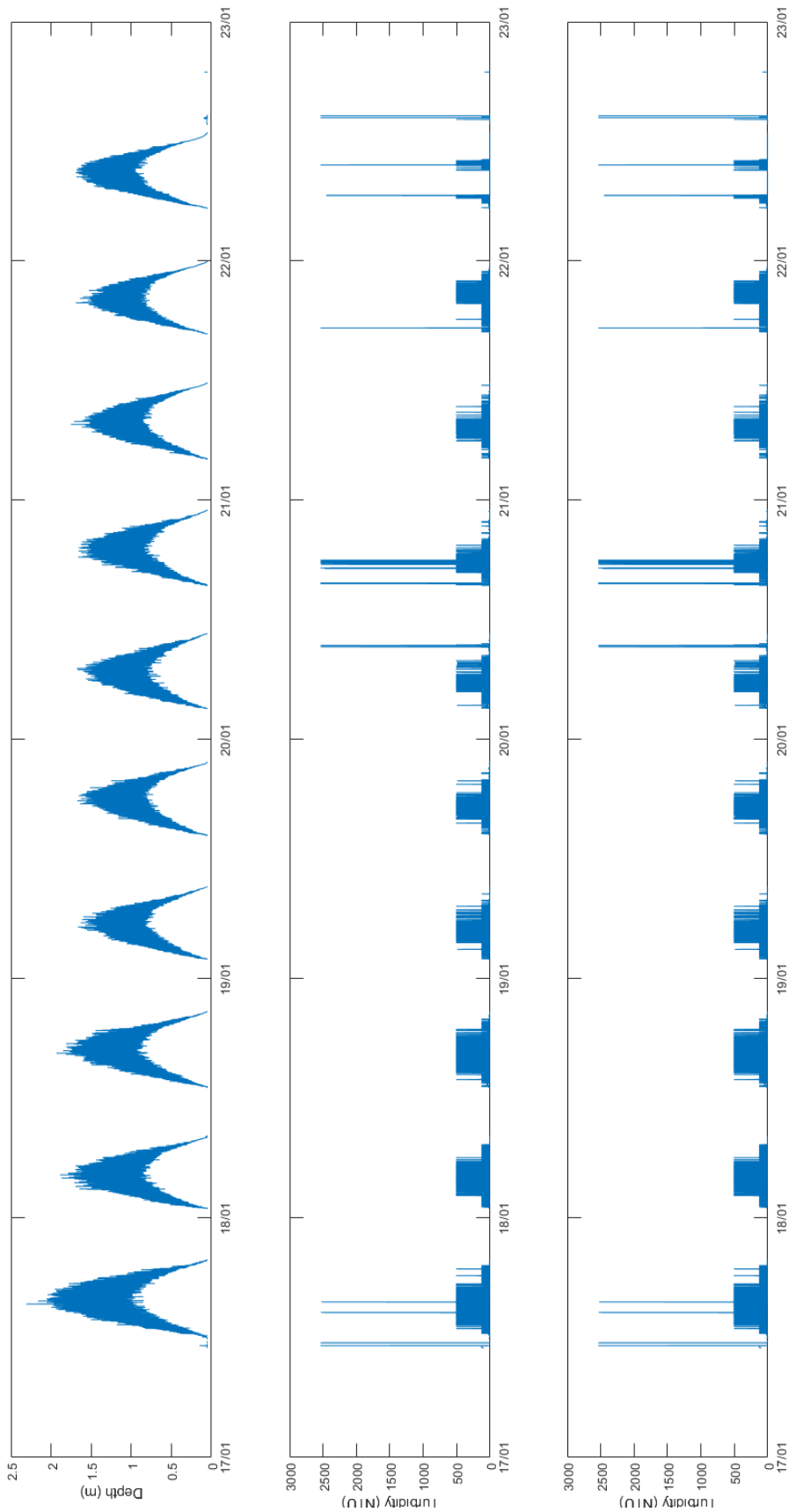
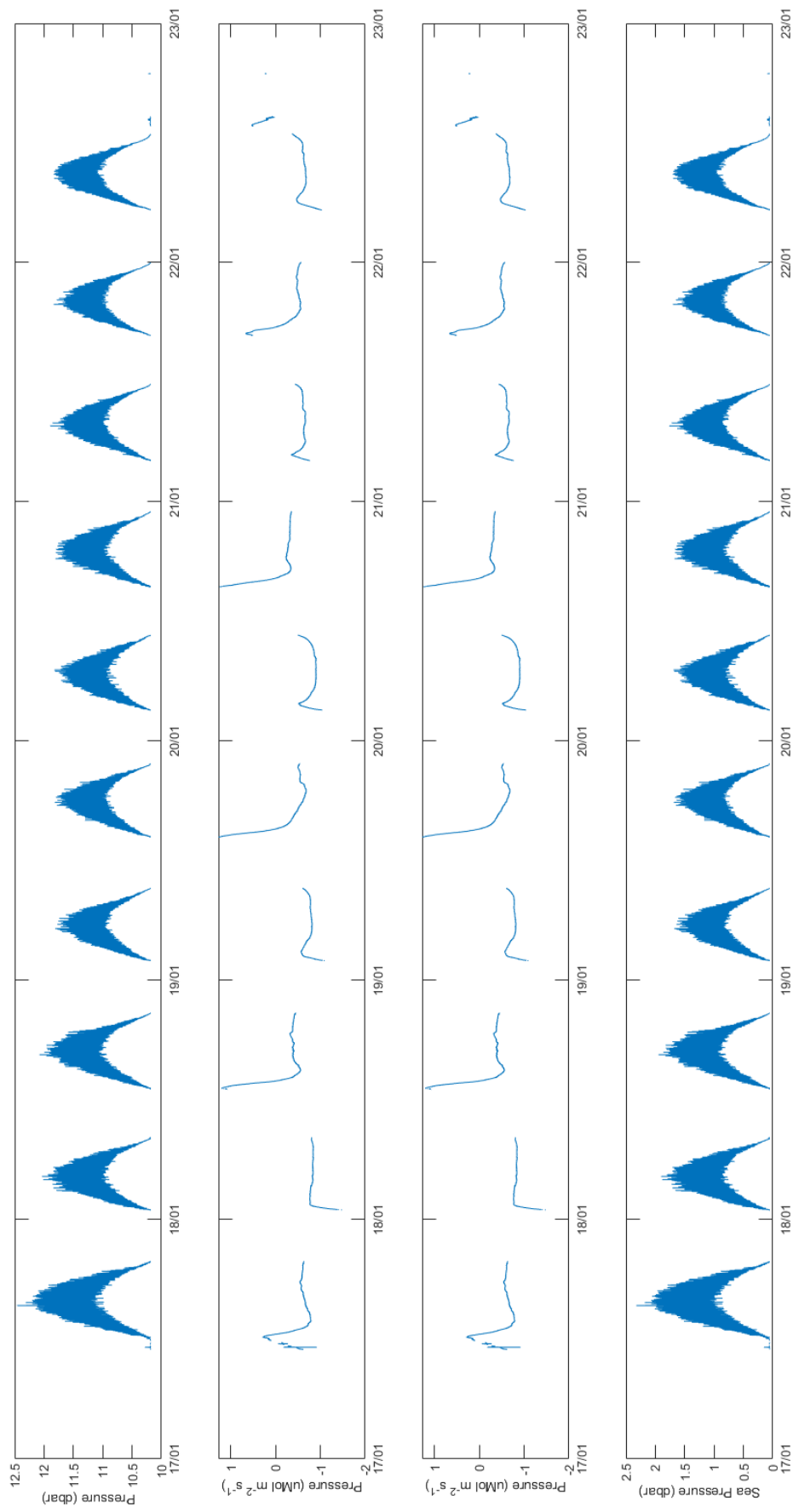


Figure 5b



Site F: Nortek Aquadopp

Figure 6a

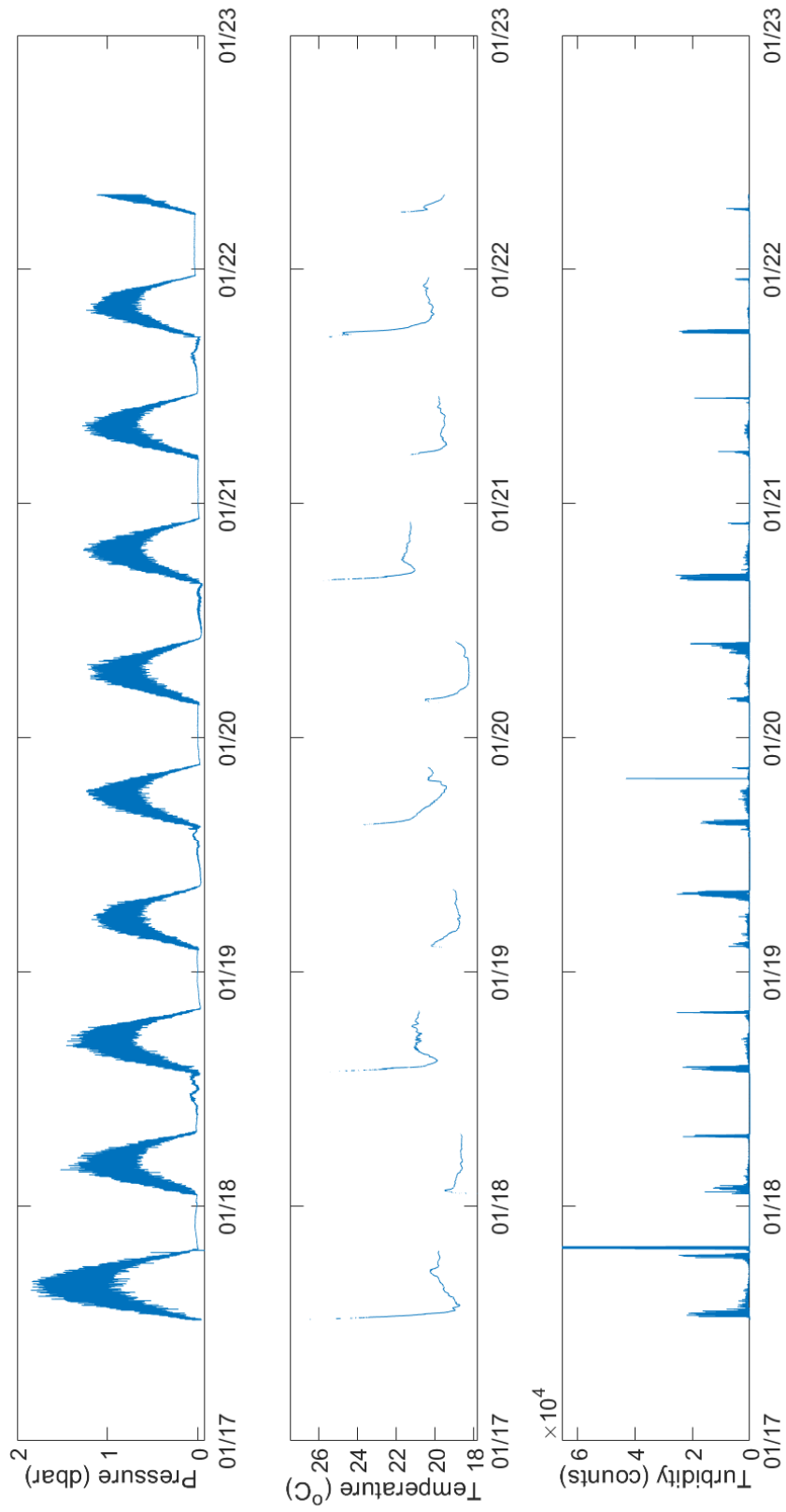




Figure 6b: Raw data

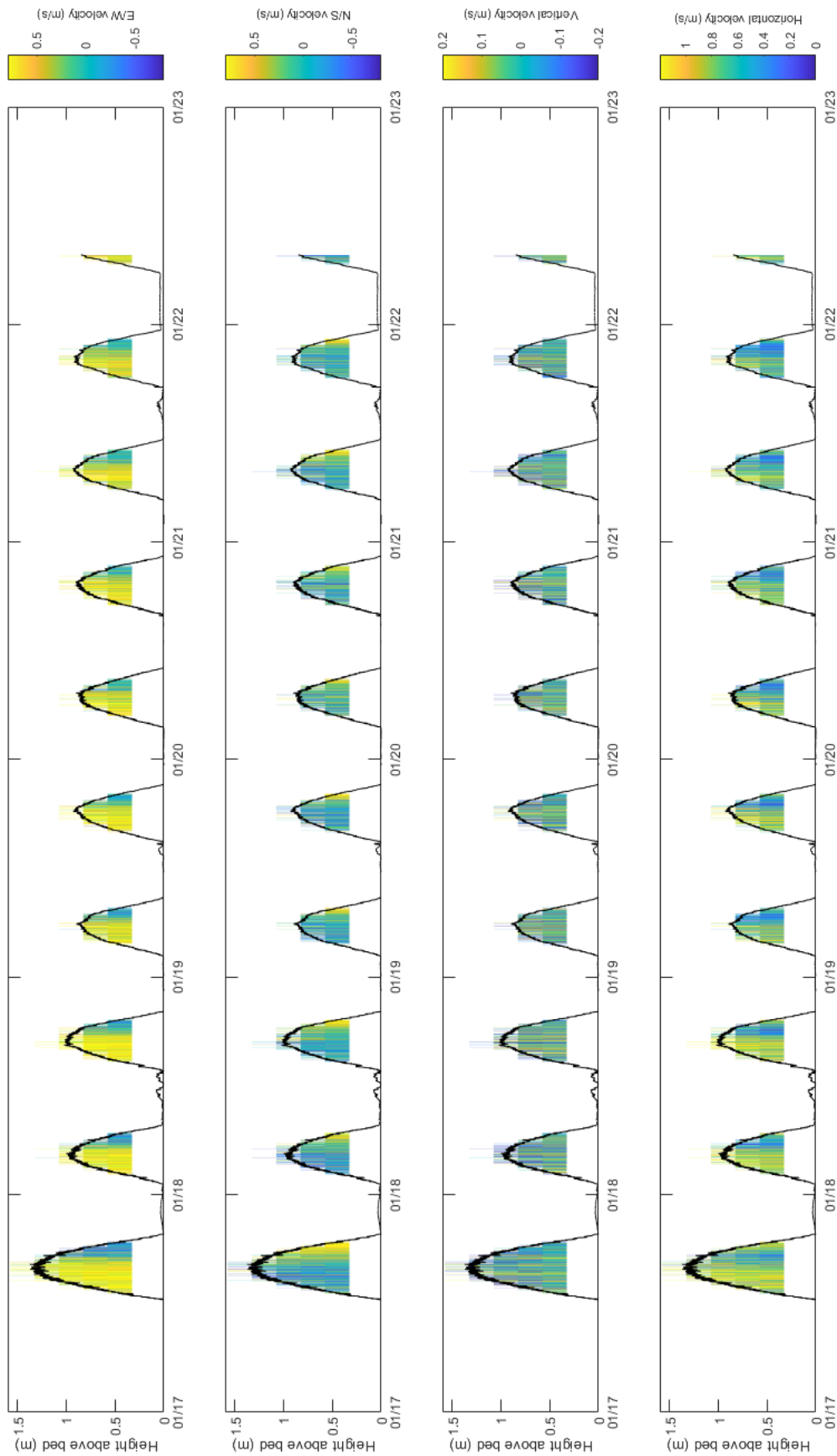
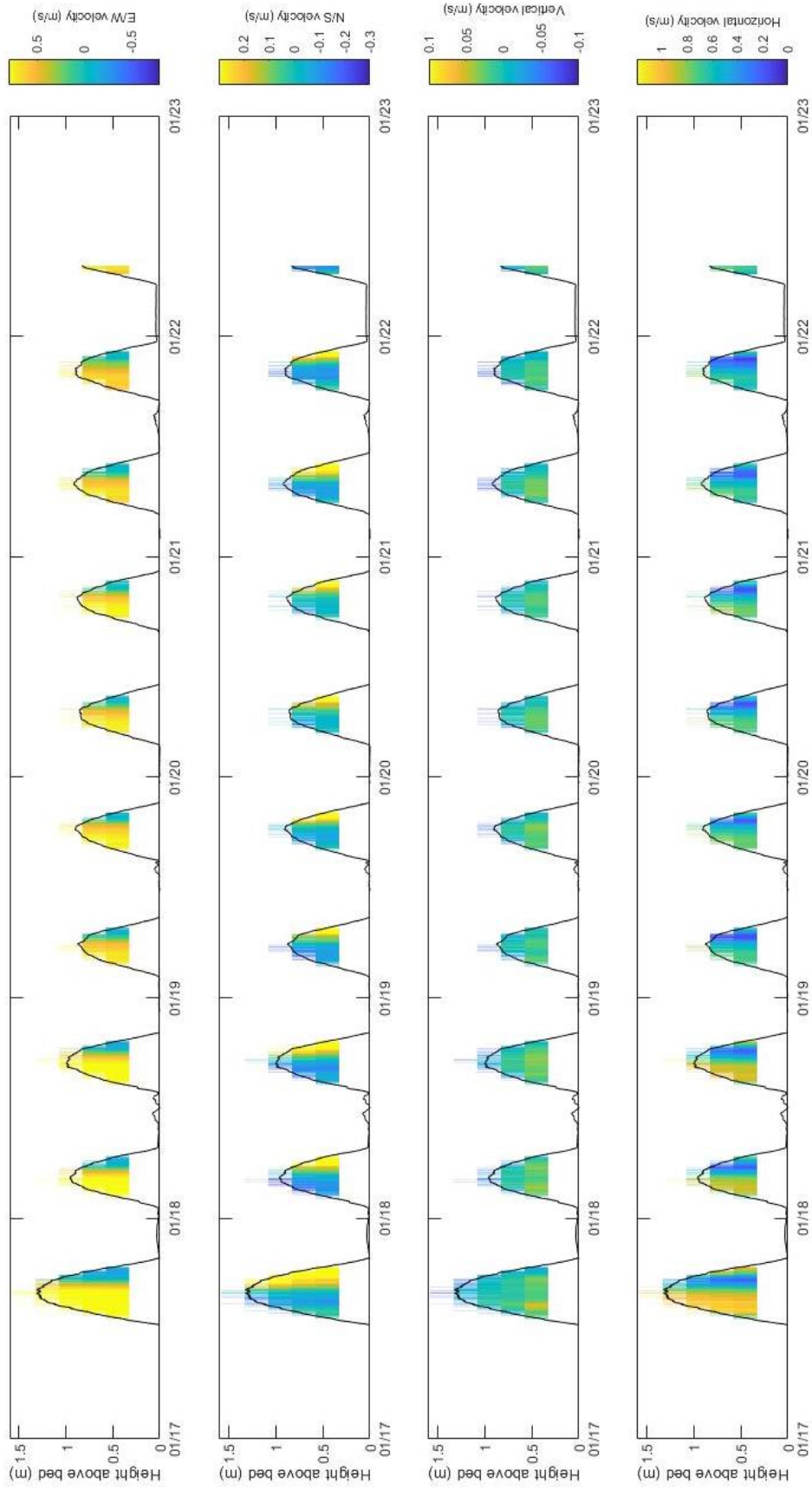


Figure 6c: Data averaged over 10 minutes



Site F: Concerto  
Figure 7a

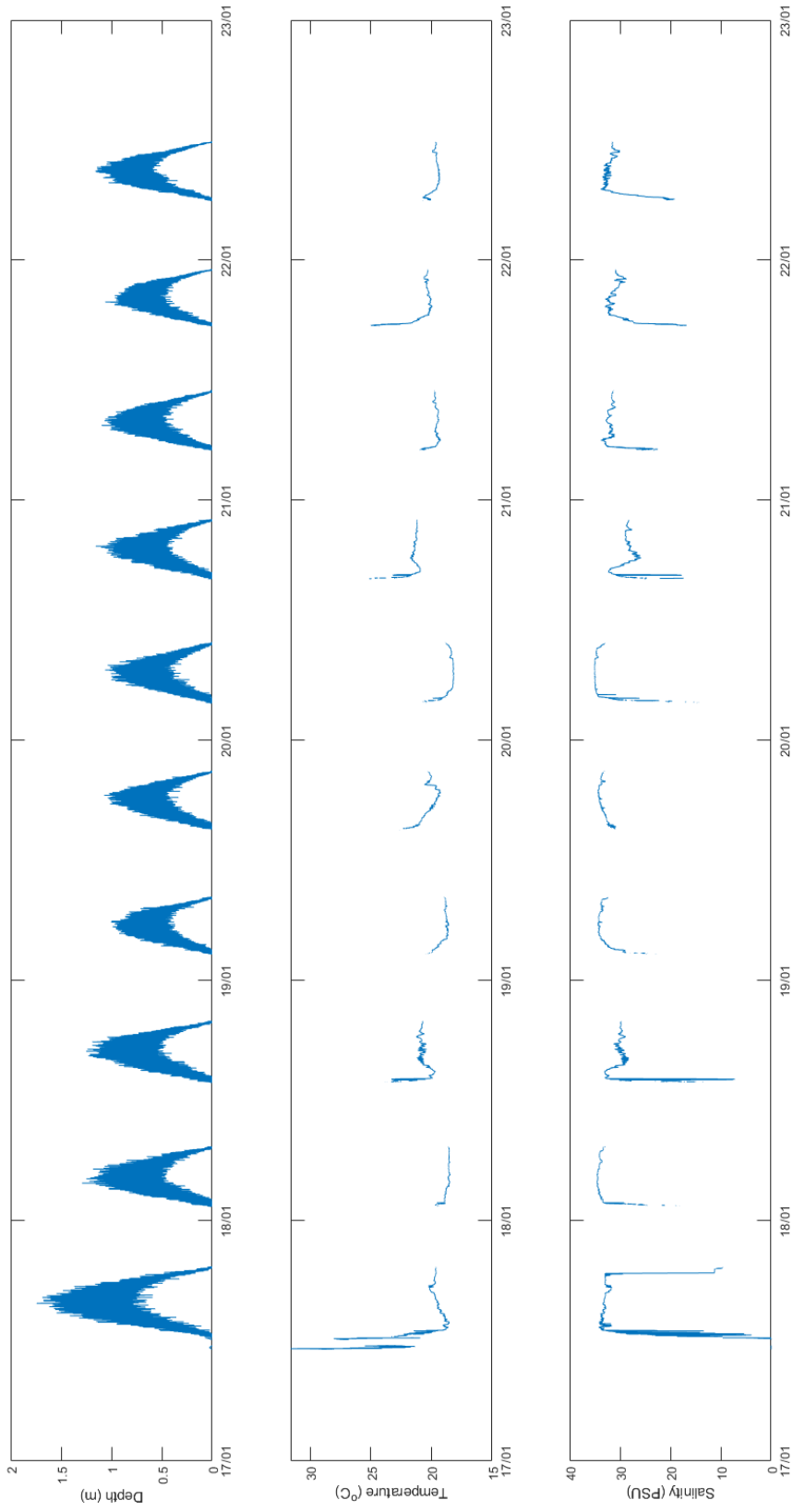


Figure 7b

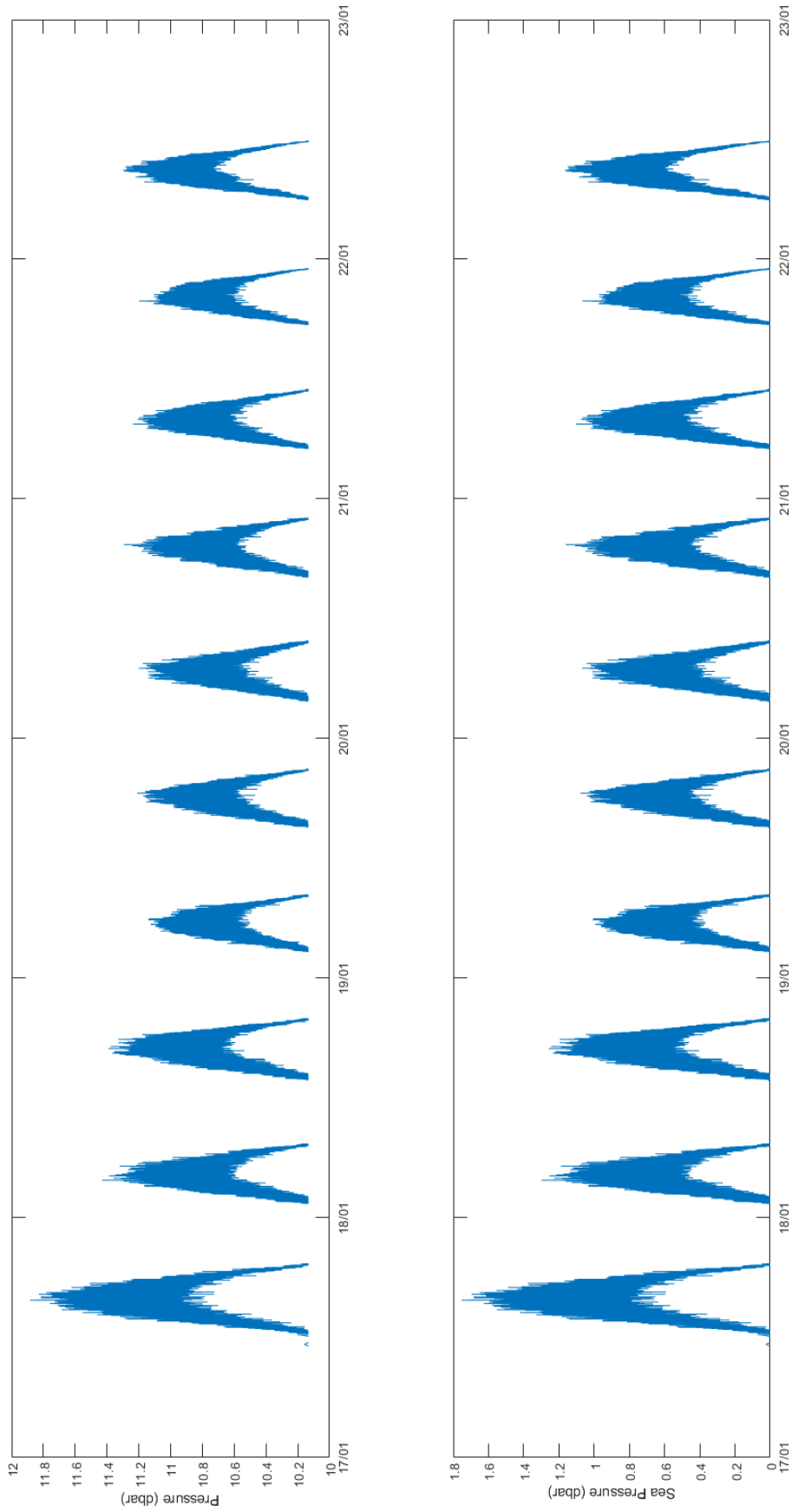
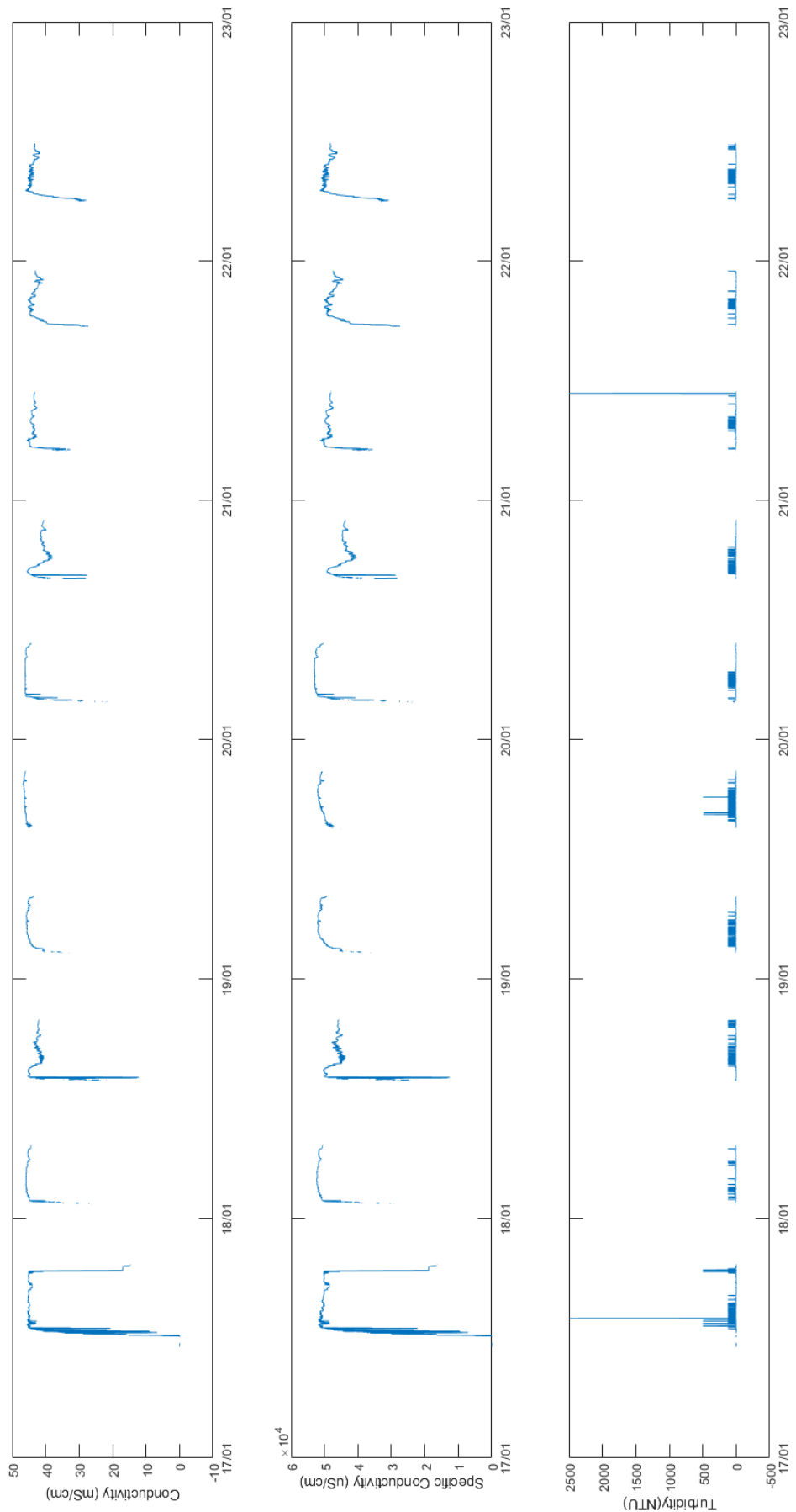


Figure 7c



Site H: Nortek Vector

Figure 8a: Raw data.

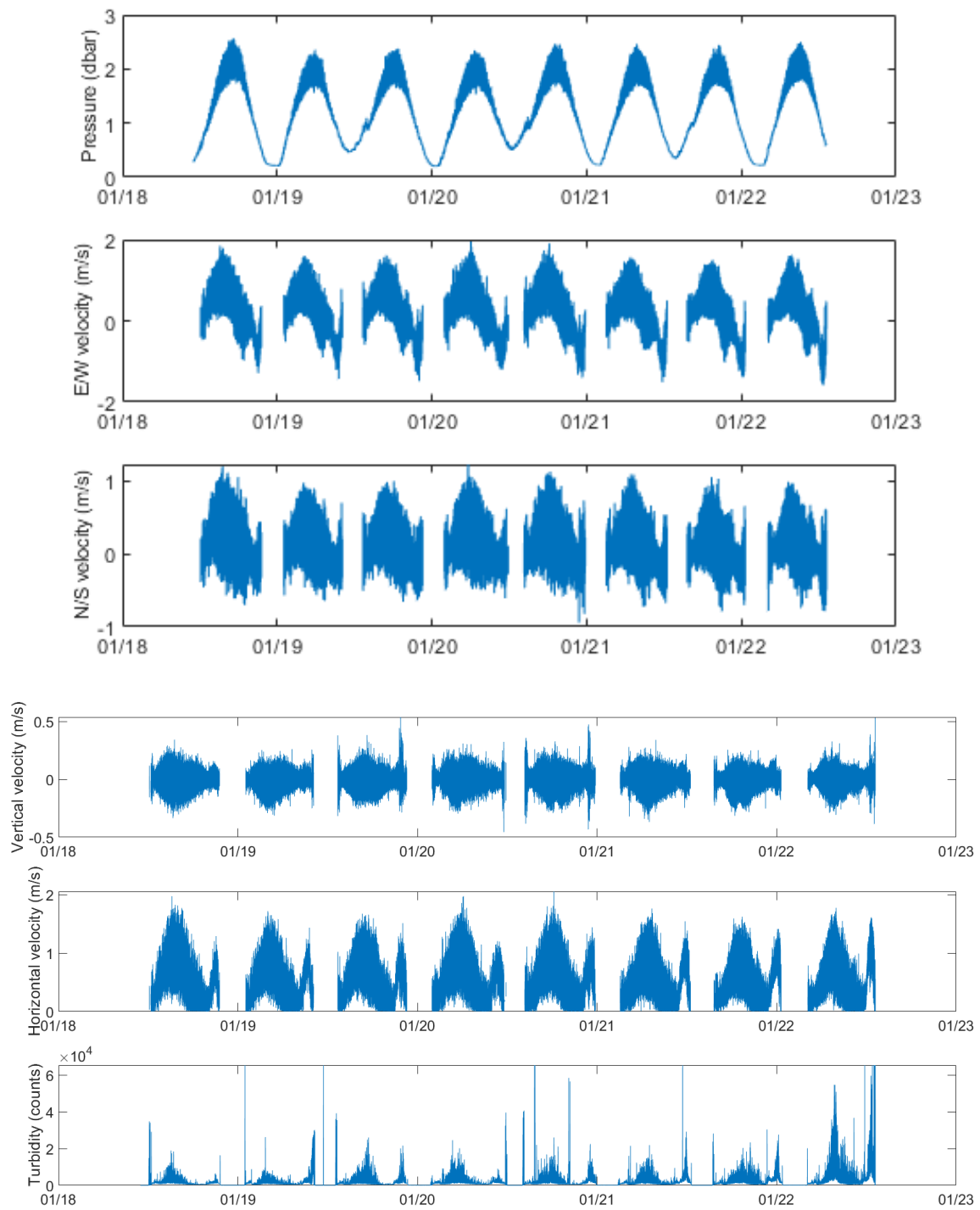
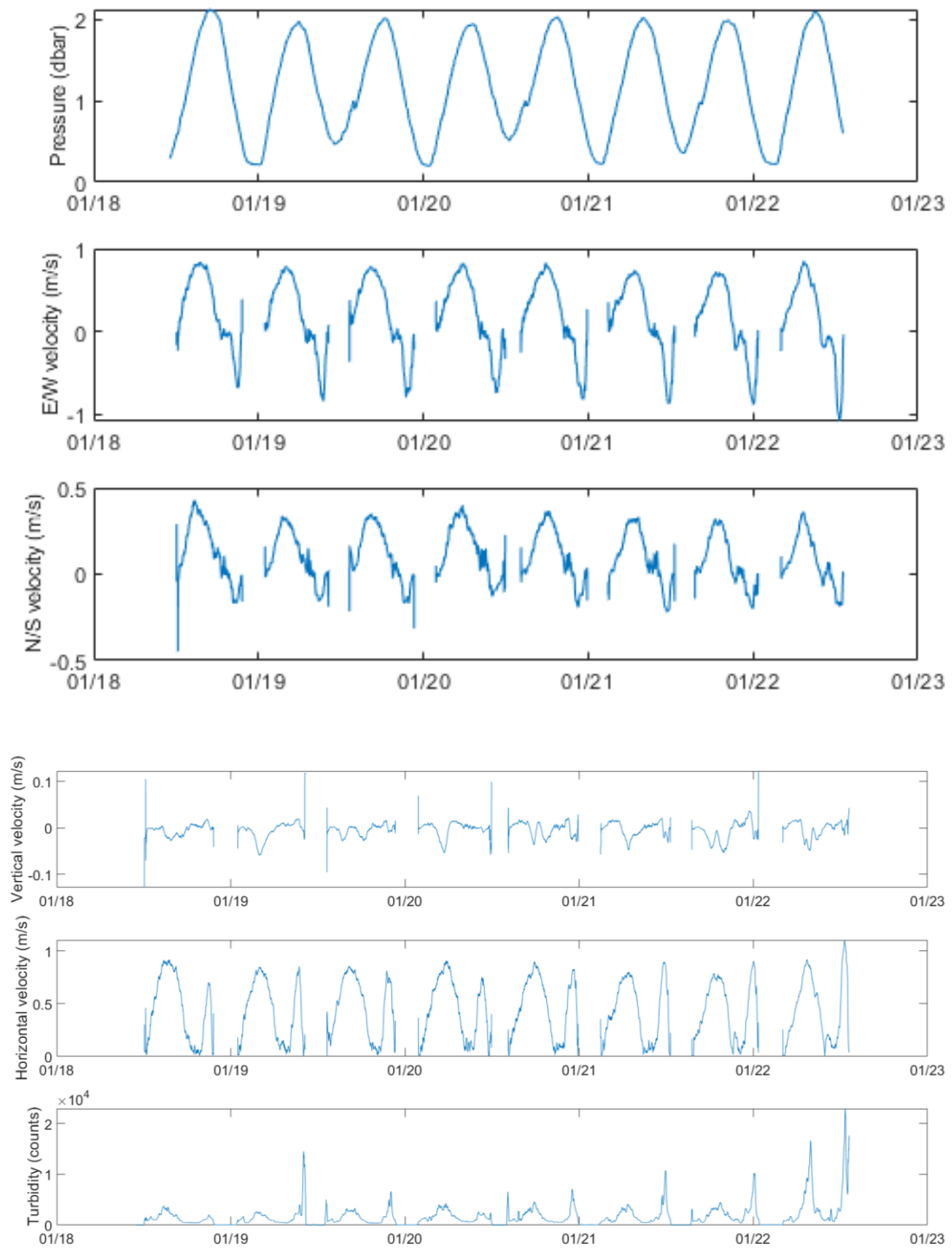



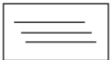
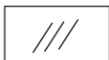
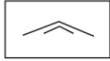
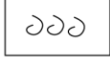



Figure 8b: Data averaged over 10 minutes

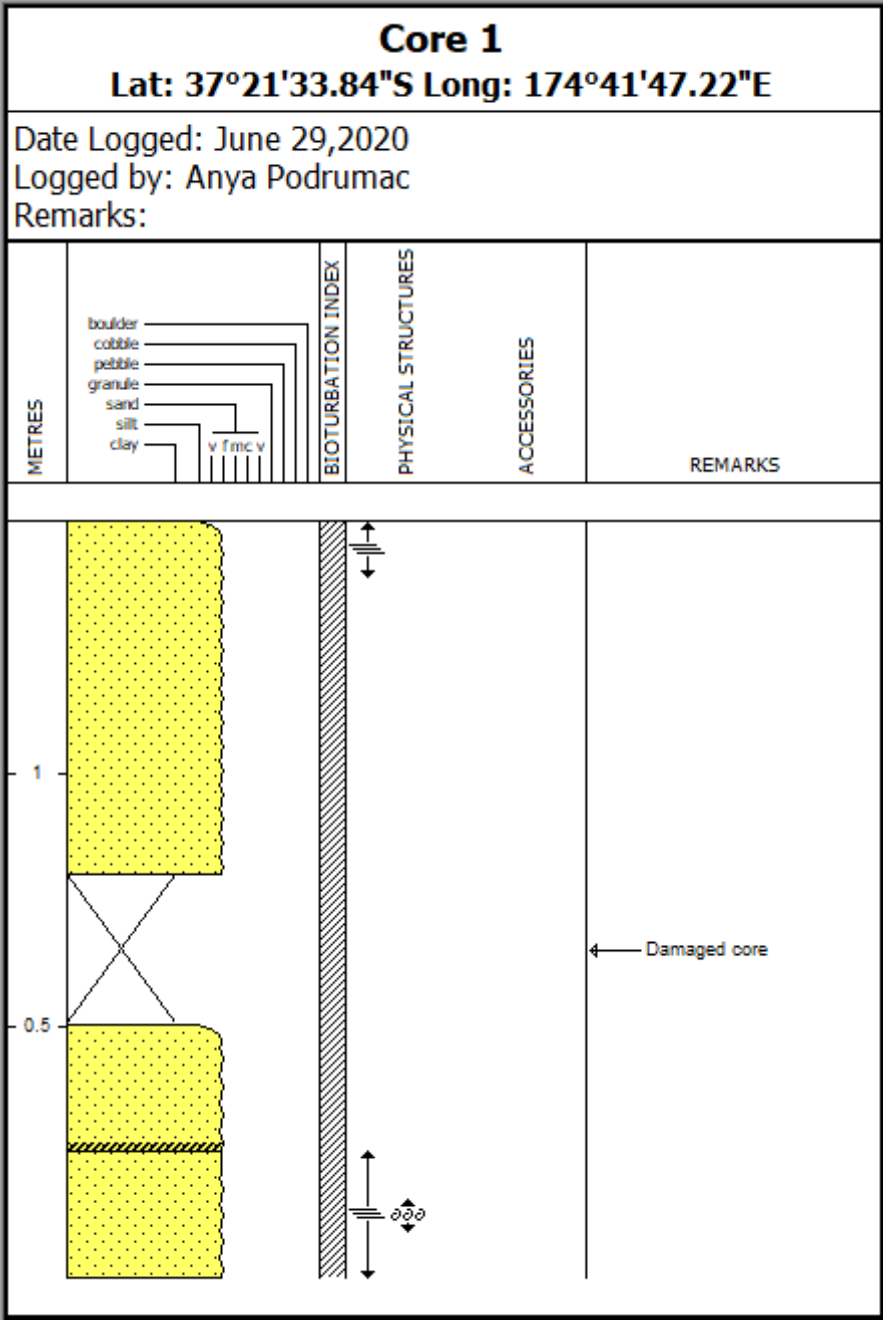


## Appendix D. Core Logs

Digital logs for cores drafted using Applecore®.

<b>LEGEND</b>	
<b>Lithology</b>	
 Sandstone	 No core / damaged core
<b>Contacts</b>	
 Gradational	
<b>Physical Structures</b>	
 Planar parallel laminated	 Planar tabular / trough cross-stratification
 Oscillatoy / combined flow ripples	
<b>Accessories</b>	
 Shell fragments	
<b>Bioturbation Index</b>	
 Barren	









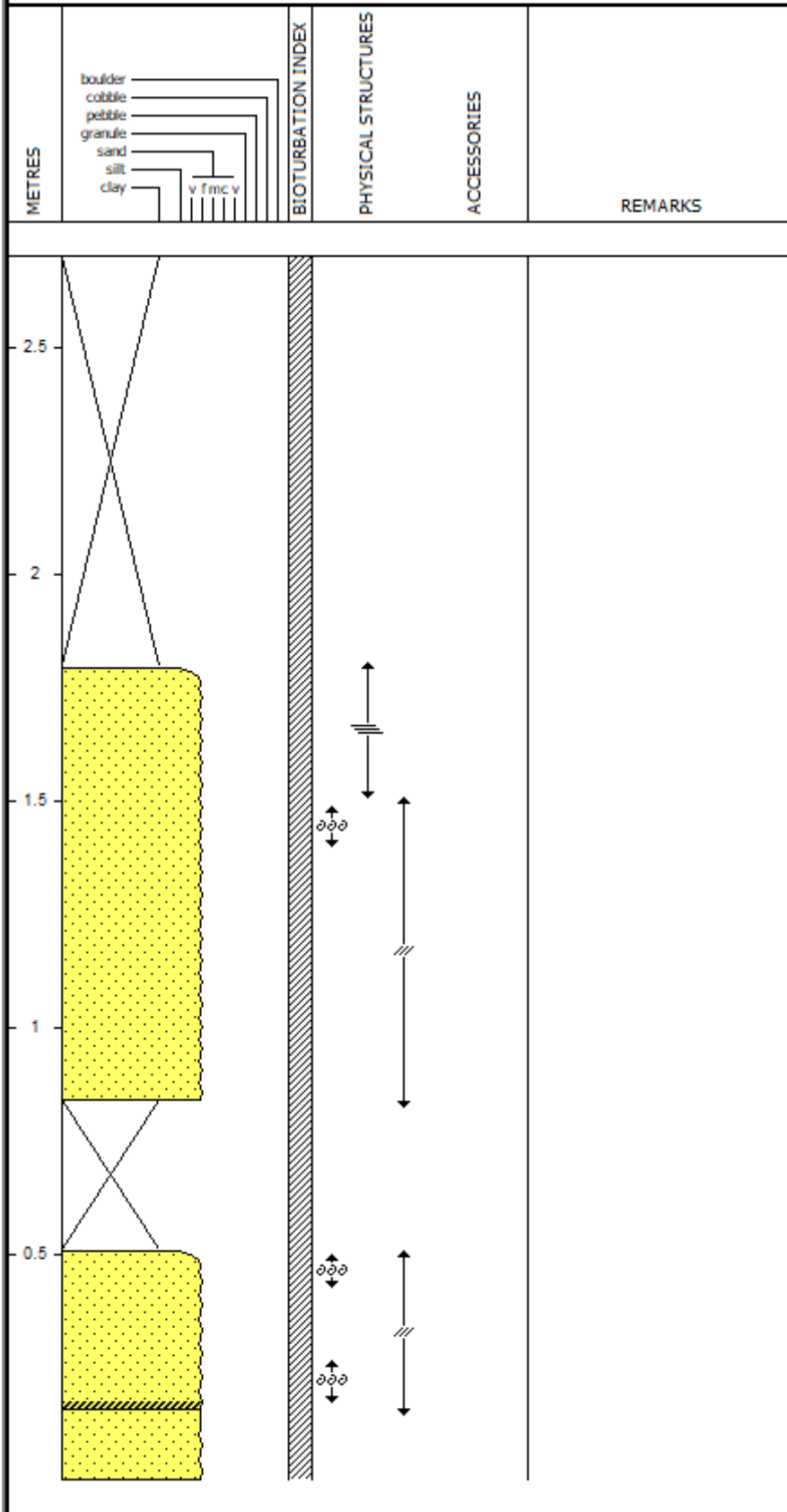
<b>Core 4</b>				
<b>Lat: 37°21'52.13"S Long: 174°42'0.9"E</b>				
Date Logged: July 6, 2020				
Logged by: Anya Podrumac				
Remarks:				
METRES		BIOTURBATION INDEX	PHYSICAL STRUCTURES	ACCESSORIES
				REMARKS
0.5				

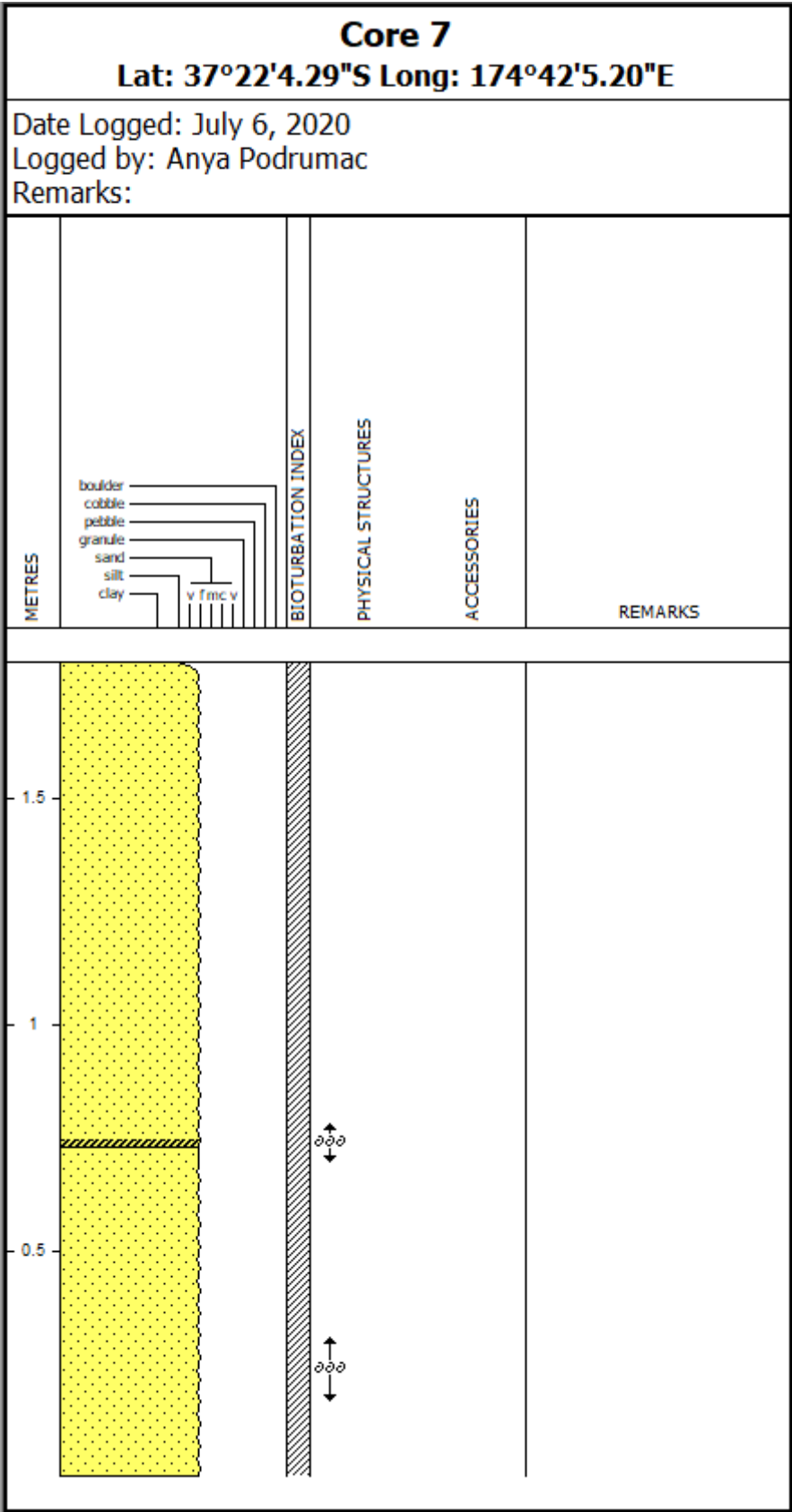


### Core 6

Lat: 37°21'47.53"S Long: 174°42'18.10"E

Date Logged: July 7, 2020  
 Logged by: Anya Podrumac  
 Remarks:

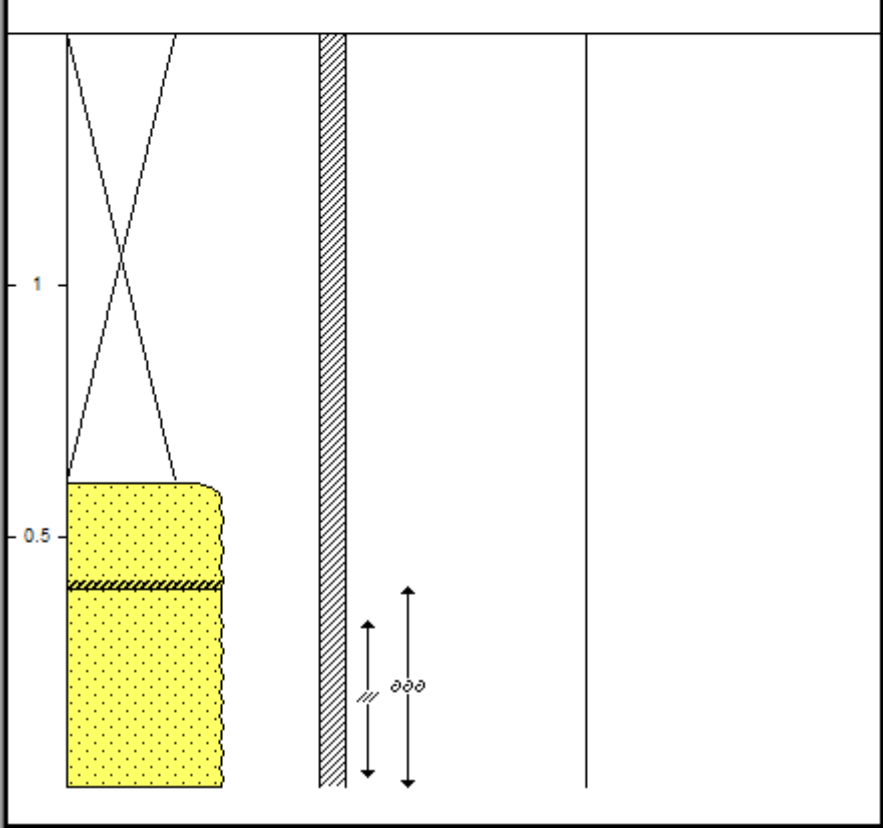




**Core 8**  
**Lat: 37°22'0.40"S Long: 174°42'13.29"E**

Date Logged: July 7, 2020  
 Logged by: Anya Podrumac  
 Remarks:

METRES	BIOTURBATION INDEX	PHYSICAL STRUCTURES	ACCESSORIES	REMARKS
--------	--------------------	---------------------	-------------	---------







## Appendix E. Core X-rays

Raw images of x-rays produced from all 9 vibracores. From core 1 on left through to core 9 on right.

